THE UNIVERSITY OF MANITOBA

LIBRARY

AUTHOR ..... WATSON, Andrew J. .....

TITLE ..... THE DYNAMICS OF THE RHODNIUS PROLIXUS FOLLICLE CELL CYTOSKELETON:

ULTRASTRUCTURE AND IMMUNOCYTOCHEMISTRY .....

.....

THESIS ..... M.Sc., 1984 .....

I, the undersigned, agree to refrain from producing, or reproducing, the above-named work, or any part thereof, in any material form, without the written consent of the author:

.....

.....

.....

.....

.....

.....

.....

.....

.....

.....

.....

.....

.....

.....

.....

.....

.....

.....

.....

THE UNIVERSITY OF MANITOBA

The Dynamics of the *Rhodnius prolixus* Follicle Cell Cytoskeleton: Ultrastructure and Immunocytochemistry

by

Andrew J. Watson

A Thesis

Submitted to the Faculty of Graduate Studies

in Partial Fulfillment of the Requirements for the

Degree of Master of Science

Department of Zoology

Winnipeg, Manitoba

June, 1984

THE UNIVERSITY OF MANITOBA

FACULTY OF GRADUATE STUDIES

The undersigned certify that they have read a Master's thesis entitled: The Dynamics of the Rhodnius prolixus Follicle Cell Cytoskeleton: Ultrastructure and Immunocytochemistry

submitted by Andrew John Watson

in partial fulfillment of the requirements for the degree of M.Sc.

The Thesis Examining Committee certifies that the thesis (and the oral examination, if required) is:

Approved [X] Not Approved [ ]

Advisor
E. Huebner

J.G. Eales

External Examiner
J. Gerrard

Chairman
M. Samoiloff

Date June 8th, 1984

THE DYNAMICS OF THE *RHODNIUS PROLIXUS* FOLLICLE CELL CYTOSKELETON: ULTRASTRUCTURE AND IMMUNOCYTOCHEMISTRY

BY

ANDREW J. WATSON

A thesis submitted to the Faculty of Graduate Studies of the University of Manitoba in partial fulfillment of the requirements of the degree of

MASTER OF SCIENCE

© 1984

Permission has been granted to the LIBRARY OF THE UNIVERSITY OF MANITOBA to lend or sell copies of this thesis, to the NATIONAL LIBRARY OF CANADA to microfilm this thesis and to lend or sell copies of the film, and UNIVERSITY MICROFILMS to publish an abstract of this thesis.

The author reserves other publication rights, and neither the thesis nor extensive extracts from it may be printed or otherwise reproduced without the author's written permission.

ACKNOWLEDGEMENTS

I would first like to thank Dr. E. Huebner for his constant support, guidance and most important for his friendship. Thank you Doc! Also a special thank you to Wade Sigurdson and Greg Kelly for countless discussions of the research and support extended throughout the course of this study. I would also like to thank the following graduate students for helping to make my M.Sc. a very enjoyable experience: Randy Baker, Odd Bres, Kevin Cash, Percy Hebert, Brent Poole, Ron Rosen, Allen Shostak and Iain Suthers. I wish to thank my mother, Marion Watson for typing the initial copy of the thesis and also Judy Bradie for making the final copy. I would like to thank the examining committee Dr. J.G. Eales, and Dr. J. Gerrard for their editorial contributions. I wish to acknowledge financial assistance from the following sources: NSERC postgraduate scholarship, NSERC research grant to Dr. E. Huebner and teaching assistantships from the Department of Zoology. Finally, I would like to thank Colleen McLeod for her support and encouragement in helping to see this thesis to its' completion.

TABLE OF CONTENTS

PAGE

Abstract 1
Introduction 3
Materials and Methods 10
Animal rearing techniques 10
Dissection techniques 10
Fixation to embedding procedures 10
Light and transmission electron microscopy 12
Detergent extraction methods 13
Basal lamina removal 13
Scanning electron microscopy of basal lamina removal 15
Detergent extraction experiments 15
Immunofluorescence methods 17
Photomicrography methods 22
Results 23
General Overview of Follicle Cell Development 23
Methodology of Cytoskeletal Visualization and Isolation 24
Fixations and buffer composition 24
Fixation 24
Tannic acid and Saponin 25
Buffer composition 26
Detergent extractions 27
Preliminary experiments 27
Basal lamina removal methods 29
1. Enzymatic digestion of the basal lamina 29
2. Ovariole ultrastructure upon basal lamina removal .. 31
3. Enzymatic and mechanical basal lamina removal 32
Detergent extraction after basal lamina removal 33
Detergent extraction with basal lamina intact 35
Immunofluorescence procedures 37
Intact follicle cell sheets 37
Sectioned material 37
1. Fixation: Paraffin embedding 37
2. Fixation: Plastic embedding 38
3. Plastic embedding media 39
4. Section thickness 39
5. Controls 40
6. Comparison of anti-tubulin antibodies 41
Characterization and Organizational Dynamics of the Follicle Cell Cytoskeleton During Oogenesis 41
Prefollicular cells 41
Previtellogenic cells 42
Vitellogenic follicles 43
Overview 43
Apical follicle cells - Details 44
Lateral follicle cells - Details 45
Post vitellogenic lateral follicle cells 47

PAGE

Figure Abbreviations 48
Figures 49
Discussion 105
Methodology of Cytoskeletal Visualization and Isolation 105
Overview 105
Fixations and buffer composition 106
Detergent extractions 109
Basal lamina removal 112
Immunofluorescence methods 116
Characterization and Organizational Dynamics of the Follicle Cell Cytoskeleton During Oogenesis 120
References 128

Abstract

The follicular epithelium of Rhodnius prolixus undergoes significant morphogenetic alterations during an oogenic cycle. Cell shape and cell to cell contacts vary from tall columnar tightly apposed cells during previtellogenesis to decreased cell height, irregular shape and reduced cell to cell contact during vitellogenesis. The transformation from a tightly packed epithelium to one with large extracellular spaces is known as patency and provides the pathway for extraovarian yolk precursors to reach the oocyte.

Application of transmission electron microscopy to normal and detergent extracted follicle cell preparations in combination with basal lamina removal, revealed that cytoskeletal elements play an integral part of the lateral follicle cell shape change during patency. Microtubules and microfilaments occur in all follicle cell stages and subtypes. Immunofluorescent anti-tubulin localization in follicle cell sheets and paraffin and plastic sections allowed the visualization of the pattern of microtubule distribution.

Upon initiation of vitellogenesis the follicle cell microtubular cytoskeleton undergoes a reorganization from the well organized longitudinal cylindrical arrangement of previtellogenic follicle cells to the random arrangement of the patent lateral follicle cells. Microtubules in these cells are less packed, shorter and oriented both circularly and longitudinally. Only the lateral follicle cells undergo patency while apical cells remain columnar and tightly apposed. Microtubules become a dominant cytoplasmic constituent of the apical cells retaining the longitudinal cylindrical organization.

Microfilaments are most abundant in the patent lateral follicle cells, arranged in a subplasmalemmal zone around the cell. Microfilaments are also found in the lateral arms connecting adjacent vitellogenic lateral follicle cells and in the apical microvilli of these cells.

The reorganization of the microtubular cytoskeleton and the appearance of the subplasmalemmal microfilaments are key events which contribute to the cell shape change associated with patency. This study has shown that patency involves a more complex interaction of cellular processes than previously thought.

Introduction

The mechanisms involved with the maintainence and regulation of cell shape is a major area of basic cell biological research. Cytoskeletal components (microtubules, microfilaments and intermediate filaments), are intimitely associated with the modulation of cell shape in many diverse systems such as: tissue culture cell systems (Osborn and Weber, 1977; Trotter et al., 1978; Wolosewick and Porter, 1979 and Albertini et al., 1984), chromatophores (Schliwa et al., 1978; Beckerle and Porter, 1983), nucleated erythrocytes (Barrett and Dawson, 1974; Bertolini and Monaco, 1976 and Cohen, 1978), brush borders of intestinal epithelial cells (Mooseker, 1976; Hirokawa and Heuser, 1981 and Hirokawa et al., 1982) and the manchette surrounding the spermatid nucleus during spermatogenesis (Dustin, 1978). Burnside (1978) and (Warren and Burnside, 1978) have clearly shown the involvement of actin and myosin filaments and microtubules in modulating the light and dark adaptation of fish retinal cone and rod, photoreceptor cells. However, very few studies have investigated the contribution of cytoskeletal mediated cell shape changes to developmental processes. Amphibian neurulation is one example, where cytoskeletal mediated cell shape changes are directly linked to a developmental process (Karfunkel 1971; and Burnside 1973).

With the existing ultrastructural and physiological background data available, the Rhodnius follicle provides an excellent experimental model to study the modulation of follicle cell shape changes during patency and its role in oogenesis.

The insect ovary is a cell interacting system where the oocyte depends on specific cell interactions with accessory cells (Huebner, 1984b). The meroistic insect ovary types have two accessory cell types; nurse cells and follicle cells (Huebner, 1984a,b). The nurse cells and oocytes are sister cells derived from germ tissue, and exist in a syncytical association (Huebner, 1984 a,b). The follicle cells, are mesodermally derived cells which form a simple epithelium around the developing oocyte (Huebner, 1984 a,b). The follicle cells have multiple functions including the regulation of the transport of yolk proteins from the hemolymph to the oolemma (Huebner and Anderson, 1972a; Pratt and Davey, 1972abc; Davey and Huebner, 1974; Abu-Hakima and Davey, 1977a; Huebner and Injeyan, 1980, 1981; Davey, 1981 and Telfer et al., 1982) and also the production of the secondary egg coat or chorion (Beament, 1946).

The basic ultrastructural features of the meroistic telotrophic ovariole of Rhodnius are established (Huebner, 1982, 1984). For the purpose of orientation and to provide a framework for the results, a brief summary of the ovariole structure follows (See Huebner, 1984). The telotrophic ovariole can be divided into 2 compartments, an apical tropharium containing the nurse cell syncytium, and the vitellarium containing the developing oocytes and associated prefollicular and follicular cells. The nurse cell syncytium and oocytes develop and function in association with specialized mesodermally derived somatic cells. Small oocytes (at the base of the tropharium) are embedded in the prefollicular tissue which eventually forms a follicular epithelium around each growing oocyte. The somatic cells surrounding the nurse

cells form a thin sheet of cells, the inner sheath. The entire ovariole is surrounded by a basal lamina or tunica propria.

Egg production is initiated by ingestion of a blood meal, which triggers the neuroendocrine system that regulates oogenesis (Pratt and Davey, 1972 a,b,c). A key element in the control is the release of juvenile hormone (JH) from the corpus allatum (Pratt and Davey, 1972 a,b,c). JH acts on both the fat body to initiate production of vitellogenin yolk proteins, and on the ovary to regulate their uptake (Pratt and Davey, 1972 a,b,c; Davey and Huebner, 1974; Huebner and Injeyan, 1980). Within the ovary, JH acts primarily on the follicle epithelium (Davey and Huebner, 1974 and Huebner and Injeyan, 1980). Evidence exists that its action is exerted in both previtellogenesis and vitellogenesis (Abu-Hakima and Davey, 1975). The previtellogenic follicle epithelium arises from the association of prefollicular cells with the oolemma (Masner, 1968; Huebner and Anderson, 1972 and Huebner, 1984b) and is characterized as a tightly packed layer of columnar cells. These initially form a sufficient cell number by mitosis, then cease mitosis and become binucleate (Huebner and Anderson, 1972). Thus, from mid to late previtellogenesis through vitellogenesis and chorion formation the follicle undergoes differentiation with no increase in cell number (Huebner and Anderson, 1972 and Huebner, 1984b). JH exposure at the onset of vitellogenesis results in a change in the lateral follicle cell volume and shape which is manifested by the appearance of large extracellular spaces within the epithelium (Huebner and Anderson, 1972; Pratt and Davey, 1972; Davey and Huebner, 1974; Abu-Hakima and Davey, 1977 a; Huebner and Injeyan, 1980; Davey, 1981 and Huebner and Injeyan, 1981). The follicle responds optimally to JH exposure only if

the follicle cells have become competent to enter vitellogenesis by exposure to JH during previtellogenesis (Abu-Hakima and Davey, 1975). The formation of these extracellular spaces (process of patency) is a key step in oocyte differentiation, since these spaces provide the route for the movement of these yolk precusors from the hemolymph to the oolemma. The regulation of patency is thus, central to the regulation of vitellogenesis. It is important to note that patency arises only in the lateral follicle cells and not in the apical or basal follicle cells (Huebner and Anderson, 1972 and Huebner, 1984b). Once vitellogenesis is completed, the lateral follicle cells greatly increase their cellular volume through the build-up of organelles and become tightly joined, thus eliminating the extracellular spaces (Huebner and Anderson, 1972 and Abu-Hakima and Davey, 1977a). These cells then begin to secrete the layers of the secondary coat or chorion (Beament, 1946).

Davey and co-workers have extensively studied the mechanisms of lateral follicle cell patency formation (Abu-Hakima and Davey, 1977 a,b,c; Abu-Hakima and Davey, 1979; Ilenchuk, 1980; Davey, 1981 and Ilenchuk and Davey, 1983). They have concluded that the observed decrease in cell volume and cell shape changes in the lateral follicle cells occurs due to the JH stimulation of increased Na^+ K^+ ATPase activity in the follicle cell membranes. This is theorized to lead to a pumping out of fluid from the follicle cells, which causes a sharp reduction in cell volume, creating the formation of the extracellular spaces and cell shape changes.

Although the role of the follicle cell cytoskeleton has been briefly noted (Huebner, 1976), Davey and co-workers have tended to discount its importance to the overall process of patency (Abu-Hakima

and Davey, 1977a & c). As noted earlier, cytoskeletal elements are known to play an important role in the modulation of cell shape in a wide variety of eukaryotic cell systems. It is difficult to envisage consideration of the mechanisms involved with cell shape control in any eukaryotic cell system without consideration in detail, of the cytoskeletal contribution. The presence of microtubules in Rhodnius follicle cells, is established (Huebner and Anderson, 1970, 1972; Abu-Hakima and Davey, 1977c) as are microfilaments (Abu-Hakima and Davey, 1977c). Furthermore cytoskeletal inhibitors such as colchicine or cytochalasin B also inhibit the patency response, normally observed with JH treatment (Huebner, 1976, Abu-Hakima and Davey, 1977c). In order to fully understand the role of the cytoskeleton in Rhodnius follicle cells, an accurate and detailed study of its abundance, orientation and dynamics during an oogenesis cycle is essential. This thesis research was conducted to re-assess and extend our knowledge of the role of the cytoskeleton in the Rhodnius follicle cell shape change.

The general objectives of this study are to determine the organization of the follicle cell cytoskeleton and to determine if a rearrangement of the cytoskeletal elements is correlated with the onset of patency.

Most research involved with the localization of cytoskeletal proteins has utilized tissue culture cell systems as research models. For this reason the common techniques involved with cytoskeletal localization had to be modified as only intact follicles were used in this study. An integration of a variety of approaches was undertaken. Examination of normal live preparations with various types of routine light microscopy and fixed preparations with transmission and scanning

electron microscopy was conducted. In addition to enzymatic digestion and mechanical removal of the basal lamina, detergent extraction methods were applied. Finally, indirect immunofluorescence methods using anti-tubulin and anti-actin binding to whole permeabilized ovarioles or sections of paraffin and plastic embedded ovarioles provided a third approach.

Although the literature is repleat with single cell methods (Lazarides and Weber, 1974; Weber and Groeschel-Stewart, 1974; Weber et al., 1975; Osborn and Weber, 1982 and Herman et al., 1983), the application of immunofluorescence methods to thicker tissue preparations has only recently been attempted (Bussolati et al., 1980; Byers and Fujiwara, 1982; Hogan and Smith, 1982 and White et al., 1983). Since it is important to relate cell shape changes to the in vivo situation. The application of these techniques to intact tissues (although more difficult), will lead to a much clearer understanding of the developmental process under study. The use of intact tissues ensures the maintainence of normal cell to cell interactions, a quality which is obviously lost through the use of single cell systems.

Within this framework, the four specific objectives of this study were: (1) To develop and extend the methodology required to isolate and visualize the follicle cell cytoskeleton; (2) To determine if the follicle cells contain an interacting cytoskeleton composed of microtubules and microfilaments; (3) To investigate the changes in cytoskeletal organization during follicle cell differentiation from the prefollicular cell stage through chorion formation; and (4) To compare the cytoskeletal organization of the lateral and apical follicle cells,

to establish if a correlation exists between the onset of patency and reorganization of the cytoskeleton in the lateral follicle cells.

Materials and Methods

Animal rearing techniques

Animals were maintained at 27°C in high humidity using routinely established methods (Huebner and Anderson, 1972a). Only mated adult females were used for experiments and these animals were fed regularly at appropriate intervals to obtain ovarioles at all the specific stages of oogenesis.

Dissection techniques

The ovaries were dissected and transferred to a 35mm Petri dish containing Rhodnius saline (Maddrell, 1969), or usually calcium free Rhodnius saline + 2mM ethylene glycol bis (B-amino ethyl ether) N-N'-tetracetic acid (EGTA). The 7 ovarioles composing each ovary were separated in the saline by removing the entangling tracheoles. Once separated, a fine electrolytically sharpened tungsten needle (Juurlink and Dell, 1980) is inserted between the ovariole and the sheath is removed. The ovarioles were desheathed and separated in this manner for all experiments, including normal fixations.

Fixation to embedding techniques

Ovarioles from mated females fed within one week of dissection were used, thus ensuring only healthy ovarioles encompassing all stages of follicle development were fixed.

Thirteen different fixations were used in this part of the study. The fixatives used were variations of 2 fixatives: (1) a modified Karnovsky fixative (Karnovsky, 1965), containing 2.5% glutaraldehyde,

1.0% paraformaldehyde and 0.05% $CaCl_2$ in 0.1M sodium cacodylate buffer pH 7.2 and (2) a microtubule stabilizing fixative, (Luftig et al., 1977) containing 5.0% glutaraldehyde, 1mM $MgSO_4$, 1mM GTP, and 2mM EGTA in 100 mM piperazine-N-N'-bis [2-ethane sulfonic acid] (PIPES) buffer, pH 6.9.

The 13 different variations used were as follows: (1) modified Karnovsky's; (2) modified Karnovsky's + 0.1% wt/vol tannic acid (TA); (3) modified Karnovsky's + 0.5% wt/vol TA; (4) modified Karnovsky's + 0.5% wt/vol TA + 0.05% wt/vol Saponin (Maupin and Pollard, 1983); (5) Luftig's fixative; (6) 3.0% glutaraldehyde in 100mM PIPES buffer pH 6.9, + 8.5 mM $MgCl_2$, 10mM EGTA + 1mM GTP; (7) 3.0% glutaraldehyde in 100 mM Pipes buffer pH 6.9 + 8.5mM $MgCl_2$, 10mM EGTA, + 1mM GTP + 0.5% wt/vol TA: (8) 3.0% glutaraldehyde in 60 mM Pipes + 25mM (N-2-Hydroxyethyl-perazine-N'2 ethane Sulfonic acid) HEPES buffer, pH 6.9, + 8.5mM $MgCl_2$ + 10mM EGTA + 0.1% wt/vol TA; (9) 4.0% glutaraldehyde in PHEM buffer (Schliwa and Von Blerkom, 1981), 60mM Pipes + 25mM HEPES buffer pH 6.9 + 2mM $MgCl_2$, 10 mM EGTA: (10) 3.0% glutaraldehyde in PHEM buffer pH 6.9 + 1mM GTP; (11) fix #10 + 0.5% wt/vol TA: (12) fix #11 + 0.05% wt/vol Saponin and (13) #11 + 0.1% Saponin.

The primary fixative used in most of the experiments was fixative #10. Fixations using tannic acid with or without Saponin were conducted to provide better preservation and visualization of microfilaments.

Ovarioles were fixed for 1 hour at 4°C, washed once in the appropriate buffer and then postfixed for 15 minutes in 0.5% wt/vol osmium tetroxide (OsO_4) in 0.1M sodium cacodylate buffer, pH 7.2. Keeping the OsO_4 postfixation time as short as possible is important since OsO_4 exposure can cause a breakdown of microfilament structure

(Maupin-Szamier and Pollard, 1978). Rapid dehydration in an ascending (-20°C) ethanol series, (70%, 80%, 95%, and 100%) follows post-fixation. Once in 100% ethanol the vials are left to warm to room temperature and then are given 4 changes of fresh 100% ethanol at 30 minute intervals. Subsequently there is a change to a 1:1 mixture of propylene oxide and 100% ethanol for 15 minutes, followed by two, 15 minute changes of pure propylene oxide. Infiltration overnight in a 1:1 mixture of the epon-araldite embedding medium (Anderson and Ellis, 1965) and propylene oxide is next followed by embedding in flat moulds using a fresh embedding mixture (Anderson and Ellis, 1965).

Light and transmission electron microscopy

Semi-thin (1uM) epoxy sections were cut with a Sorvall-Porter Blum MT2B ultramicrotome using glass knives made with a LKB knifemaker type 7801B. The sections were heat fixed on clean glass slides and were stained with 1.0% toluidine blue in 1.0% sodium borate solution by heating the stain covered slides. After rinsing under running water and air drying, the slides were mounted with immersion oil and then viewed and photographed with a Zeiss photomicroscope II.

For transmission electron microscopy, thin sections were cut on glass knives with the Sorvall Porter Blum MT2B ultra-microtome and were mounted on 200 mesh hexagonal grids. Sections were first stained in a saturated solution of uranyl acetate in 50% ethanol for 30 minutes, followed by a wash with 50% ethanol, and then stained in lead citrate (Venable and Coggershall, 1965) for 1 minute. Grids were examined in either an AEI 6B or AEI 801S transmission electron microscope at an accelerating voltage of 60KV.

Detergent extraction methods

In normal TEM preparations the density of cellular cytoplasm can often obscure the presence of cytoskeletal elements, making their detection difficult. This problem can be reduced by the production of detergent insoluble cytoskeletal models by exposing tissue samples to detergent extraction conditions using non-ionic detergents such as Triton X-100 or Saponin in combination with a cytoskeletal stablization buffer. The resulting solubilization of cell membranes, and extraction of cytoplasmic cell constituents, except for a detergent insoluble cytoskeleton, leads to an increased visualization of the cell cytoskeleton.

When intact ovarioles are exposed to detergent extraction conditions, the ovarian basal lamina expands outward, trapping the extracted cytoplasmic cell constituents within the periovariole space. This result, indicated that in order to achieve an unrestricted extraction of cellular material it was essential to remove the basal lamina prior to the application of detergent extraction methods.

Basal lamina removal

Enzymatic digestion of basal lamina was conducted with the following enzymes: collagenase V: elastase type I and III; trypsin types III and IX and protease (pronase VIII) (all Sigma Chemical Co.). Initial experiments included these enzymes in combination with one of the following 8 salines or buffers: (1) microtubule stabilization buffer (MS buffer), 100mM Pipes buffer pH 6.9, x 2.5mM $MgCl_2$, 1mM EGTA, and 2.5% vol/vol Dimethylsulfoxide (DMSO) (Batten et al., 1980); (2) MS buffer minus DMSO; (3) MS buffer + 2mM EGTA: minus DMSO (4) Rhodnius

saline (NaCl 3.74, KCl 0.319, $CaCl_2 + 2H_2O$, 0.148, $MgCl_2 + 6H2O$, 0.863, $Na\ HCO_3$ 0.4284, $Na\ H_2PO_4 + 2H_2O$, 0.336 and glucose, 3.06; all grams/500 mls) (Maddrell, 1969); (5) calcium free saline (CF saline); (6) calcium + magnesium free saline (CMF saline); (7) CF saline + 2mM EGTA and (8) CMF saline + 2mM EGTA.

Desheathed ovarioles were transferred into a 35mm Petri dish containing the enzyme digestion solution at 20°C where they were left for times ranging from 10 minutes to 3 hours. Ovarioles were then washed at least 4 times in fresh saline or buffer to ensure complete removal of the enzyme. This was shown to be adequate since the results were identical to preliminary trypsin trials which included the use of trypsin soybean inhibitor (25mg/ml), (Sigma Chemical Co.) following enzyme exposure.

Ovarioles left in enzyme solution for times exceeding 30 minutes became very fragile, making handling of the ovarioles for the subsequent exposure to detergent extraction techniques very difficult. Furthermore, this change in ovariole integrity suggested the enzyme likely begins to act on the ovariole tissues as well as the basal lamina in the longer digestions. To circumvent this problem a modified method of basal lamina removal was developed. Trypsin III or protease VIII (pronase) digestion was carried out until the basal lamina separated from the ovariole (10 min.). Mechanical removal of the basal lamina was then carried out in fresh enzyme-free-medium by grabbing the separated terminal filament of each ovariole. The basal lamina is then removed by pulling the terminal filament with attached basal lamina through the meniscus of the saline, leaving the ovariole in the solution. Physical damage to the ovarioles does not occur and the exposure of the ovarian

cells to enzyme is minimized. This is not only vital for the ease of application of the detergent extraction methods but also reduces the possibility of cell structural alteration prior to extraction.

Assessment of the enzyme action on the ovarioles was made by in vitro light microscopical observation using phase contrast and differential interference contrast microscopy with a Zeiss photomicroscope II. Representative ovarioles from each experiment were also fixed in modified Karnovsky's and processed routinely for sectioning and examination with both light and TEM.

Scanning electron microscopy (SEM) of basal lamina removal

Groups of desheathed ovarioles digested in 1.0% trypsin III in CF saline + 2mM EGTA for 20, 30, 45 minutes and 1 hour, washed 4 times with fresh saline following digestion, were fixed in modified Karnovsky's fixative and further processed for SEM observation. The steps following dehydration included transfer into acetone, exchange of the acetone with liquid carbon dioxide (CO_2) in a Sorvall Critical Point Dryer, and routine critical point drying (Lutz and Huebner, 1980). Samples are then mounted on stubs with double sticky tape, gold coated in a Balzers sputter coater and viewed in a Cambridge Stereoscan Scanning Electron Microscope. Examination of specimens on the SEM was carried out with the assistance of its operator, Mr. Bert Luit.

Detergent extraction experiments

Various detergent extractions were performed on desheathed ovarioles with and without their basal lamina present in 35mm Petri dishes containing the detergent extraction solution. Following

detergent extraction the ovarioles were washed a minimum of 4 times by fresh buffer and then fixed using modified Karnovsky fixative for some of the preliminary extraction experiments and 3.0% glutaraldehyde in PHEM buffer + 1mM 6TP pH 6.9, for all the remaining detergent extraction experiments. Subsequent, tissue processing for light and transmission electron microscopical observation was carried out as already described.

Since the literature on the application of detergent extraction methods to intact tissues is limited, several experiments were performed, varying detergent concentration, extraction duration and buffer composition. Two initial experiments were conducted using ovarioles which had their basal laminae removed by 1 hour digestion with 1.0% trypsin III in CF saline + 2mM EGTA. Groups of ovarioles were detergent extracted with either Triton X-100 or Saponin (0.1% to 1.0%) in microtubule stabilization buffer (Batten et al., 1981). Following detergent extraction all ovarioles in these experiments were fixed with modified Karnovsky fixative.

Subsequent extraction experiments were as follows: (1) 0.5% vol/vol Triton X-100 in PHEM buffer for 10 minutes (2) 0.1% vol/vol Triton X-100 in PHEM buffer for 10 and 15 minutes (3) 0.3% wt/vol Saponin in PHEM buffer for 1 minute intervals up to 10 minutes (4) 0.5% vol/vol Triton X-100 in Pipes 60mM and Hepes 25mM buffer pH 6.9 + 8.5mM $MgCl_2$, 10mM EGTA, for 5 minutes (5) 0.5% vol/vol Triton X-100 in Pipes 60mM and Hepes 25mM buffer pH 6.9 + 8.5mM $MgCl_2$, 10mM EGTA + 1mM GTP + 30% glycerol for 5 minutes (6) 0.5% vol/vol Triton X-100 in PHEM buffer pH 6.9 + 1mM GTP + 20% glycerol for 10 minutes (7) 0.5% vol/vol Triton X-100 in PHEM buffer pH 6.9 + 1mM GTP + 10% glycerol for 10 minutes (8) 0.5% vol/vol Triton X-100 in PHEM pH 6.9 + 1mM GTP for 10 minutes.

All ovarioles used in these extractions had their basal laminae removed by the brief trypsinization, mechanical removal method. Following detergent extraction, they were fixed with 3.0% glutaraldehyde in PHEM buffer pH 6.9 + 1mM GTP.

The final detergent extraction experiment was applied to ovarioles with the basal lamina intact. Ovarioles were desheathed and then detergent extracted in 0.5% vol/vol Triton X-100 in PHEM buffer pH 6.9 + 1mM GTP for 2,5, 10 and 15 minutes. For these ovarioles, 3.0% glutaraldehyde in PHEM buffer pH 6.9 + 1mM GTP was used for the fixation.

Immunofluorescence methods

An extensive literature has demonstrated that immunocytochemical techniques provide a powerful tool to visualize the presence and organization of cytoskeletal elements. In this study, indirect immunofluorescence methods were employed to localize the distribution of tubulin and actin within the follicle cell epithelium. The application of these methods to whole ovarioles, and intact follicle cell sheets involved the development of specific methods of tissue handling, and tissue preparation to obtain the most optimal resolution of the fluorescence pattern within the follicle cell epithelium.

Fixation methods required special consideration since the preservation of the antigenicity of the cytoskeletal proteins, occurs often at the expense of ideal ultrastructural preservation. An additional problem is nonspecific background fluorescence resultant from the use of some fixation agents and embedding media.

The primary (1°) antibodies used were: (1) rabbit anti-tubulin against chicken embryo brain tubulin (Miles Laboratories), (2) rabbit anti-actin against chicken back muscle actin (Miles Laboratories), and (3) rabbit anti-tubulin against sea urchin tubulin (kindly supplied by Dr. Keigi Fujiwara, Dept. of Anatomy, Harvard Medical School). The secondary (2°) antibody for all experiments was fluorescein conjugated goat anti-rabbit IgG (Miles Laboratories).

Initial experiments attempted to apply these methods to intact follicle cell sheets. The follicle cell sheets were prepared as follows: follicle cell cylinders were first formed by flushing out the ooplasm of isolated follicles with a micropipette. The ends of this cylinder were then cut with either a microscalpel or fine iris scissors. The cylinder is then cut up one of its lateral surfaces to form a flattened sheet of follicle epithelium. Results from these experiments showed the follicle cells were too thick to observe any fine resolution of the fluorescence pattern within the cells. Attempts to flatten these cells to improve the resolution involved squashing the follicle cell sheets in between two coverslips, prior to fixation.

Several different fixations were applied to the follicle cell sheets. The following fixations were used: (1) 3.7% vol/vol formalin for 20 minutes followed by postfixation in -20°C methanol for 5 minutes and -20°C acetone for 2 minutes (Weber et al., 1975), (2) 3.7% vol/vol formalin for 20 minutes, followed by exposure to 0.2% vol/vol Triton X-100 in Pipes 60mM and Hepes 25mM buffer pH 6.9 + 8.5mM $MgCl_2$, 10mM EGTA for 4 minutes, (3) 1 hour trypsin III digestion, 1.0% wt/vol in CMF saline, then fixation in 3.7% vol/vol formalin for 15 minutes followed by exposure to 0.2% vol/vol Triton X-100 in Pipes 60mM and Hepes 25mM

buffer pH 6.9 + 8.5mM $MgCl_2$, 10mM EGTA for 4 minutes, (4) 1 hour 1.0% wt/vol trypsin III digestion in CMF saline then fixation in 3.7% vol/vol formalin 15 minutes followed by postfixation in -20°C methanol, 5 minutes and -20°C acetone 2 minutes and (5) 90% methanol, -20°C + 50mM EGTA pH 6.0 for 15 minutes (Harris et al., 1980). None of these fixations resulted in optimal resolution of the fluorescence within the follicle cells.

In order to obtain better resolution of the fluorescence, these methods were subsequently adapted to paraffin and plastic embedded tissue sections. Fixations for paraffin embedded desheathed ovarioles were as follows: (1) Bouins, 14 hours, (2) 10% buffered formalin in 0.1M sodium phosphate buffer, 14 hours, (3) modified Karnovsky's, 1 hour, (4) 3.0% wt/vol paraformaldehyde + 0.5% vol/vol glutaraldehyde in PHEM buffer + 1mM GTP, 1 hour and (5) 1.0% wt/vol paraformaldehyde in PHEM buffer + 1mM GTP for 20, 40 minutes and 1 hour. Following fixation, ovarioles were dehydrated, and routinely processed for paraffin embedding in Tissue Prep 56.5°C, [R], (Humason, 1979).

To evaluate plastic embedding as an alternative to paraffin embedding, desheathed ovarioles were also fixed in: (1) Bouins, 8 hours; (2) 3.0% wt/vol paraformaldehyde, + 0.5% vol/vol glutaraldehyde in PHEM buffer pH 6.9 + 1mM GTP, 1 hour, (3) 3.0% wt/vol paraformaldehyde in PHEM buffer pH 6.9 + 1mM GTP, 1 hour, (4) 4.0% wt/vol paraformaldehyde, 0.1% vol/vol glutaraldehyde in PHEM buffer pH 6.9 + 1mM GTP, 1 hour, (Tomasek et al., 1982) and (5) 1.0% wt/vol paraformaldehyde in PHEM buffer pH 6.9 + 1mM GTP for 20, 40 minutes, and 1 hour times. These ovarioles were processed for embedding in Epon-Araldite (Anderson and Ellis, 1965) as described.

[R] Fisher Scientific

To investigate the influence of plastic embedding media constituents on the amount of background nonspecific fluorescence, desheathed ovarioles were fixed in 1.0% wt/vol paraformaldehyde in PHEM buffer pH 6.9 + 1mM GTP for 1 hour. They were then processed for embedding in one of the 5 different plastic embedding media: (1) JB-4 methacrylate, (2) Epon-Araldite (Anderson and Ellis, 1965), (3) Taab Transmit light microscopy resin, (4) Araldite (Luft, 1961) and (5) Araldite (Coulter, 1967).

Procedures for processing ovarioles for fixations to plastic embedding were as noted previously except for JB-4 methacrylate and Taab Transmit resin. For JB-4 methacrylate embedding, ovarioles are dehydrated to 95% ethanol, infiltrated in the infiltration mixture overnight, then are placed in the embedding mixture and polymerized at room temperature. For Transmit resin embedding, ovarioles were dehydrated to 100% ethanol, then transferred through two 15 minute changes of acetone and infiltrated in mixtures of acetone and the resin infiltration solution (1:1 for 1 hour, then 1:3 for 3 hours). The ovarioles were then embedded in a fresh resin embedding mixture and polymerized at 60°C for 24 hours.

Paraffin sections (5-10 μ M) were cut using a Jung rotary microtome. The sections are deparaffinized in toluene, hydrated with a descending ethanol series and then placed in phosphate buffered saline (PBS), Dulbeccos (8 gm . NaCl, 0.2 gm . KCL 0.2 gm. KH_2PO_4, 1.15 gm. Na_2HPO_4 and 0.1 gm . $MgCl_2$/l). Plastic sections (1-2 μ M) were cut on glass knives using a Sorvall Porter Blum MT2B ultramicrotome, and were mounted on glass slides as described. Plastic was removed from the tissue sections by placing the slides in a coplin jar of saturated NaOH in

absolute ethanol for up to 30 minutes dependent upon the particular plastic (Lane and Europa, 1965; Maxwell, 1978 and Bussolati et al., 1980). The slides were then placed in 100% ethanol and hydrated in a descending alcohol series to PBS.

The procedures for all the immunofluorescent experiments were as follows. The slides are supported on two clean glass microscope slides in a 100mm Petri dish, containing a piece of moist filter paper to provide a high humidity. The Petri dishes are then placed in an incubator at 37°C. For the initial 1 hour incubation the sections are flooded in a large pool of 1.0% wt/vol solution of bovine serum albumin (BSA) type V, (Sigma Chemical Co.) in PBS. The incubation is followed by a quick rinse in PBS. The slides are then placed back in the Petri dishes and similarily incubated for another hour in the 1° antibody. A 1:10 dilution of the Miles anti-tubulin or anti-actin in PBS containing 1.0% wt/vol BSA type V was used. Dilution of Dr. Fujiwara's anti-tubulin was 1:50 antibody to BSA-PBS solution. Following this incubation the slides are washed at least 4 times with fresh PBS for 15 minutes. They are then incubated for a third hour in the 2° antibody, the Miles fluorescein conjugated goat anti-rabbit IgG, diluted 1:16 with BSA-PBS solution. Following this incubation the slides are washed in PBS again as above. After mounting the slides in 50% glycerol in PBS, they were examined with a Zeiss photomicroscope II equipped for epi and transmitted fluorescence microscopy.

Fluorescence controls for each experiment included the following. (1) paraffin or plastic removed from the section to measure auto-fluorescence, (2) Paraffin or plastic removed, incubated in PBS only (3) Paraffin or plastic removed and incubated in 1.0% wt/vol BSA in

PBS, (4) Paraffin or plastic removed, incubated in 1.0% wt/vol BSA in PBS, followed by incubation in 1:16 dilution of 2° antibody in BSA-PBS solution, (5) Comparison of the fluorescence patterns of anti-tubulin and anti-actin binding and (6) check of the tubulin labelling in the microtubule rich trophic core and trophic cords, an *in situ* positive control.

Photomicrography methods

Routine light micrographs and scanning electron micrographs were taken with Kodak Panatomic-X 135 film. This film was developed in either Kodak Microdol-X (1:3 dilution) or Acufine (Acufine Inc.) according to manufacturer's specifications. Transmission electron micrographs were taken on Kodak Electron microscopic film 4489, and were developed in Kodak D-19 (1:2 dilution). Fluorescence light micrographs were taken on Kodak Tri-X Pan 135 film at ISO 1000. This film was developed in Acufine developer (Acufine Inc.). Prints of micrographs were made on Ilford stabilization papers, using a Beseler enlarger. Stabilized prints were fixed, washed, dried and glossed.

Results

General Overview of Follicle Cell Development

The following summary of the follicle cell developmental ultrastructural changes during an oogenesis cycle provides an introductory framework for the sections that follow. For a more detailed background see Lutz and Huebner, 1980; Huebner and Injeyan, 1981 and Huebner, 1984b.

Follicle cell development is initiated from prefollicular tissue located at the base of the tropharium (Figs. 1, 2). This tissue is composed of small spindle shaped prefollicular cells containing a single nucleus surrounded by sparce amounts of cytoplasm (Fig. 2). Through their association with small oocytes these cells produce early previtellogenic follicles (Figs. 1, 3). The prefollicular cells proliferate by mitoses until the required follicle cell number is reached. After proliferation, a final mitotic division without cytokinesis occurs forming a tightly packed columnar epithelium of binucleate follicle cells (Fig. 3). During previtellogenesis the oocyte undergoes rapid growth by receiving cytoplasmic components from the nurse cell syncytium via the trophic cords (Fig. 1). Although the amount of cytoplasm in the follicle cells increases during previtellogenesis, the tightly packed cells maintain their columnar shape (Fig. 3).

The subsequent, major phase of oogenesis is vitellogenesis, involving the incorporation and storage of yolk proteins and patency of the lateral follicle cells. Only the lateral follicle cells change

their shape from the tall columnar previtellogenic condition to the irregularly shaped patent condition (Figs. 1, 4, 5, 6). The lateral follicle cells maintain contacts with one another through lateral arms (Figs. 1, 6). Apical and basal follicle cells of the same vitellogenic follicle do not undergo any shape change (Figs. 1, 5). They remain tall and columnar without extracellular spaces forming between them.

Following vitellogenesis the lateral follicle cells greatly increase their cytoplasmic volume, become tightly packed, and accumulate organelles in preparation for chorion formation, the final phase of oogenesis (Fig. 7).

With this brief overview in mind the findings of this study can be presented. The results relating to the development and modification of the techniques required to visualize the follicle cell cytoskeleton are presented first. This is followed, by descriptions of the cytoskeletal arrangements, and changes in the organization of the cytoskeletal components in the follicle cells during oogenesis.

Methodology of Cytoskeletal Visualization and Isolation

Fixations and buffer composition

The various combinations of fixation agents and buffers were conducted not only to achieve optimal preservation of cytoskeletal elements in the normal fixations, but also to insure the maintainence and preservation of these elements upon application of detergent extraction methods.

Fixation

For normal fixation of desheathed ovarioles, very little difference was noted with the use of either modified Karnovsky's or the 3.0%

glutaraldehyde fixation (Figs. 8, 9, 11, 12). The modified Karnovsky's fixation resulted in slightly better overall fixation in terms of preservation of membrane structures and organelles such as mitochondria (Fig. 9). The glutaraldehyde fixations did however preserve microtubules *in situ* and no obvious differences between numbers of microtubules or their orientation within the follicle cells was evident between either fixation (Figs. 9, 12). The concentration of glutaraldehyde used, affected the ovariole ultrastructure. Both 5.0% glutaraldehyde (Luftig *et al.*, 1977) and 4.0% glutaraldehyde caused shrinkage of the oocytes and the nurse cell lobes resulting in the formation of spaces between these lobes (Fig. 10). Small shrinkage localized to the inner sheath cells is sometimes observed with 3.0% glutaraldehyde (Fig. 11). The modified Karnovsky's did not create any shrinkage of ovariole components (Fig. 8).

Tannic Acid (TA) and Saponin

The addition of TA (0.5% wt/vol or 0.1% wt/vol) to the prefixation medium was largely unsuccessful since the TA did not readily enter the cells if added to the fixative alone (Fig. 15). In this case, only the cell membrane and a few areas of microfilaments running just under the cell membrane become very darkly stained (Figs. 14, 15). With the addition of either 0.05% wt/vol or 0.10% wt/vol Saponin to the prefixation medium the TA penetrates into the cells (Fig. 16). The TA still darkly demarks the cell boundaries and in some cases produces a flocculant accumulation in the extracellular spaces between vitellogenic lateral follicle cells (Figs. 13, 16). Very little difference was observed between the addition of 0.05% wt/vol or 0.10% wt/vol, Saponin

as TA entered the cells at either concentration. The TA does not specifically bind only to cytoskeletal elements, but also to all intracellular membranes, such as mitochondria, nuclear membranes, rough endoplasmic reticulum (RER) and ribosomes (Figs. 14, 16).

Microtubules and in particular microfilaments are made more visible in thin sections compared to sections of tissue in which TA and Saponin was omitted from the prefixation (Figs. 15, 16). Overall, the addition of 0.5% TA and 0.05% Saponin to the 3.0% glutaraldehyde in PHEM buffer pH 6.9 + 1mM GTP fixative resulted in the best preservation and easiest visualization of the cytoskeletal elements within the follicle cell epithelium.

Buffer composition

The buffer constituents can greatly influence the retention of cytoskeletal elements, particularly when detergent extraction techniques are applied to tissues prior to fixation. Buffers can also affect the overall ovariole ultrastructural preservation.

For normal fixations the 0.1 m sodium cacodylate buffer resulted in good preservation of ovariole ultrastructure and excellent fixation of cytoskeletal elements (Figs. 9, 29). This buffer, however lacks the constituents required for the maintainence of cytoskeletal elements, during the highly permeable conditions associated with detergent extraction.

The remaining buffers are variations of cytoskeletal stabilization buffers containing the necessary constituents for the maintenance of cytoskeletal elements, within detergent extracted tissues. All of them did not maintain the normal ovariole ultrastructure. The 100mM Pipes pH

6.9 buffer caused a rapid (within 10 min) shrinkage of all oocytes and nurse cells (Fig. 31). The attempt to compensate for this shrinkage by reducing the buffer concentration to 75mM resulted in even greater shrinkage of the nurse cell lobes (Fig. 32). The addition of 8.5mM $MgCl_2$ (concentration in Rhodnius saline) to 100mM Pipes pH6.9 buffer reduced, but did not completely prevent the shrinkage. The use of PHEM buffer eliminated this shrinkage problem (Fig. 11). Normal ovariole morphology is maintained for several hours when 60mM Pipes with 25 mM Hepes is used. This buffer does not require 8.5mM $MgCl_2$ to maintain the normal ovariole morphology so the $MgCl_2$ concentration was reduced to 2mM $MgCl_2$ (Schliwa and Von Blerkom, 1981). The final component is the addition of 1mM GTP to the buffer. This is important for the maintainence of polymerized microtubules (Weisenberg, 1972) and was therefore included in the PHEM buffer for subsequent detergent extractions and fixations.

Detergent extractions

Preliminary experiments

These initial experiments were conducted on desheathed ovarioles with an intact basal lamina. Although the optimal fixation (3.0% glutaraldehyde in PHEM buffer pH 6.9 + 1mM GTP) and extraction buffer (PHEM buffer pH 6.9 + 1mM GTP) were not used in these experiments, several important results related to the changes in ovarian ultrastructure, and the maintainence of cytoskeletal elements within the follicle cells, exposed to detergent extraction conditions were obtained.

Ovarioles, exposed to detergent extraction buffer solutions become opalaent. Within a few minutes of exposure the basal lamina separates from the entire ovariole surface, expanding outward (Figs. 17, 18, 19, 20, 67, 68).

Comparison of Triton X-100 concentrations (0.125%, 0.25%, 0.50% and 1.0%) showed that detergent concentration is not as important as extraction time since extracted cells were obtained using all 4 concentrations (Figs. 23, 24). The Triton X-100 solubilizes the cell membranes very quickly (within the first minute) but does not solubilize the entire cell membrane as pieces of membrane can be observed even after 15 minutes extraction (Fig. 24). Following cell membrane solubilization the cytoplasmic constituents, including mitochondria, Golgi, and RER are rapidly extracted and lose their normal appearance (Figs. 24, 25, 69, 71). Microtubules, oriented in small groups located just within the cell boundary, along the lateral edges of the follicle cells, were observed after the detergent extraction (Figs. 26, 27, 28). Nuclei and nuclear envelopes are resistant to Triton X-100 extraction, retaining a normal appearance for up to 15 min. exposure time (Fig. 24). By 15 minutes the follicle cells and nurse cell lobes are highly extracted, retaining only a cell outline surrounding an almost completely empty cytoplasm containing the nuclei (Figs. 17, 18, 23, 24).

Two major problems of adapting these detergent extraction methods to intact desheated ovarioles, were indicated by these preliminary experiments. One problem involved the retention of extracted cytoplasmic components by the expanded basal lamina (Figs. 18, 20, 22, 67). This retention of the extracted material in a zone around the ovariole, reduced the visibility of non-extracted elements within the

cells, thus obscuring the advantage of detergent extraction, in increasing the visualization of the cytoskeletal elements. The second problem is that cytoskeletal elements including both microtubules and microfilaments were often observed within the basal lamina trapped extracted material (Fig. 21).

To overcome these problems, methods were developed to enzymatically digest and remove the basal lamina. Also glycerol was added to the extraction buffer in an attempt to prevent the movement of microtubules out of the follicle cells during detergent extraction.

Basal lamina removal methods

1. Enzymatic digestion of the basal lamina

Elastase types I and III at all concentrations did not result in the digestion and removal of the basal lamina even after 3 hours (Figs. 34, 35). The basal lamina did however separate from the ovariole upon exposure to elastase (Fig. 34). This was most evident over the apical tip of the tropharium where it separated as a double layer (Fig. 34) (See Huebner, 1984b).

Collagenase V had no affect on the basal lamina structure, as the basal lamina remained intact and tightly adherent to the ovariole throughout incubation in this enzyme solution.

Trypsin types III and IX consistently removed the basal lamina from all regions of the ovariole (Fig. 39). Within 10 minutes digestion the entire basal lamina separates from the ovariole as a single layer and expands outward (Fig. 36). This separation first occurs in the region between the base of the tropharium and the previtellogenic follicle, and

then proceeds anteriorly towards the tropharium tip (Figs. 36, 61). Separation of the basal lamina over the larger vitellogenic follicles occurs later in the digestion. Complete basal lamina digestion occurs first over the large vitellogenic follicles and last over the apical end of the tropharium. These areas correspond to the thinnest and thickest areas of the ovarian basal lamina respectively. All concentrations of the trypsin from 0.5% to 1.0% digested the basal lamina. A 1.0% trypsin solution completely digested the basal lamina after one hour (Fig. 39). Trypsin type III was more consistent than type IX in its action, thus it was used in favor over type IX for most of the digestions.

Trypsin digestion was ineffective in Rhodnius saline as ovarioles exposed for 1 hour or longer still retained an intact closely adherent basal lamina. Trypsin digestion was most effective in the 100mM Pipes pH 6.9 buffer (MS buffer) but was also very effective in salines lacking calcium. Since ovariole morphology was maintained better in these salines than the MS buffer, trypsin digestions were done in calcium free salines (Figs. 30, 31, 32). The basal lamina separates from the ovariole faster and is much easier to remove if 2mM EGTA is present in the saline. Overall trypsin type III (1.0%) in CF saline + 2mM EGTA for 1 hour was judged the most effective method for routine total digestion of the basal lamina.

Protease VIII (pronase) also consistently digested the basal lamina within 1 hour. Protease had the added advantage of being the only enzyme tested that worked in Rhodnius saline. However, since protease is a very general proteolytic enzyme the risk of enzymatic damage to the ovariole structure was greater with protease use than trypsin.

2. Ovariole ultrastructure upon basal lamina removal

Prior to removal the basal lamina forms an investing blanket over the ovariole surface (Fig. 33). Fig. 37a,b,c,d displays a series of SEM micrographs illustrating the basal lamina structure at various trypsin digestion times (15,20,30, and 45 minutes). The entire basal lamina is not digested evenly, instead the trypsin selectively digests holes through the basal lamina (Fig. 37A). The holes progressively enlarge and by 1 hour digestion time no trace of the basal lamina is left (Figs. 37, b,c,d, 39).

Following basal lamina removal the ovariole maintains its normal shape (Fig. 39). The inner sheath cells covering the nurse cell lobes of the tropharium, round up, and display long tenuous connecting arms which join with arms from adjacent cells (Figs. 38, 40, 62) (see also Huebner, 1984b). The nurse cell lobes often alter their shape as well by forming long pointed projections (Figs. 38, 40).

Prefollicular cells and previtellogenic follicle cells round up and also extend a number of thin projections and blebs from their surface (Figs. 41,44,45). TEM micrographs show that the rounded previtellogenic follicle cells still contain numerous microtubules and also a normal complement of cell organelles (Figs. 46, 47). The projections eminating predominantly from the prefollicular cells contain microfilaments, but the larger cytoplasm filled blebs associated with the previtellogenic follicle cells do not contain any obvious concentrations of microfilaments. Vitellogenic follicle cells maintain their shape and normal ultrastructure (Figs. 42, 66). The extracellular spaces, characteristic of patency, remain along with the lateral cell to cell connections (Figs. 42, 43).

The principle problem with using the 1 hour trypsin basal lamina digestion is that the trypsin can act directly on the ovarian cells over a considerable time since holes are digested through the basal lamina within 15 minutes (Fig. 37A). The ovarioles become very fragile during the digestion, making subsequent handling during the detergent extraction techniques very difficult. A more serious concern is that the trypsin may alter the cell structure causing a change in the cytoskeletal structure and/or arrangement.

Polarizing micrographs of the same ovariole after 30, 45, and 60 minutes of trypsin digestion display a progressive decrease in birefringence of the microtubule rich trophic core and trophic cords (Figs. 57, 58, 59). Over the normal 1 hour trypsin digestion the birefringence decreases significantly and by 2 hours can disappear all together.

These observations could in part be due to the CF saline + 2mM EGTA, but the disappearance of birefringence in this saline alone normally takes place only after a considerably longer period (several hours). These results suggest that prolonged exposures to the enzyme solutions should be avoided and thus led to the development of the faster mechanical basal lamina removal method.

3. Enzymatic and mechanical basal lamina removal

Separation of the basal lamina from the tropharial tip occurs after only 10 minutes exposure to digestion solutions (Fig. 61). Removal is easily accomplished by grabbing the separated basal lamina (Fig. 60).

This method of basal lamina removal results in the maintainance of a more normal ovariole ultrastructure. Nurse cell lobes remain closely associated together, with the rounded-up inner sheath cells positioned in close contact with the nurse cells (Fig. 62). The small oocytes and prefollicular tissue also maintain a more normal morphology (Figs. 63, 64). The prefollicular cells still round up and produce some surface blebs, but generally they retain much closer contacts with one another than following the 1 hour trypsin digestion (Figs. 64, 65). The vitellogenic follicle cells remain in close contact with the oocyte surface and no unusual ultrastructural changes appear in these cells (Fig. 66).

The ovarioles are much less fragile following basal lamina removal by this method and the application of detergent extraction procedures are more easily extended to these ovarioles. This method of basal lamina removal is far superior to the previous method and is an efficient means of removing the ovarian basal lamina.

Detergent extraction after basal lamina removal

Although the initial extraction experiments involved the 1 hour trypsin digestion they did reveal differences between the effectiveness of Triton X-100 and Saponin extraction of the ovarioles. Saponin achieved the same degree of cell extraction at much lower concentrations (0.1% for 10 mins) than Triton X-100. Triton X-100 (up to 0.5% for 10 mins) still leaves a considerable amount of cytoplasmic material within the cells (Fig. 71). The absence of the basal lamina does result in an unrestricted extraction of the cytoplasmic components (Figs. 48, 49, 50, 51, 52, 53). But the problem of microtubules being displaced out of the

cells along with the extracted cytoplasmic constituents persisted. In extreme extractions very few microtubules were observed within the extracted follicle cells (Fig. 53).

The ovarioles were observed to withstand the rigors of the detergent extraction procedures better, when the shorter exposure to trypsin digestion followed by mechanical basal lamina removal method was used. As with intact ovarioles Triton X-100 concentrations from 0.1% to 0.5% were all effective. Extractions for 10-15 minutes using 0.5% Triton X-100 is sufficient for complete extraction of follicle cell contents excluding the nuclei, while a slightly longer period is necessary for 0.1% Triton X-100 concentrations. The Saponin, as in earlier experiments achieved the same degree of extraction at lower concentrations. Concentrations of 0.1% to 0.3% Saponin for 10 minutes were sufficient for complete follicle cell extraction. Since control over cell extraction was more difficult with Saponin due to the short time and concentration required, Triton X-100 was preferred.

As in initial experiments relatively few microtubules remained within the follicle cells after extraction of cell contents. A few longitudinally oriented microtubules remain along the lateral edges of previtellogenic follicle cells in close proximity to remnants of cell membrane (Fig. 52).

Attempts to curb the displacement or extraction of polymerized microtubules were made by adding glycerol at various concentrations (30%, 20% and 10%) to the extraction medium (Figs. 54, 55, 56). This, however, did not improve the results. Drastic shrinkage occurred in all components of the ovariole, including the follicle cells, particularly with the use of 30% glycerol (Figs. 54, 55). But even 10% glycerol

addition caused severe shrinkage of the nurse cell lobes and follicle cells (Fig. 56).

Detergent extraction with basal lamina intact

Since the above experiments illustrated that removal of the basal lamina resulted in the unavoidable loss of polymerized microtubules from the follicle cells, detergent extraction with the basal lamina intact was re-evaluated and modified despite the problems noted earlier. The retention of the extracted material between the basal lamina and the ovarian cells permits better control over the progression of the extraction and also allowed the detection of the displaced polymerized microtubules. These points, reduced the initial disadvantage of leaving the basal lamina intact during detergent extraction.

The effect of time on the progression of cell extraction was clearly observed in this experiment (Figs. 67, 68, 69, 71, 72). The basal ends of the follicle cells become completely extracted before the detergent solution even begins to extract the apical ends (Figs. 67, 71). The retention of extracted material beneath the basal lamina is also clearly evident (Fig. 67). Within 2 minutes, the extraction has penetrated to the depth of the first nucleus while the cell membranes are still predominantly intact (Figs. 67, 69). The cells contain large amounts of cytoplasm and cell organelles such as mitochondria still often appear normal (Figs. 67, 69). By 5 minutes the cell membrane contains many breaks and the extraction has disrupted all membraneous organelles except for the nuclei (Fig. 71). The basal end of these cells is still more extracted than the apical ends (Fig. 71). After extraction for 15 minutes, very little cytoplasm is left within the cell

no organelles retain their usual morphology and only small traces of cell membrane remain (Figs. 68, 72).

Numerous microtubules are observed within these cells (Figs. 73, 74, 75, 76). The numbers seen depend on the length of time of extraction and on the position of the microtubules within the cells. The microtubules do not form an interconnecting network within the follicle cells (Fig. 74). Instead they are distributed individually (Figs. 73, 74). The detergent extractions have suggested that the microtubular cytoskeleton in the follicle cell epithelium is composed of independent, non-interacting groups of individual microtubules. This pattern of microtubule organization makes the preparation of an isolated follicle cell cytoskeleton by the application of detergent extraction techniques very difficult as this organization results in the loss of microtubules from the fully extracted follicle cell preparations. Microtubules are very evident in the follicle cells after only 2 minutes, and even 5 minutes extraction (Figs. 73, 74). But by 10 minutes extraction time or longer only a few microtubules remain within the cells, (Figs. 75, 76).

Since, microtubules remain polymerized in the trapped extracted material this indicates that the buffer conditions are suitable for the maintainence of polymerized microtubules and their loss from the cells is not likely due to depolymerization. Microtubules remaining in follicle cells after 15 minutes extraction are usually localized just under the remaining remnants of the lateral cell membrane, near the nuclei (Figs. 75, 76). The presence of the cell membrane and nearby nucleus likely reduce the potential for displacement of the microtubules from the cell.

Immunofluorescence Procedures

Intact follicle cell sheets

Application of anti-tubulin and anti-actin immunofluorescence methods to isolated follicle cell sheets or nurse cell lobes resulted in a diffuse pattern of fluorescence, within the cell (Figs. 77, 78). The various fixation and cell permeabilization methods did not affect the pattern of fluorescence observed. The follicle cell sheets withstood the acetone-methanol method of cell permeabilization better than exposure to the brief Triton X-100 extractions. Attempts to increase the resolution of the fluorescence pattern by fixing the squashed follicle sheets between two coverslips also did not increase the resolution of the observed fluorescence.

Sectioned material

Several factors influence the resolution of the fluorescence pattern observed in follicle cell sections. These are: (1) fixation (2) embedding media and (3) section thickness. Also, in order to distinguish the specificity of fluorescence the results must be compared to various control preparations. Controls reveal the pattern and amount of nonspecific background autofluorescence the various preparative methods impart to the tissue sections.

1. Fixation: Paraffin embedding

The best combination of tissue preservation and detail of fluorescence pattern observed in paraffin embedded tissue was with the 3.0% paraformaldehyde and 0.5% glutaraldehyde fixation (Fig. 80). With this fixation, dense bands of fluorescence along the lateral edges of

the apical vitellogenic follicle cells become apparent (Fig. 80). Thinner lines of fluorescence are revealed at the apical ends of these cells (Fig. 80). These thin lines are not observed with Bouins fixation or 1.0% paraformaldehyde fixation (Figs. 79, 82). Tissue shrinkage is often associated with the 1.0% paraformaldehyde (Fig. 96) fixation. Although the modified Karnovsky's fixation provides excellent tissue preservation, it imparted a bright background autofluorescence which overwhelmed any specific fluorescence. Fixations with 4.0% paraformaldehyde and 0.1% glutaraldehyde and the 3.0% paraformaldehyde fixative were not as optimal as the 3.0% paraformaldehyde + 0.5% glutaraldehyde fixative.

2. Fixation: Plastic embedding

The use of plastic embedding media greatly increases the background nonspecific fluorescence (Figs. 93, 94). The combination of their use with glutaraldehyde fixation (concentrations as low as 0.1% glutaraldehyde) further increases the background nonspecific fluorescence. For plastic embedding, the 1.0% paraformaldehyde fixative gave the best results (Fig. 83). It imparted the least amount of background non-specific fluorescence to plastic embedded tissue, despite its less than optimal general fixation and induced tissue shrinkage (Figs. 93, 96).

The specific fluorescence pattern observed using this fixation correlated well with the pattern seen with the other fixations and with observations on paraffin embedded tissue sections (Figs. 80, 83). The tissue shrinkage created by this fixation was predominantely localized to the small oocytes at the base of the tropharium and the nurse cell

lobes (Fig. 96). The follicle cells always maintained a normal morphology following this fixation (Fig. 83).

3. Plastic embedding media

The amount of background nonspecific fluorescence observed varied with the type of plastic embedding media used. The affect of the plastic embedding medium on the background fluorescence persisted even upon removal of the medium from the sections by exposure to the saturated NaOH in absolute alcohol solution (Figs. 93, 94). The ease of tissue sectioning also varied between the plastics.

The Epon-Araldite mixture (Anderson and Ellis, 1965) provided the best combination of low background fluorescence, consistent removal in the NaOH solution and ease at sectioning. The Taab transmit and JB-4 methacrylate plastics both caused the brightest background fluorescence observed. The Araldite embedding media gave a low background but required a longer exposure to the NaOH for plastic removal and also were not as easy to section as the other plastics.

4. Section thickness

Section thickness greatly affected the fluorescence resolution obtained. Comparison of 10 μM paraffin sections with 5 μM thick sections reveals a brighter fluorescence in the 10 M sections but also less detail in the fluorescence pattern (Figs. 80, 81). The best fluorescence resolution was with the 1 μM plastic sections (Fig. 83). Discrete thin strands of fluorescence discernable in follicle cell plastics sections are not detectable in similiar preparations using thicker paraffin sections (Figs. 80, 81, 83).

5. Controls

For paraffin sections once the embedding medium is removed, the background is very low (Figs. 84, 85, 87, 88, 90). Incubation of the sections in the BSA-PBS solution reduces the nonspecific fluorescence that can arise from exposure to the 2° fluorescein conjugated goat-anti rabbit IgG (Figs. 85, 86, 88, 89). The addition of 0.5% glutaraldehyde increases the background slightly in all the controls compared to Bouins fixative (Figs. 85, 88). The controls illustrate that nonspecific background fluorescence was not a major problem with paraffin embedded tissue.

It is important to note that although the background is brighter in plastic sections, no specific fluorescence pattern occurs (Figs. 93, 94). The BSA-PBS incubation greatly reduced the intensity of the background in plastic sections also (Fig. 92).

The presence of the microtubule rich trophic core and cords provided a useful <u>in situ</u> control to verify the anti-tubulin binding (Figs. 95, 96, 98). Specific labelling as indicated by a very bright fluorescence occurred in both paraffin and plastic embedded tissue sections (Figs. 95, 96, 98).

An additional control for the specificity of anti-tubulin binding is the variation in fluorescence pattern observed when anti-actin binding is assessed (Figs. 99, 100, 101, 102). With anti-actin binding no fluorescence occurs in the trophic core or in particular the trophic cords (Fig. 97). The pattern of fluorescence in the follicle cells (all stages) is also quite different from that of anti-tubulin binding (Figs. 99, 100, 101, 102). Instead of the long continuous strands of fluorescence observed with anti-tubulin binding, anti-actin binding is

localized as small discrete patches within the follicle cells (Figs. 100, 101).

6. Comparison of anti-tubulin antibodies

Both the Miles Laboratories anti-tubulin and Fujiwara's anti-tubulin displayed identical patterns of fluorescence within the follicle cells. Fujiwara's anti-tubulin gave more consistent results, required less antibody per experimental run and remained reactive while stored for many months at 4°C. The Miles laboratories anti-tubulin was not as consistent from run to run as it did not seem to maintain its antigenicity during storage periods as long as Fujiwara's antibody.

Characterization and Organizational Dynamics of the Follicle Cell Cytoskeleton During Oogenesis

Prefollicular cells

Immunofluorescent localization of tubulin in prefollicular cells reveals a bright band of fluorescence along the lateral cell edges under the cell membrane and a second brighter band parallel to the basal lamina (Fig. 103). The second band only exists at the basal end of those prefollicular cells resting on the basal lamina (Fig. 103).

The TEM results confirm the microtubular orientation suggested by the immunofluorescence results. Prefollicular cells contain relatively small numbers of microtubules compared to previtellogenic and vitellogenic (lateral and apical) follicle cells (Figs. 104, 109, 121, 132). Microtubules are oriented longitudinally near the lateral cell membrane (Fig. 105). Cross sections of microtubules are not seen in these lateral cell regions in longitudinal planes of section (Fig. 105).

The bright band of fluorescence parallel to the basal lamina, in the basal ends of prefollicular cells is due to groups of microtubules oriented at right angles to the lateral microtubules (Figs. 106, 107). These are the only microtubules observed in cross section profiles in longitudinal sections of prefollicular cells.

Dense regions of microfilaments, which normally exclude ribosomes and other cell organelles were not commonly found within the prefollicular cells, except at the basal ends of those cells in contact with the basal lamina in the same position as the cross sectioned groups of microtubules (Figs. 106, 107).

Previtellogenic cells

The fluorescence pattern of late previtellogenic follicle cells displays a very bright and regular distribution of fluorescence restricted to the lateral edges of these cells (Fig. 108). Very little fluorescence is observed elsewhere in the cytoplasm including the area near the basal lamina (Fig. 108).

Grazing, longitudinal sections, just under the cell membrane and cross-sections of late previtellogenic follicle cells, reveal abundant bands of longitudinally oriented microtubules (Figs. 109, 113). This dense distribution of microtubules was never observed in prefollicular cells. Early previtellogenic follicle cells show a similiar pattern but have fewer microtubules than in late previtellogenic follicle cells. Longitudinal sections deeper into the cells including the nucleus in the plane of section also show numerous microtubules longitudinally oriented along the lateral edges of the cell, just beneath the cell membrane (Figs. 110, 111, 112).

The longitudinally oriented microtubules are very long and do not associate or connect with one another, but are arranged parallel to one another (Fig. 111). In detergent extraction preparations this identical orientation and distribution of microtubules along the cell lateral edges is also observed (Fig. 112).

These observations suggest that the longitudinally arranged microtubules encircle the cell circumference in the form of a cylinder running just under the cell membrane. It is important to note that very few microtubules are not longitudinally oriented in the previtellogenic follicle cells. The microtubules are most concentrated in the cell area occupied by the two nuclei. Cross sections of previtellogenic cells above or below the nuclei contain smaller numbers of microtubules than cross sections of the middle regions of these cells (Figs. 113, 115, 116).

Dense microfilament accumulations are not commonly observed in the previtellogenic follicle cells. However, microfilaments are present in the basal ends of these cells, similar to their distribution in prefollicular cells contacting the basal lamina (Fig. 114).

This pattern of microtubular organization persists even in the lateral follicle cells during the initial early onset of extracellular space formation (Fig. 117). Dramatic changes in the microtubular organization of the lateral follicle cells does however become evident as vitellogenesis and patency progress.

Vitellogenic follicles

Overview

Immunofluorescent preparations of mid-vitellogenic follicles illustrate that the apical follicle cells have a dramatically different fluorescence distribution than the patent lateral follicle cells (Fig. 118). The principle difference is the bright longitudinal bands of fluorescence along the lateral edges of the columnar apical follicle cells (Fig. 118). The lateral follicle cells do not show a bright, concentrated fluorescence within their cytoplasm (Fig. 118). Instead the fluorescence observed is confined to discrete strands which do not take on an organized configuration. This irregular, random pattern contrasts dramatically with that of both the apical vitellogenic and previtellogenic follicle cells (Figs. 108, 118, 119).

Apical follicle cells - Details

The apical follicle cells show a pattern of longitudinal fluorescence similar to previtellogenic follicle cells (Figs. 108, 119, 120). In addition, the apical and basal areas of the apical cells show a more diffuse fluorescence, in paraffin sections (Fig. 119). With plastic sections, this diffuse fluorescence can be resolved as thin strands running longitudinally, with the fluorescence in the basal end of the cell being brighter than the apical end (Fig. 120).

TEM results, confirm the bright immunofluorescence staining is due to microtubule accumulations. In longitudinal sections, dense bands of long slender microtubules extend the entire lateral length of the cell (Figs. 121, 122, 123, 124, 125). Their configuration is very similar to that of late previtellogenic follicle cells, namely a cylinder of

longitudinal microtubules under the cell membrane. Examination of a variety of planes of section through the apical follicle cells substantiates this pattern of distribution (Figs. 121, 123, 126, 129, 130). Grazing tangential sections, showing large areas of the cell cortex, dramatically reveal the microtubular abundance (Fig. 121). These dense accumulations of microtubules in the apical follicle cells, are greater than those of any other follicle cell stage or substage. They are also the longest microtubules observed in any follicle cell type. The combination of their length and large numbers makes them a dominant cytoplasmic feature of these cells.

As the microtubules extend into the basal and apical ends of the apical cells their arrangement becomes less regular, and their numbers begin to decrease (Figs. 127, 128). This presumably accounts for the more diffuse and irregular immunofluorescence staining in these cell regions.

As in previtellogenic follicle cells, areas of microfilament densities are rarely observed in the apical follicle cells. Even regions near the basal lamina do not have prominent microfilament accumulations in contrast with the following observations on the lateral follicle cells.

Lateral follicle cells - Details

The immunofluorescence results show the irregular pattern of thin anatomizing strands of fluorescence characteristic of patent lateral follicle cells (Figs. 131, 134). No evidence of bright lateral bands of fluorescence similar to that of apical follicle cells was found in these cells.

TEM sections reveal numerous microtubules within the lateral follicle cells (Figs. 132, 135, 136). Compared with the apical cells, these microtubules are shorter in length and are not organized in parallel fashion but rather irregularly so various microtubule planes of section are seen in any one plane of section (both longitudinal and cross sections) (Figs. 132, 136). This is quite unlike the pattern of microtubule orientation within the apical follicle cells.

The lateral vitellogenic follicle cells characteristically contain a subplasmalemmal band of microfilaments which encircles the cells' perimeter (Figs. 132, 133, 135). No other follicle cell stage or subtype was observed to contain this microfilament ring. The microfilamentous areas can be discarded as dense regions of cytoplasm which excludes cell organelles, such as ribosomes (Figs. 132, 133, 135). The TA-Saponin fixation was particularly beneficial in exposing and highlighting these microfilamentous regions.

In addition to the subplasmalemmal filaments, the patent lateral follicle cells also display dense areas of microfilaments in the lateral arms connecting adjacent cells (Fig. 138). As the extracellular spaces enlarge during late vitellogenesis, the microfilamentous regions in the lateral arms become more extensive and microtubules become a common constituent of the arms as well (Fig. 137).

The patent lateral follicle cells produce numerous apical projections which maintain oocyte-follicle cell contact during vitellogenesis (Figs. 139, 140). These follicle cell projections and in particular, the oocyte microvilli, also contain numerous microfilament bands (Figs. 139, 140).

Post vitellogenic lateral follicle cells

Following vitellogenesis the lateral cells increase their cell volume and form a tightly packed epithelium. Immunofluorescent anti-tubulin results show a weak diffuse fluorescence around the lateral and basal extremities of these cells (Fig. 142). No bright fluorescent localization comparable to that in the previtellogenic or apical vitellogenic follicle cells is observed (Fig. 142).

Few microtubules were found in these cells (Figs. 143, 144). Of these, most become oriented parallel to the basal lamina, with only a few microtubules still localized along the lateral edges of these cells (Figs. 141, 143, 144). Clearly there is an alteration in the number and orientation of the microtubules during this last phase of follicle cell morphogenesis.

Microfilamentous areas are scarce in these cells, with only a few areas present along the lateral cell membranes (Fig. 144).

Figure Abbreviations

AF	apical vitellogenic follicle cell
B	basal lamina
EM	extracted material
F	follicle cell(s)
G	Golgi complex
IS	inner sheath cell
LF	lateral vitellogenic follicle cell
LM	light micrograph
M	mitochondria
MF	microfilaments
MT	microtubules
N	nurse cells
NU	nucleus
O	oocyte
P	plasma membrane
PF	prefollicular cell
POV	postvitellogenic follicle cell
PV	previtellogenic follicle cell
RER	rough endoplasmic reticulum
SEM	scanning electron micrograph
T	tropharium
TA	tannic acid
TC	trophic cord
TEM	transmission electron micrograph
VF	vitellogenic follicle
Y	yolk sphere

NOTICE/AVIS

PAGE(S) plates 1-28 IS/ARE ~~EST~~/SONT black + white photos

PLEASE WRITE TO THE AUTHOR FOR INFORMATION, OR CONSULT THE ARCHIVAL COPY HELD IN THE DEPARTMENT OF ARCHIVES AND SPECIAL COLLECTIONS, ELIZABETH DAFOE LIBRARY, UNIVERSITY OF MANITOBA, WINNIPEG, MANITOBA, CANADA, R3T 2N2.

VEUILLEZ ECRIRE A L'AUTEUR POUR LES RENSEIGNEMENTS OU VEUILLEZ CONSULTER L'EXEMPLAIRE DONT POSSEDE LE DEPARTEMENT DES ARCHIVES ET DES COLLECTIONS SPECIALES, BIBLIOTHEQUE ELIZABETH DAFOE, UNIVERSITE DU MANITOBA, WINNIPEG, MANITOBA, CANADA, R3T 2N2.

Plate 1

Overview of Follicle Cell Development

Figure 1. The line drawing illustrates the overall structure of a Rhodnius telotrophic ovariole (from Huebner, 1984a).

Figures 2-7. These light micrographs of 1 µM sections show structural changes the follicular tissue undergoes during an oogenesis cycle. The sequence is prefollicular cells (fig. 2), previtellogenic follicle cells (fig. 3), vitellogenic apical-lateral follicle cell junction (fig. 4), apical vitellogenic follicle cells (fig. 5), lateral vitellogenic follicle cells (fig. 6), and post-vitellogenic lateral follicle cells (fig. 7). Note the large extracellular spaces (*) between the vitellogenic lateral cells. XI,000, X500, X450, X650, X1,100, X1,000.

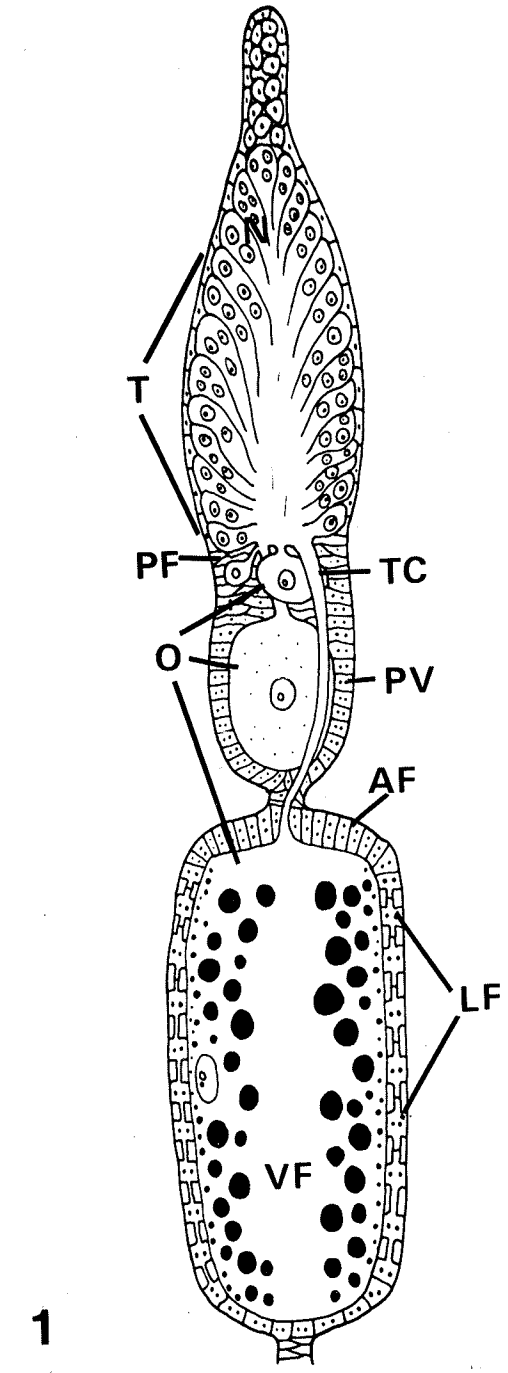

1

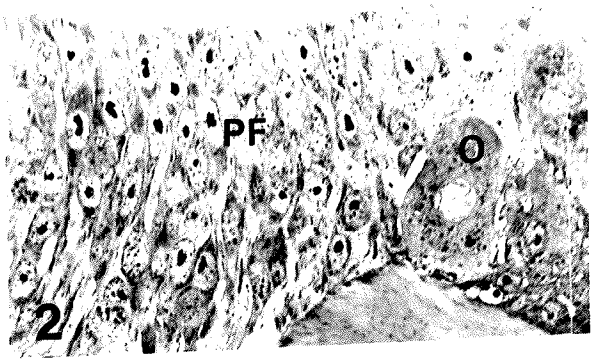

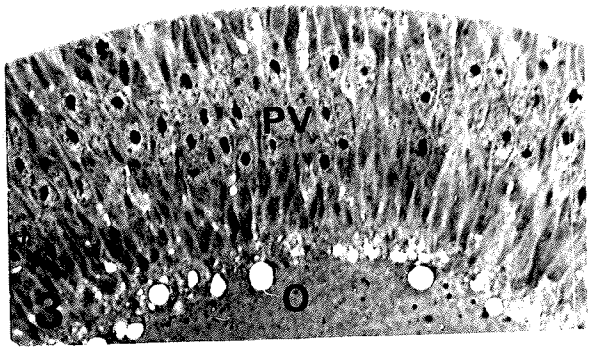





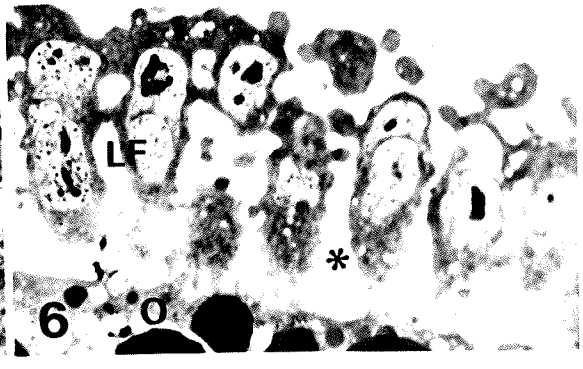

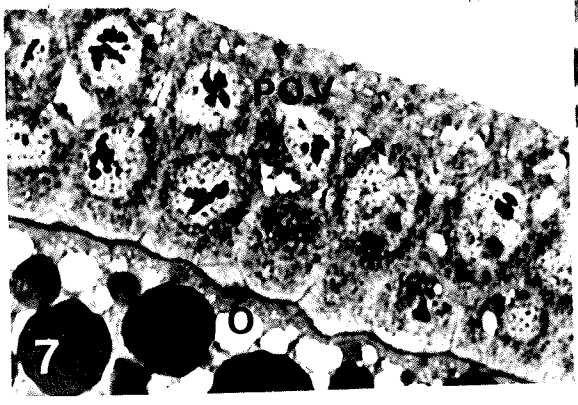

Plate 2

Assessment of Fixation

Figures 8,10 and 11, inset. These light micrographs illustrate the affects of fixation on the maintainence of normal nurse cell structure. Note the extensive shrinkage in Luftig's fixative (fig. 10) but not in the modified Karnovsky's (fig. 8) or 3.0% glutaraldehyde (fig. 11). There is slight shrinkage of the inner sheath cells in the 3.0% glutaraldehyde (fig. 11 inset). X300, X350, X350, X1,100.

Figure 9. TEM of Karnovsky's fixed apical follicle cells. Note the generally good fixation of mitochondria, nuclear envelopes and microtubules (arrows), X25,000.

Figure 12. A TEM comparable to fig. 9 but with 3.0% glutaraldehyde fixed tissue. Overall fixation quality is maintained. Note the abundant microtubule profiles (arrows). X28,000.

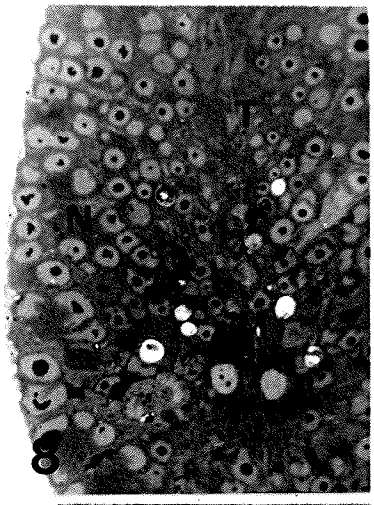

8

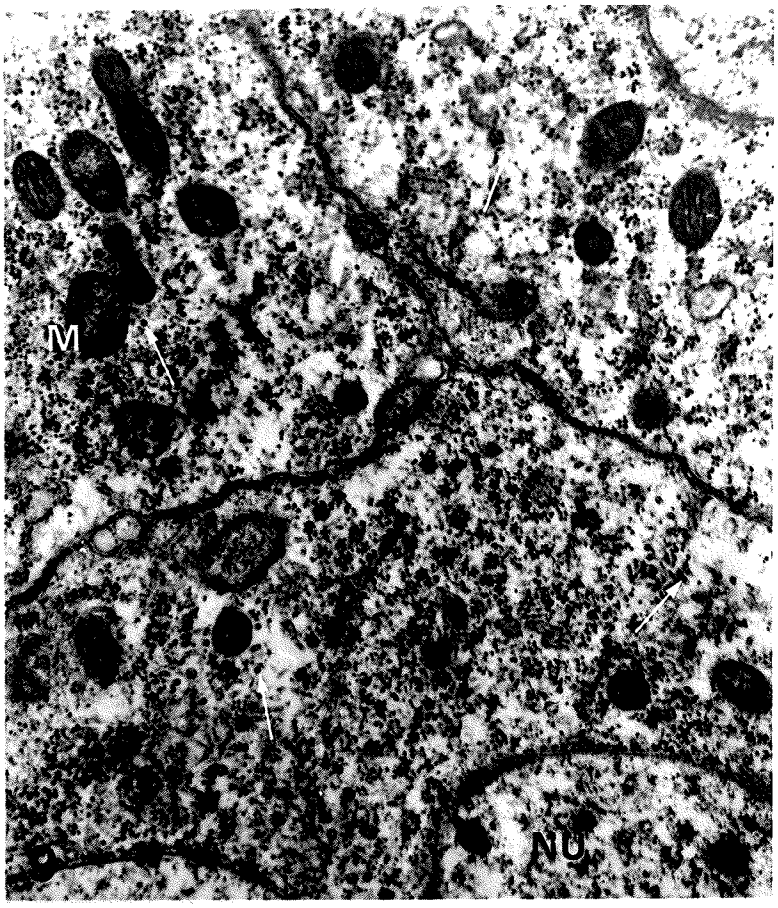



10

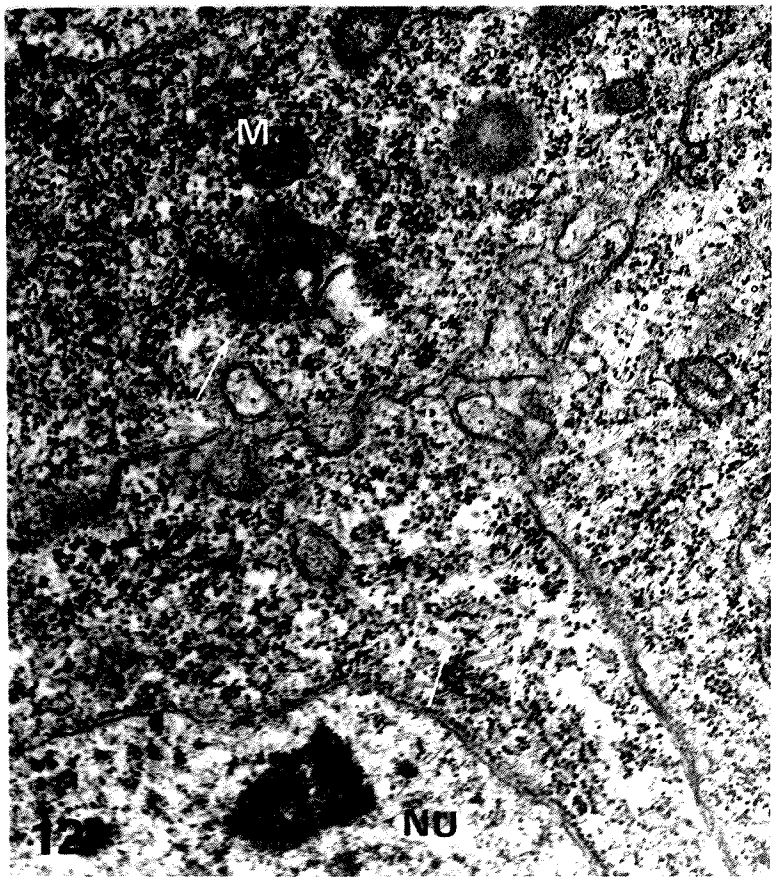

12



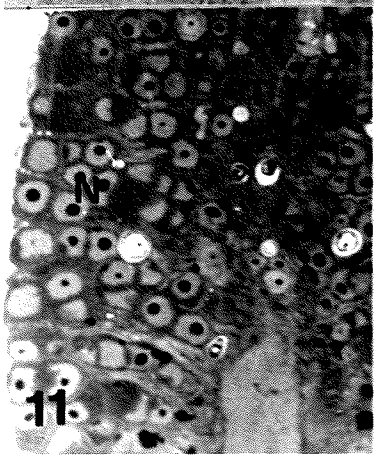

11

Plate 3

Tannic acid and Saponin Fixation

Figure 13. This TEM shows the TA (arrows) as a flocculant material in the extracellular spaces between the lateral vitellogenic follicle cells when higher TA concentrations are used. X20,000.

Figure 14. TEM illustrating the penetration of TA (arrows) just under the cell membrane, without Saponin. X55,000.

Figure 15. This TEM reveals the lack of TA penetration into the follicle cells when saponin is not used in the prefixation. X25,000.

Figure 16 and inset. The addition of Saponin facilitates penetration of TA into the cell cytoplasm: Note that, not only are the cell surfaces clearly demarked, but cytoplasmic structures like microtubules (arrows) (inset) are also more obvious. X34,000X X55,000.

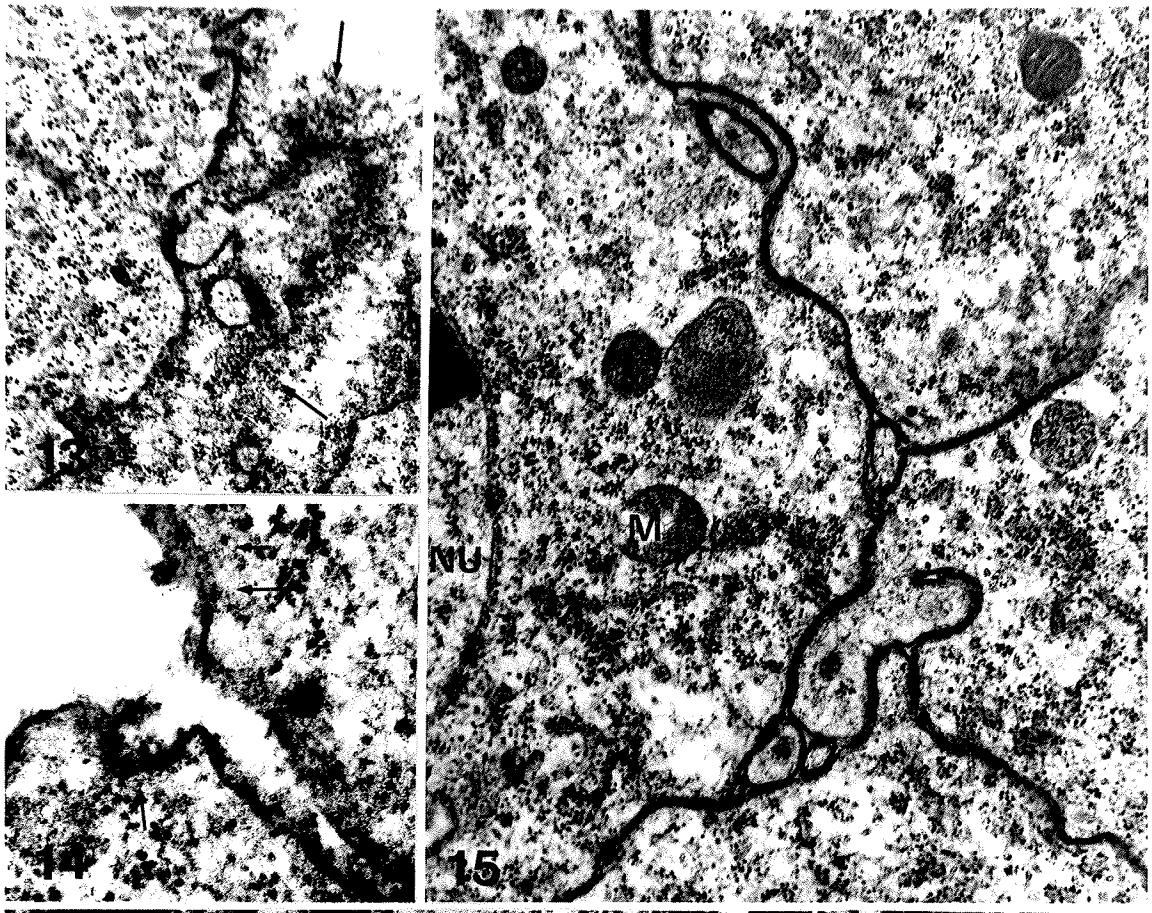
13
14
15
NU
M

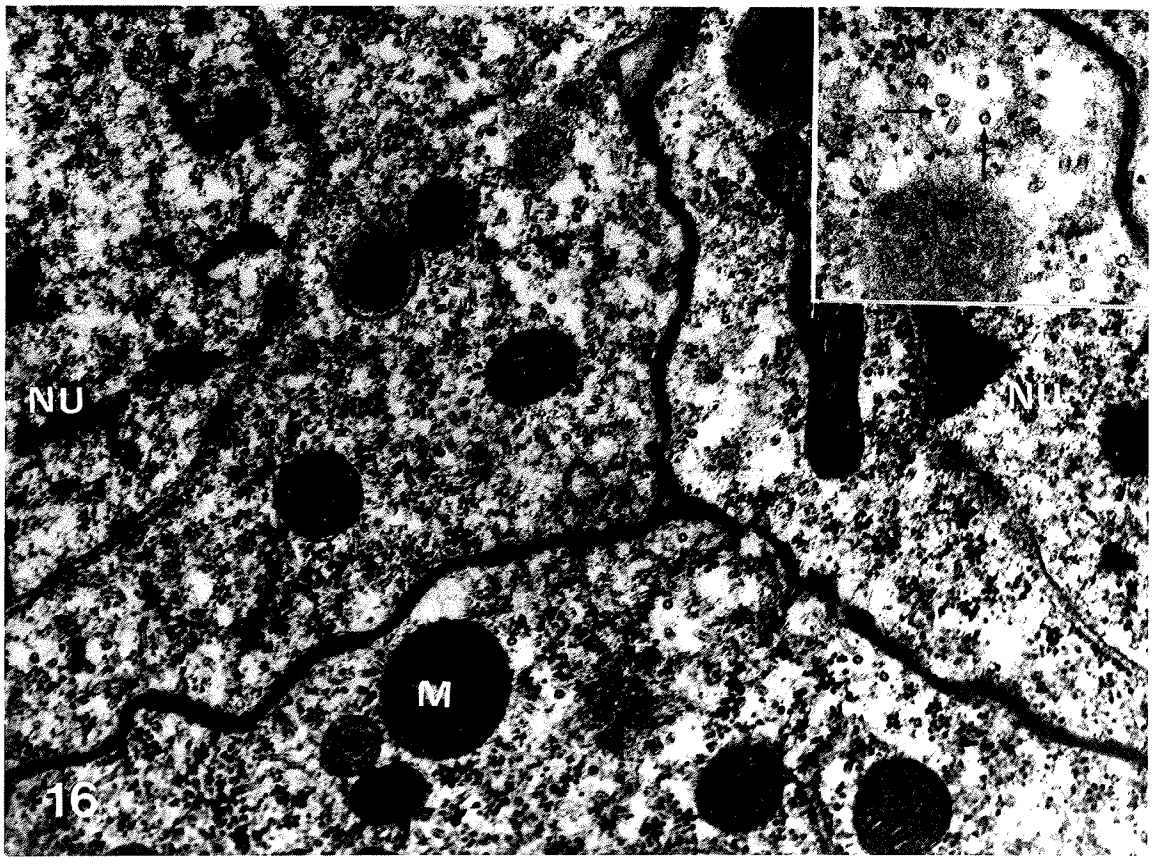
NU
M
16

Plate 4

Preliminary Detergent Extractions

Figures 17-20. The extraction of cytoplasmic constituents is illustrated by these LM's of a whole ovariole and higher magnification views of extracted nurse cells, prefollicular cells and previtellogenic follicle cells. Note that little cytoplasm remains in nurse cell lobes or prefollicular cells trapping the extracted material within the expanded basal lamina. X350, X750, X750, X550.

Figures 21 and 22. These TEM's show cytoskeletal microfilamentous material extracted outside of the cell (fig. 21), along with other cell cytoplasmic components (fig. 22). X60,000, X20,000.

Figures 23 and 24. Detergent extractions of follicle cells with 0.25% and 0.50% Triton X-100 respectively, for 15 minutes. Note loss of substantial cytoplasmic elements but the retention of the nuclear envelope and small cell membrane fragments. X8,000, X5,000.

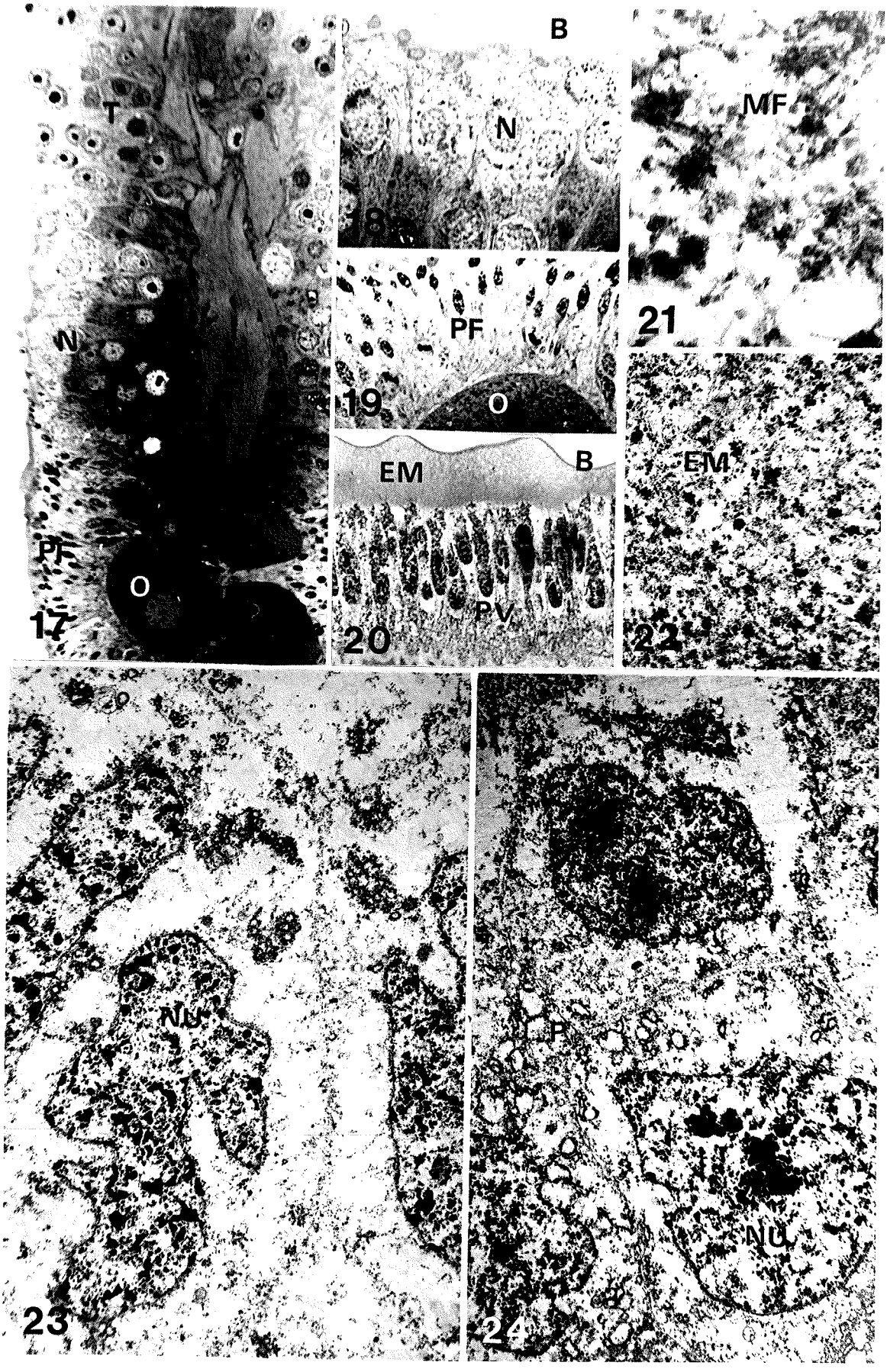
T
N
PF
O
17
B
N
18
PF
O
19
EM
B
PV
20
MF
21
EM
22
NU
23
P
NU
24

Plate 5

Preliminary Detergent Extractions

Figures 25-28. These are TEM's of Triton X-100 extracted follicle cells. Note the retention of long microtubules (arrows) near the lateral cell membrane. X15,500, X75,000, X50,000, X50,000.

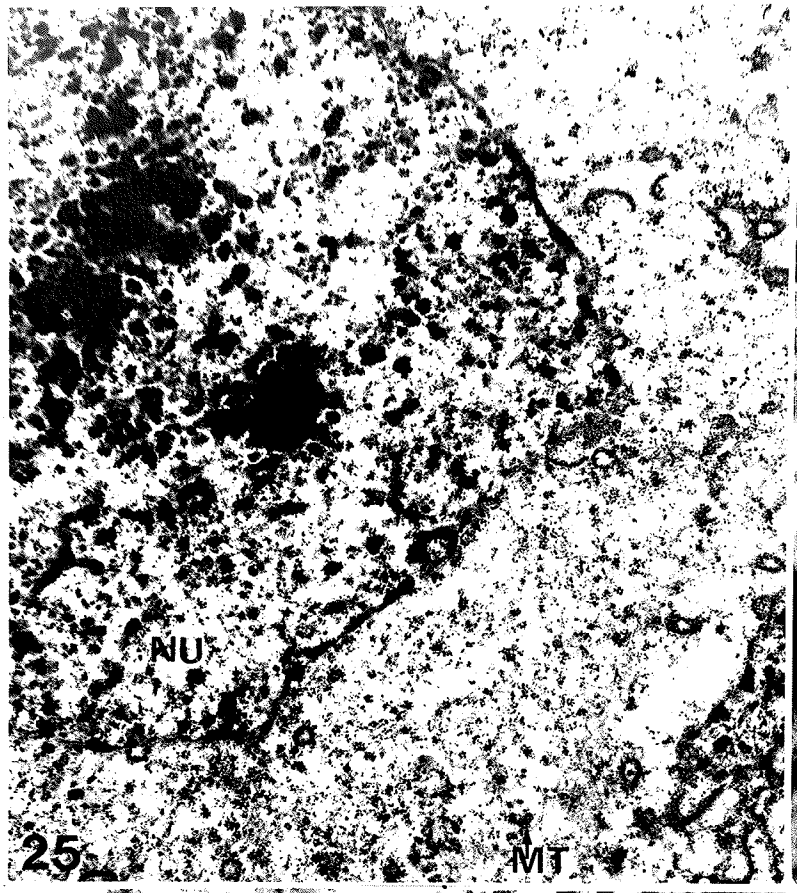
NU
MT
25

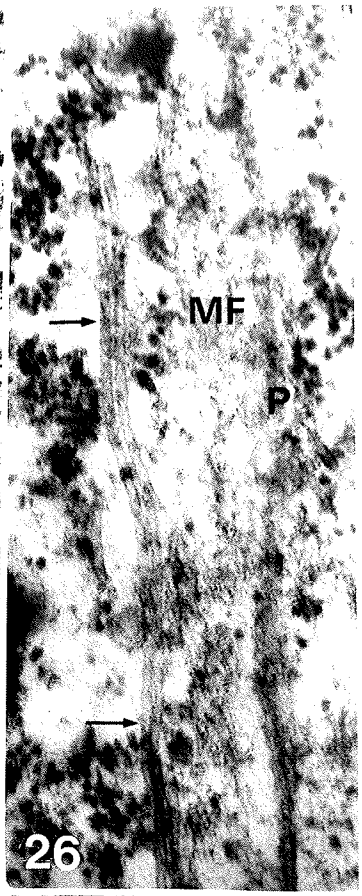
MF
P
26


P
27


P
28

Plate 6

Basement Membrane Digestion

Figures 29-32. These 1 μM epoxy sections show the nurse cell morphology after exposure to Rhodnius saline, calcium magnesium free saline, 0.1M PIPES buffer pH 6.9 and 0.075M PIPES buffer pH 6.9. X350, X250, X350, X350.

Figure 33. This SEM reveals a desheathed ovariole with an intact basal lamina. X115.

Figure 34. This Nomarski LM from Huebner, 1984b demonstrates the separation of the basal lamina at the tropharium tip during elastase digestion. Note the basal lamina is not digested. X300.

Figure 35. The effect of elastase digestion on ovariole structure is illustrated by this 1μ M epoxy section. X200.

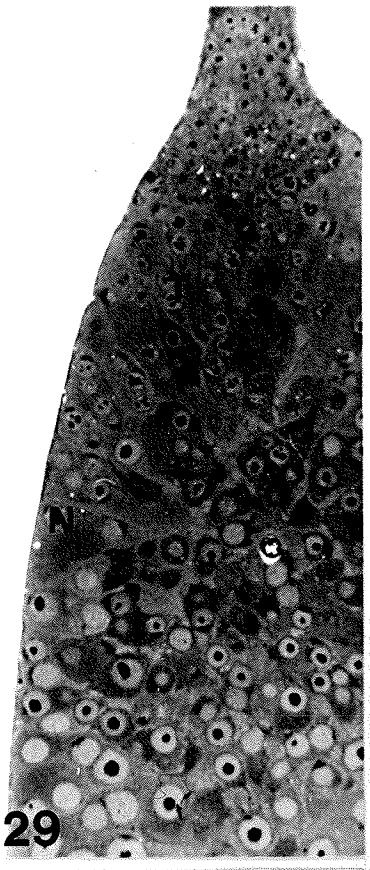

29

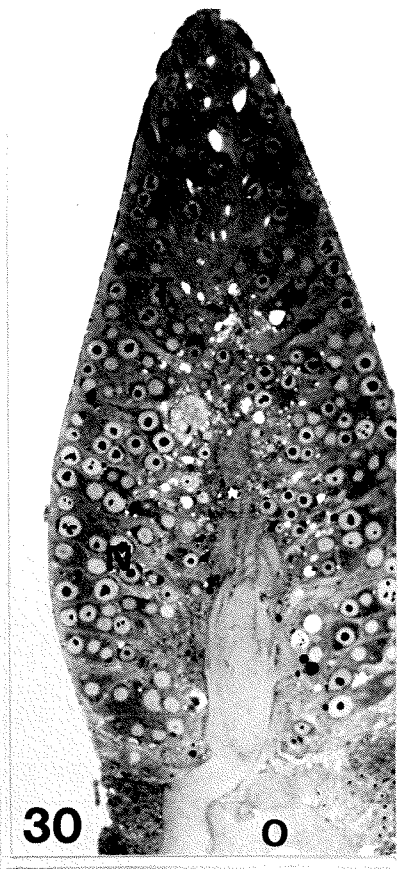

30



3

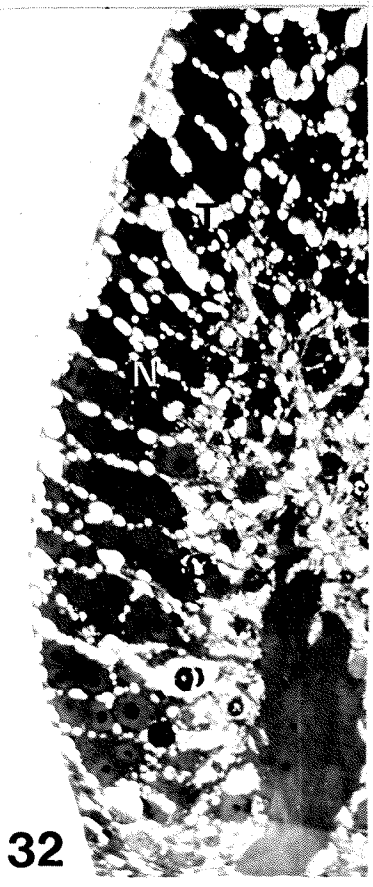

32

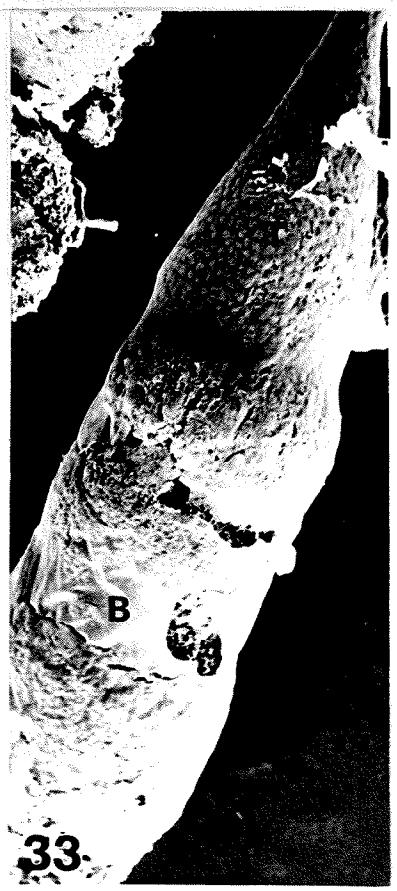

33

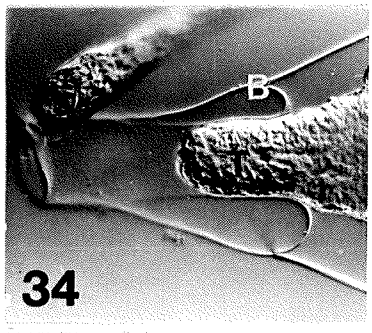

34

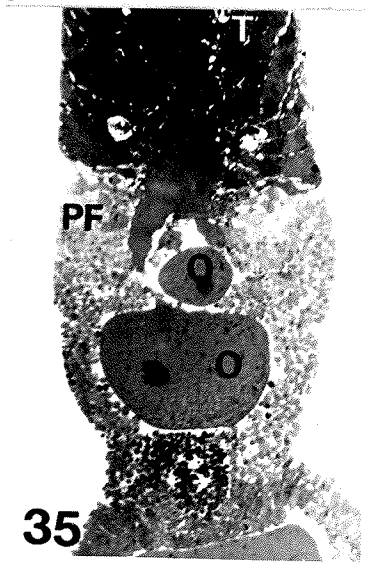

35

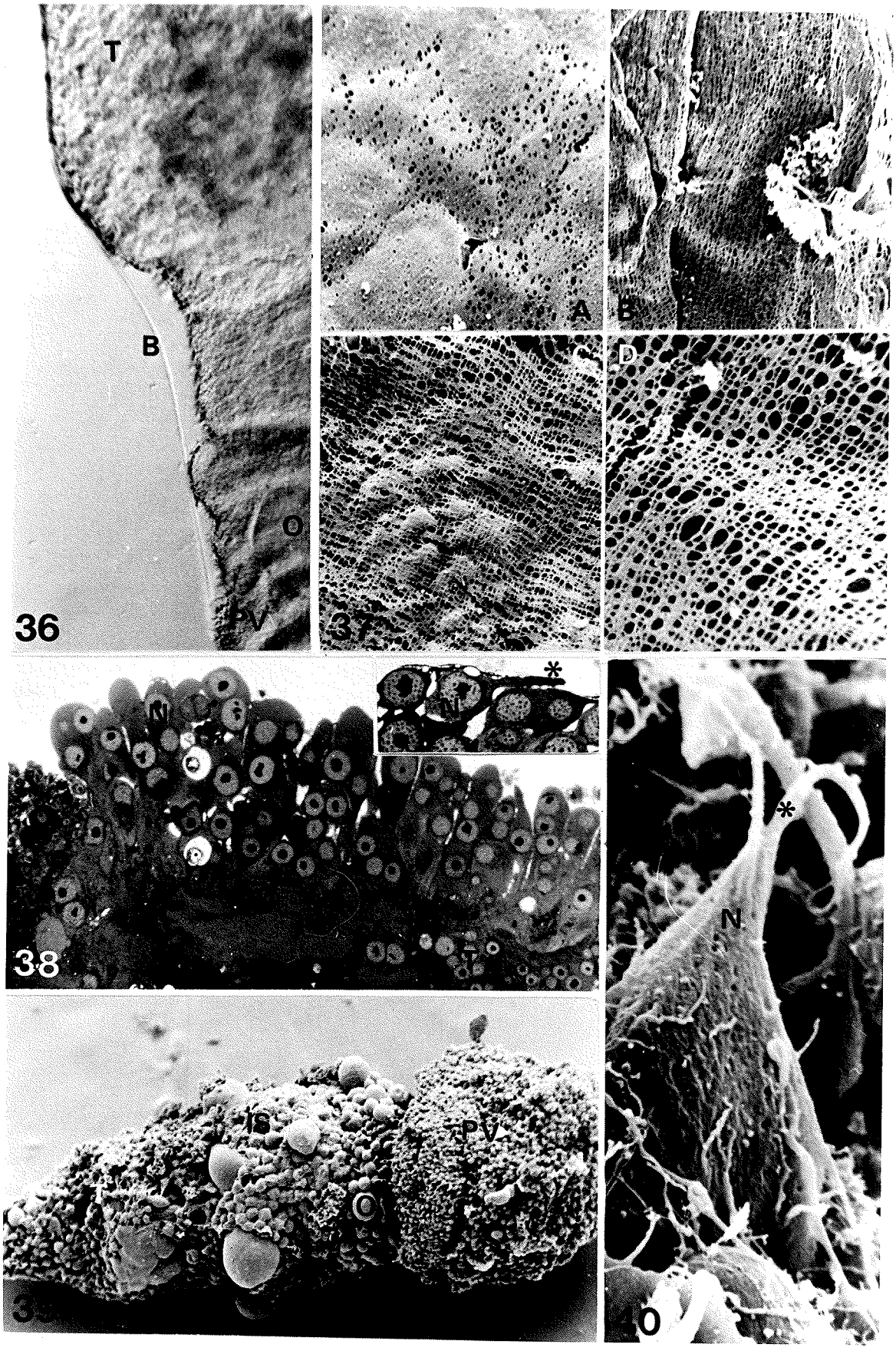
T
B
O
PV
36
A
37
B
D
N
*
38
T
IS
PV
O
39
N
*
40

Plate 8

Follicle Cell Changes Following Basal Lamina Removal

Figure 41. The rounding up of previtellogenic follicle cells is illustrated by this SEM. X750.

Figures 42 amd 43. This Nomarski LM and SEM reveal that the vitellogenic, lateral follicle cells generally maintain their normal structure and cellular interactions following basal lamina removal. X850, X1,200.

Figures 44-47. The previtellogenic follicle cell lobes and surface projections (*) are displayed in the 1 μM epoxy section (fig. 44) and low magnification TEM (fig. 45). Figures 46 and 47 reveal the presence of microtubules (arrows) and other cytoplasmic organellles in these cells. X1,000, X2,500, X25,000, X31,500.

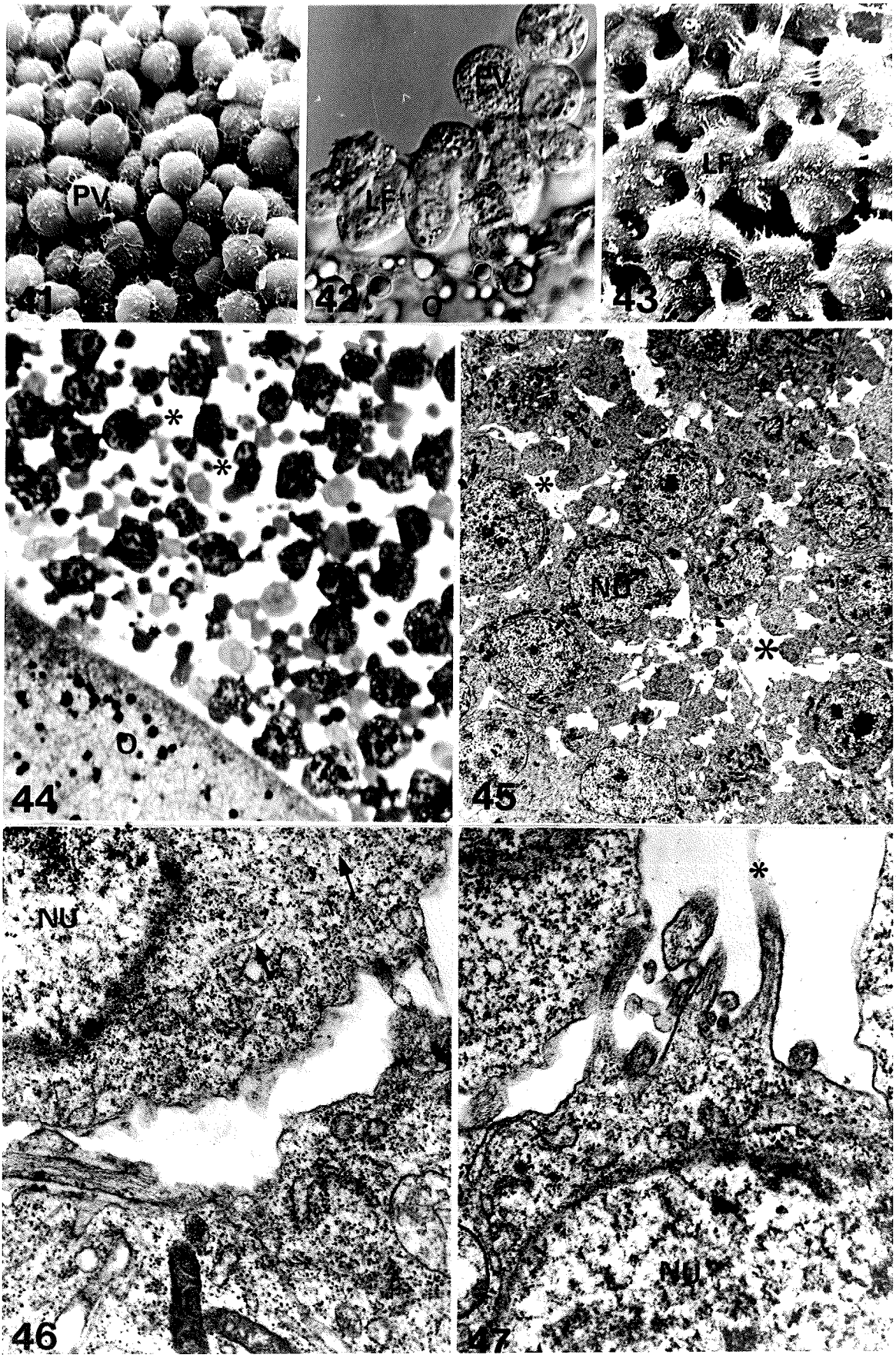
PV
41
PV
LF
42
C
LF
43
*
*
C
44
*
NU
45
NU
46
*
NU
47

Plate 9

Detergent Extraction Following Basal Lamina Removal

Figures 48-51. These LM's reveal that after basal lamina removal, detergent extracted cytoplasmic material does not remain in close proximity to the ovariole. X250, X750, X250, X500.

Figures 52 and 53. TEM's revealing the retention of very few microtubules (arrows) or other cytoplasmic constituents in extracted cells. X17,800, X14,300.

Figures 54 inset, 55 and 56. The extreme shrinkage of all ovariole components exposed to glycerol solutions is presented in these LM's. X200, X250, X550, X850.

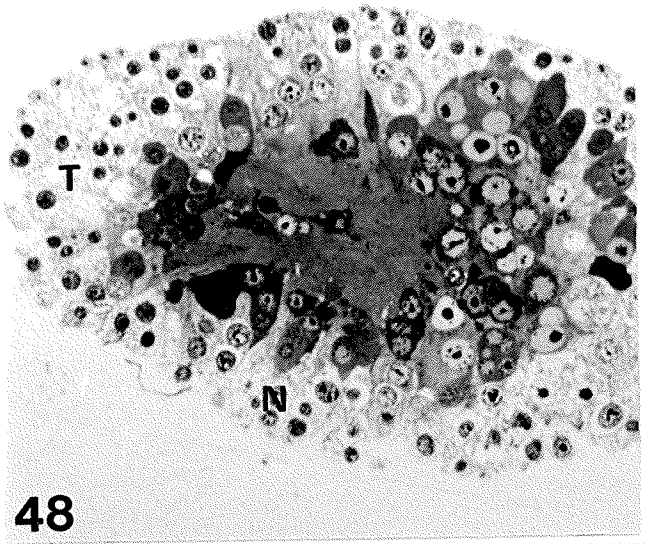
T
N
48


LF
O
49

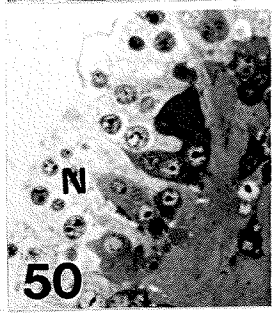
N
50

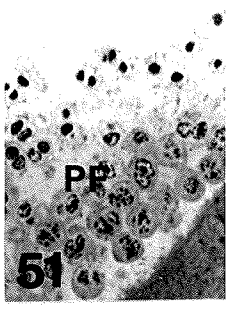
PP
51

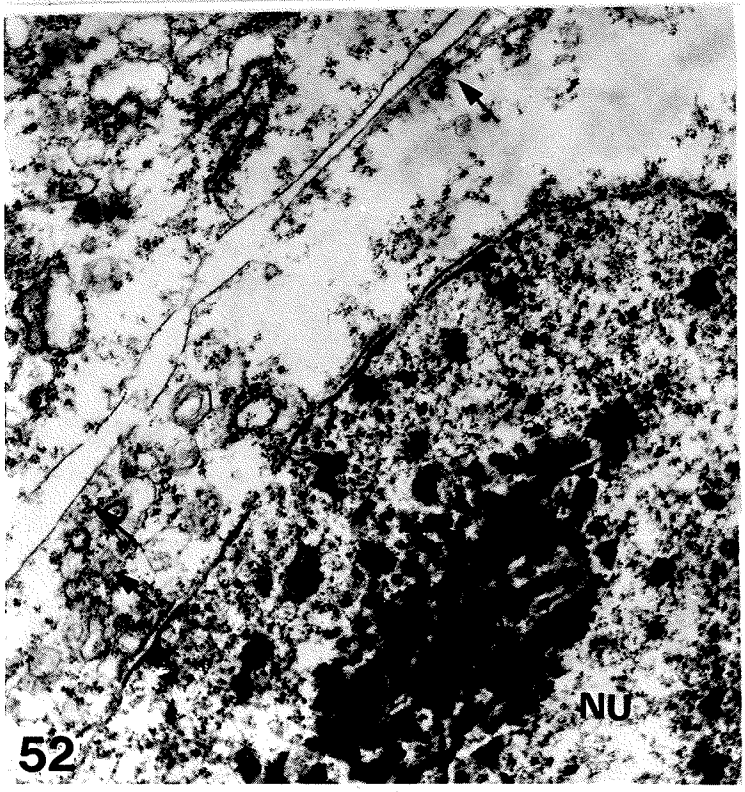
NU
52

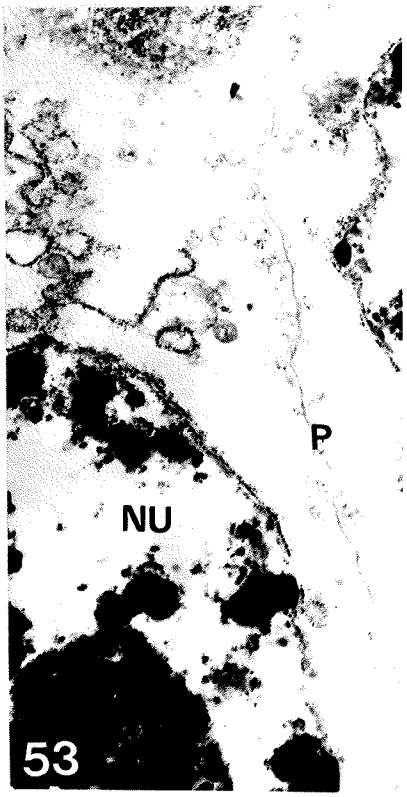
P
NU
53

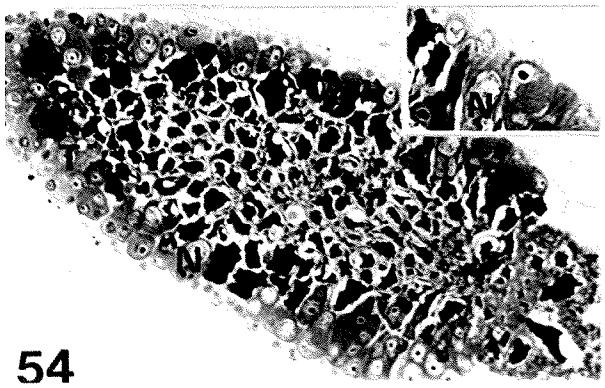
N
54

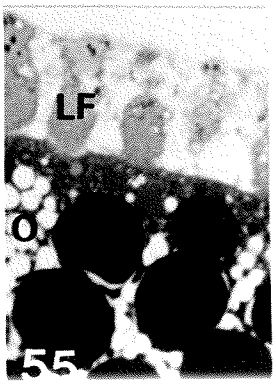
LF
O
55

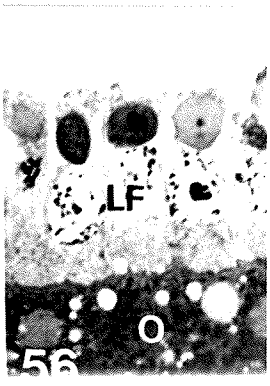
LF
O
56

Plate 10

Effects of Trypsin Digestion (1 hr.) on Trophic Core Birefringence and Ovariole Structure After Mechanical Basal Lamina Removal

Figures 57-59. These polarizing LM's show the progressive decrease in trophic core birefringence (*) in an ovariole after 20, 30 and 45 min. trypsin exposure. X175, X175, X175.

Figures 60 and 61. These Nomarski LM's show mechanically removed basal lamina and also the basal lamina separation at the tropharium tip. X200, X200.

Figures 62-64 and 66. These 1 μM epoxy sections of nurse cell lobes, small oocytes, prefollicular cells and vitellogenic lateral follicle cells show the maintenance of normal ovariole structure after basal lamina removal. X1,250, X1,100, X750, X1,250.

Figure 65. TEM showing that the prefollicular cells maintain close contact following basal lamina removal. X20,500.


57


58


59

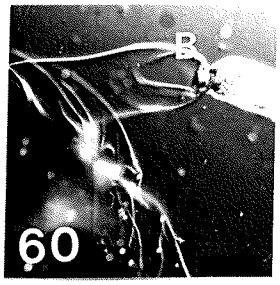
B
60

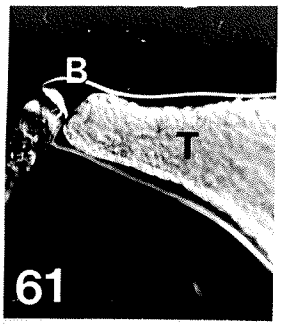
B
T
61


IS
62

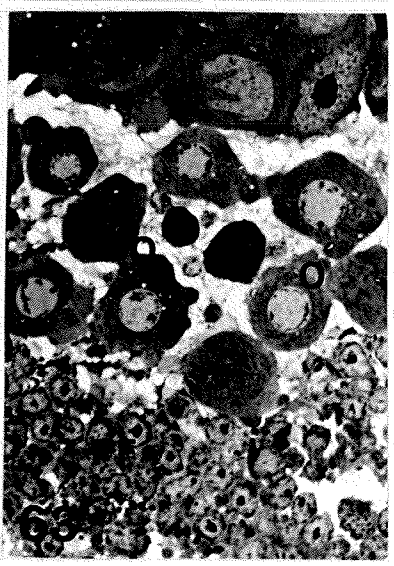
63

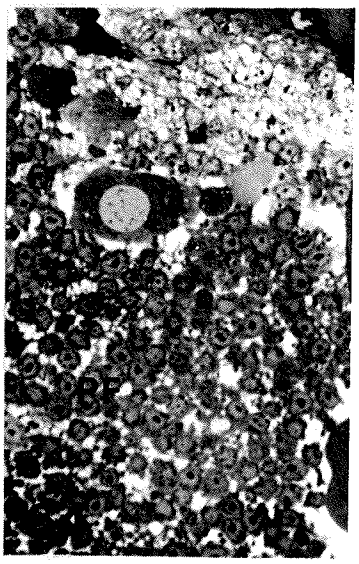

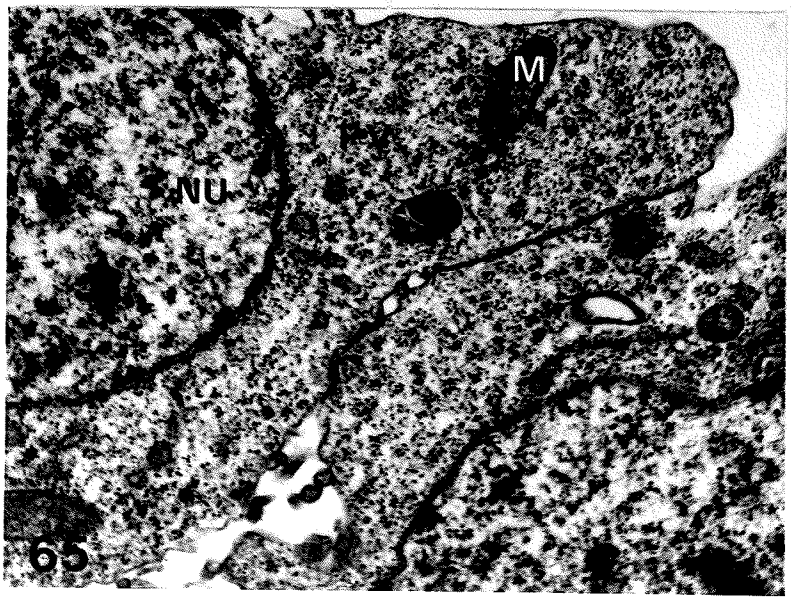
M
NU
65

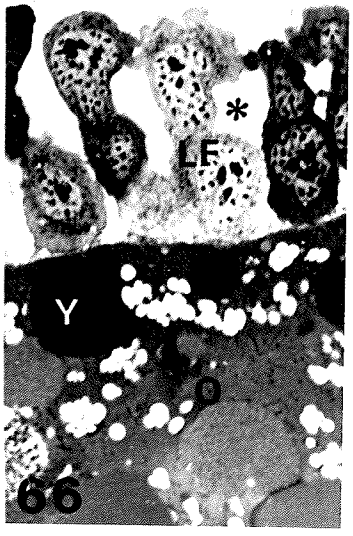
LF
Y
66

Plate 11

Detergent Extraction With Intact Basal Lamina

Figures 67 and 68. LM's showing the progression of extraction in previtellogenic follicle cells after 2 and 15 min. Triton X-100 exposure. X1,000, X1,250.

Figure 69. TEM of previtellogenic follicle cells Triton X-100 extracted for 2 minutes. X5,500.

Figure 70. The retention of extracted cell material by the basal lamina is illustrated by this TEM. X20,000.

Figure 71. TEM of previtellogenic follicle cells extracted 5 min. Note extraction of the basal end occurs before extraction of the apical end. X2,600.

Figure 72. By 15 minutes extraction time, little cytoplasmic materials remains, although nuclei retain a normal appearance. TEM. X6,000.

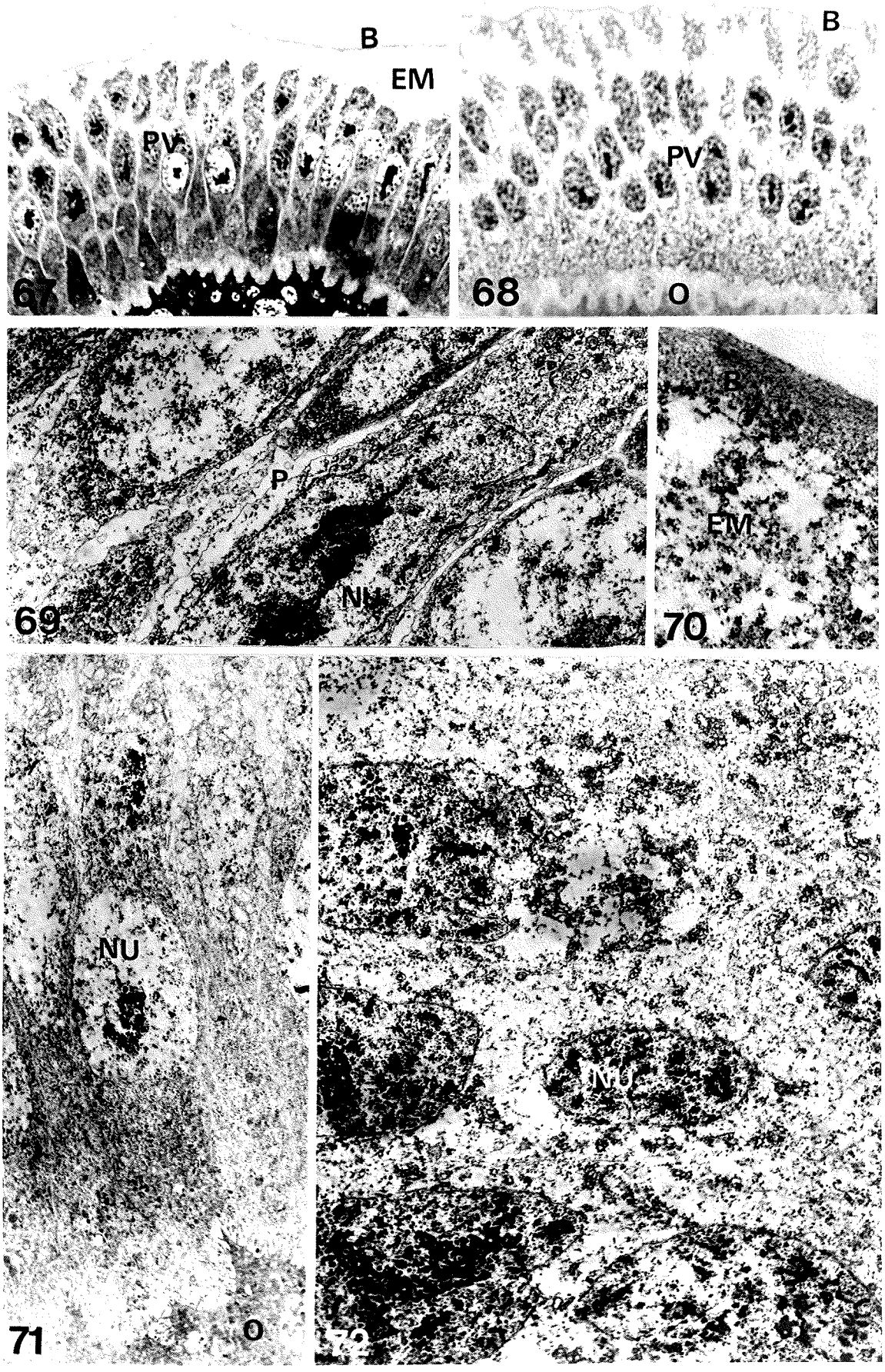
B
EM
PV
67
B
PV
68
O
P
N
69
B
EM
70
NU
71
O
NU

Plate 12

Detergent Extraction With Intact Basal Lamina

Figures 73-76. These TEM's reveal the effects of detergent extraction on the retention of microtubules within follicle cells. Numerous microtubules (arrows) observed after 2 and 5 min (figs. 73, 74). By 10 minutes, microtubules (*arrows) are primarily detected near the lateral cell nucleus (figs. 75, 76). X41,600, X76,000, X32,000, X43,000.

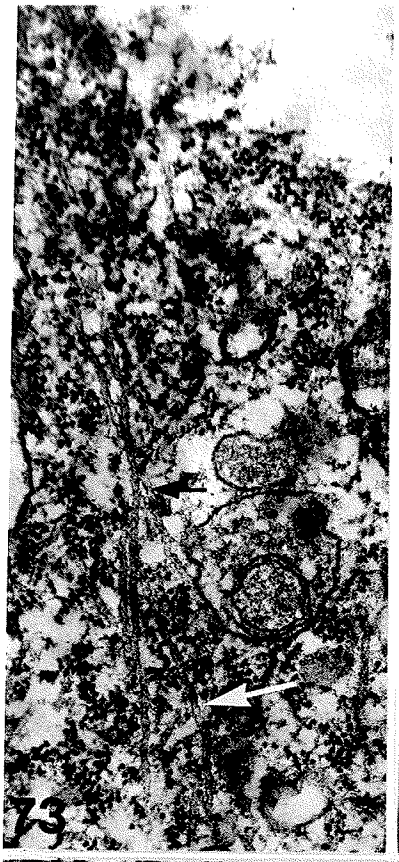
73

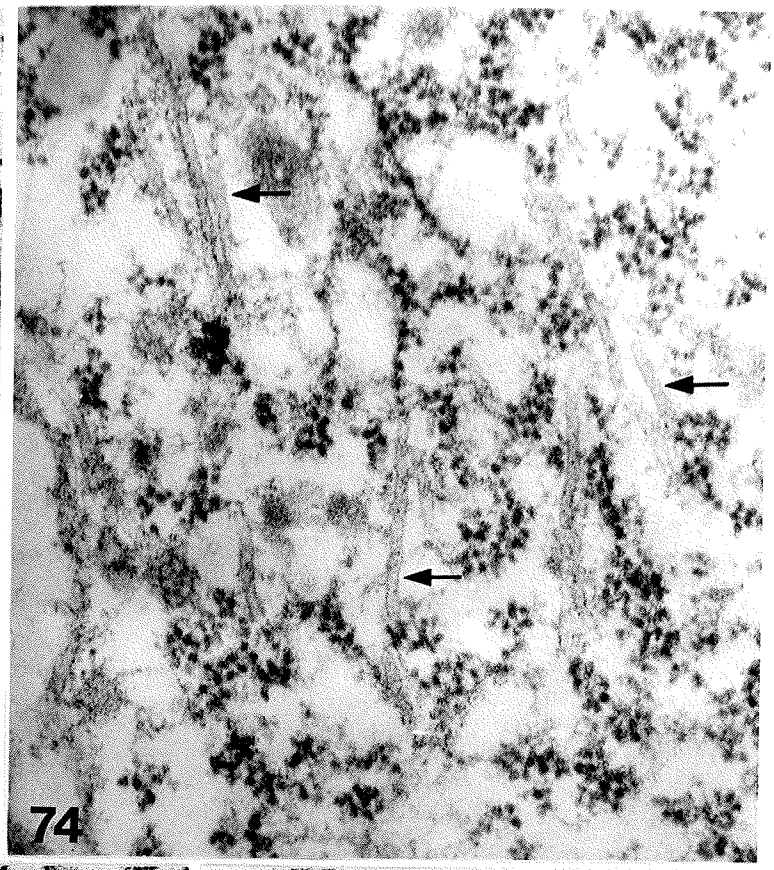
74

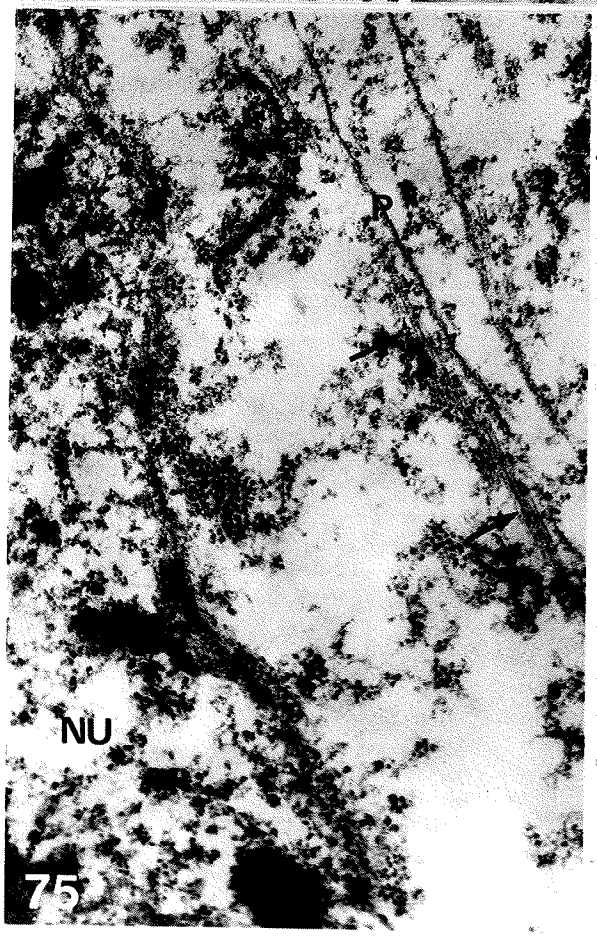
P
NU
75

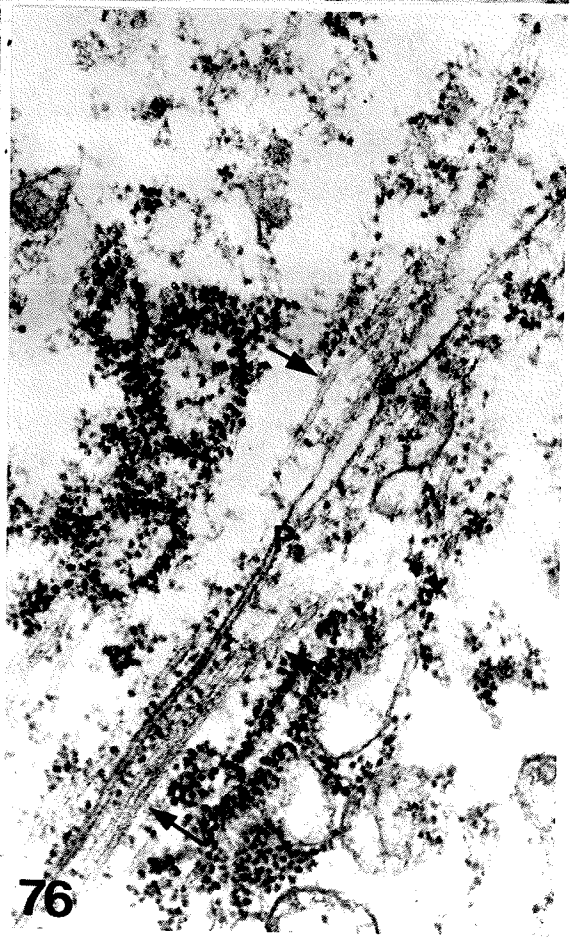
P
76

Plate 13

Immunofluorescence Trials

Figures 77 and 78. LM's of intact follicle cell sheets (fig. 77) and nurse cell lobes (fig. 78) illustrating a diffuse anti-tubulin fluorescence pattern. X1,000, X450.

Figures 79 and 80. Anti-tubulin fluorescence pattern of 5 μM paraffin and sections of apical follicle cells fixed in Bouins and 3% paraformaldehyde - 0.5% glutaraldehyde respectively. These are labelled with the Fujiwara anti-tubulin antibody. X550, X850.

Figure 81. Anti-tubulin fluorescence pattern of a 10 μM, Bouins' fixed paraffin section labelled with Fujiwara's anti-tubulin. X900.

Figure 82. Anti-tubulin fluorescence pattern of a 5 μM paraffin section of 1.0% paraformaldehyde fixed tissue labelled with the Miles anti-tubulin. X750.

Figure 83. Anti-tubulin (Miles) fluorescence pattern of a 1 μM Epon-Araldite embedded tissue section fixed with 1.0% paraformaldehyde. X1,200.

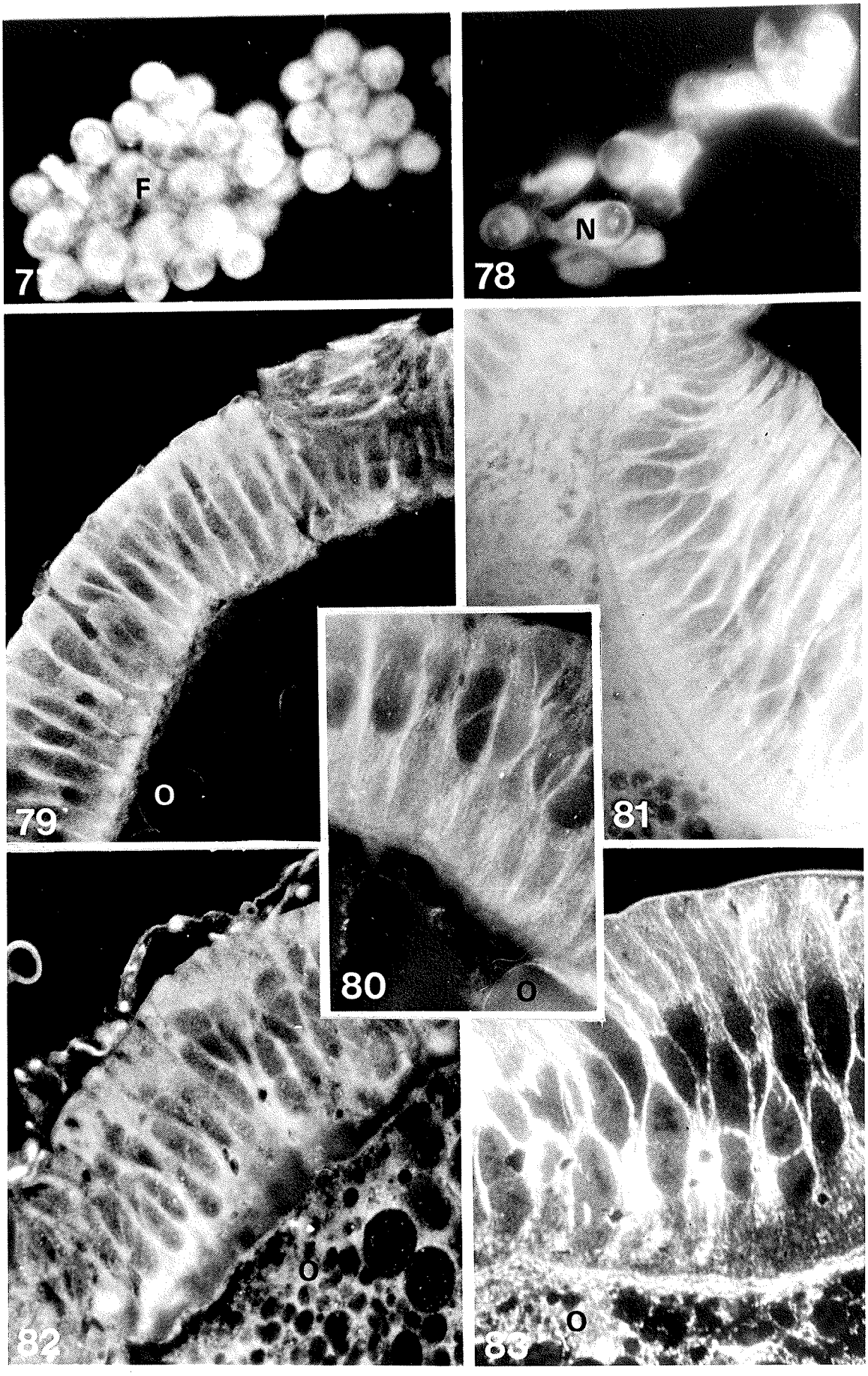
F
71
N
78
O
79
80
O
81
O
82
O
83

Plate 14

Immunofluorescence Controls

Figures 84-86. LM illustrating the background autofluorescence of Bouins' fixed paraffin embedded tissue after paraffin removal (fig. 84), 1 hour incubation in 1.0% BSA-PBS (fig. 85) and incubation in BSA-PBS followed by exposure to 2° fluorescein labelled antibody only (fig. 86). X600, X600, X600.

Figures 87-89. Background fluorescence controls for 3.0% paraformaldehyde and 0.5% glutaraldehyde fixed paraffin sections. X750, X750, X1,100.

Figures 90 and 91. Background autofluorescence of 1.0% paraformaldehyde and fixed paraffin sections (fig. 90). Fluorescence following BSA-PBS incubation and BSA-PBS, 2° fluorescein labelled antibody incubation (fig. 91). X400, X400.

Figures 92 and 93. Background fluorescence controls for Epon-Araldite and embedded tissue fixed with 1.0% paraformaldehyde following BSA-PBS incubation (fig. 92) and BSA-PBS, 2° fluorescein labelled antibody incubation (fig. 93). X800, X800.

Figure 94. Increase in autofluorescence with 3.0% paraformaldehyde - 0.5% glutaraldehyde fixation (Epon-Araldite sections) following BSA-PBS and 2° fluorescein labelled antibody incubation. X750.

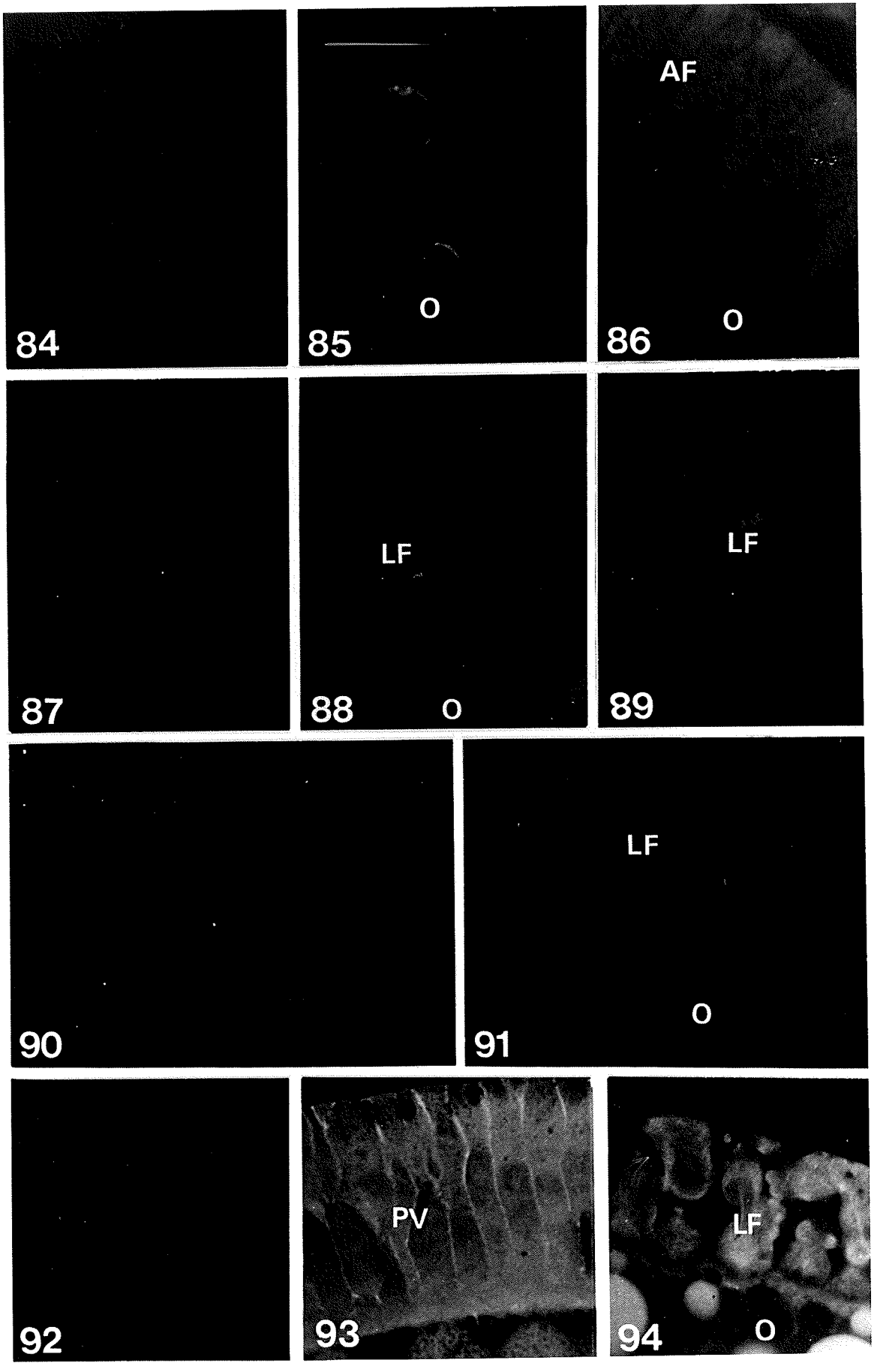
84
85
O
AF
86
O
87
LF
88
O
LF
89
90
LF
91
O
92
PV
93
LF
94
O

Plate 15

In Situ Ovariole Immunofluorescence Controls

Figure 95. Bright anti-tubulin labelled fluorescence of a trophic cord and prefollicular cells using 3.0% paraformaldehyde - 0.5% glutaraldehyde fixed Epon-Araldite 1 M section. X450.

Figure 96. Fluorescent anti-tubulin staining pattern of a trophic cord entering a previtellogenic oocyte in 1.0% paraformaldehyde fixed Epon-Araldite embedded tissue. Note the shrinkage due to fixation of the smaller previtellogenic oocytes. X1,000.

Figure 97. LM showing the absence of fluorescence in the trophic cords with anti-actin immunofluorescence labelling applied to 3.0% paraformaldehyde - 0.5% glutaraldehyde fixed paraffin sections. X750.

Figure 98. Anti-tubulin labelled fluorescence pattern of the microtubule rich trophic core, 3.0% paraformaldehyde - 0.5% glutaraldehyde fixed tissue, paraffin section. X850.

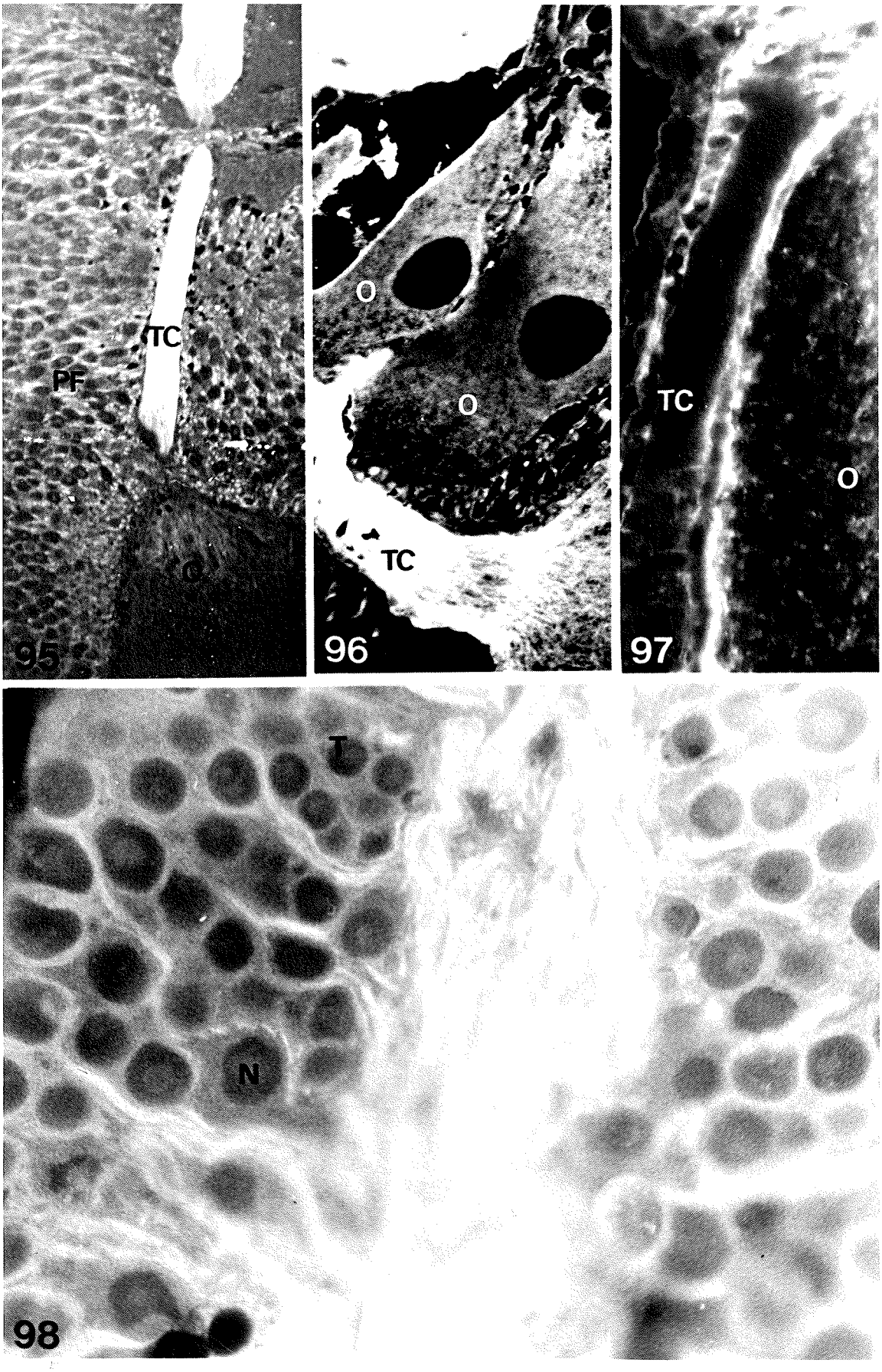
TC
PF
O
95
O
O
TC
96
TC
O
97
T
N
98

Plate 16

Anti-Actin Immunofluorescence

Figures 99-101. Anti-actin labelled fluorescence pattern of 1.0% paraformaldehyde fixed tissue (1 μM Epon-Araldite sections). Prefollicular tissue (fig. 99), previtellogenic follicle (fig. 100) and apical vitellogenic follicle cells (fig. 101). X1,000, X650, X1,000.

Figure 102. Anti-actin labelled fluorescence pattern of 1.0% paraformaldehyde fixed tissue (5 μM paraffin sections), showing apical vitellogenic follicle cells. X650.

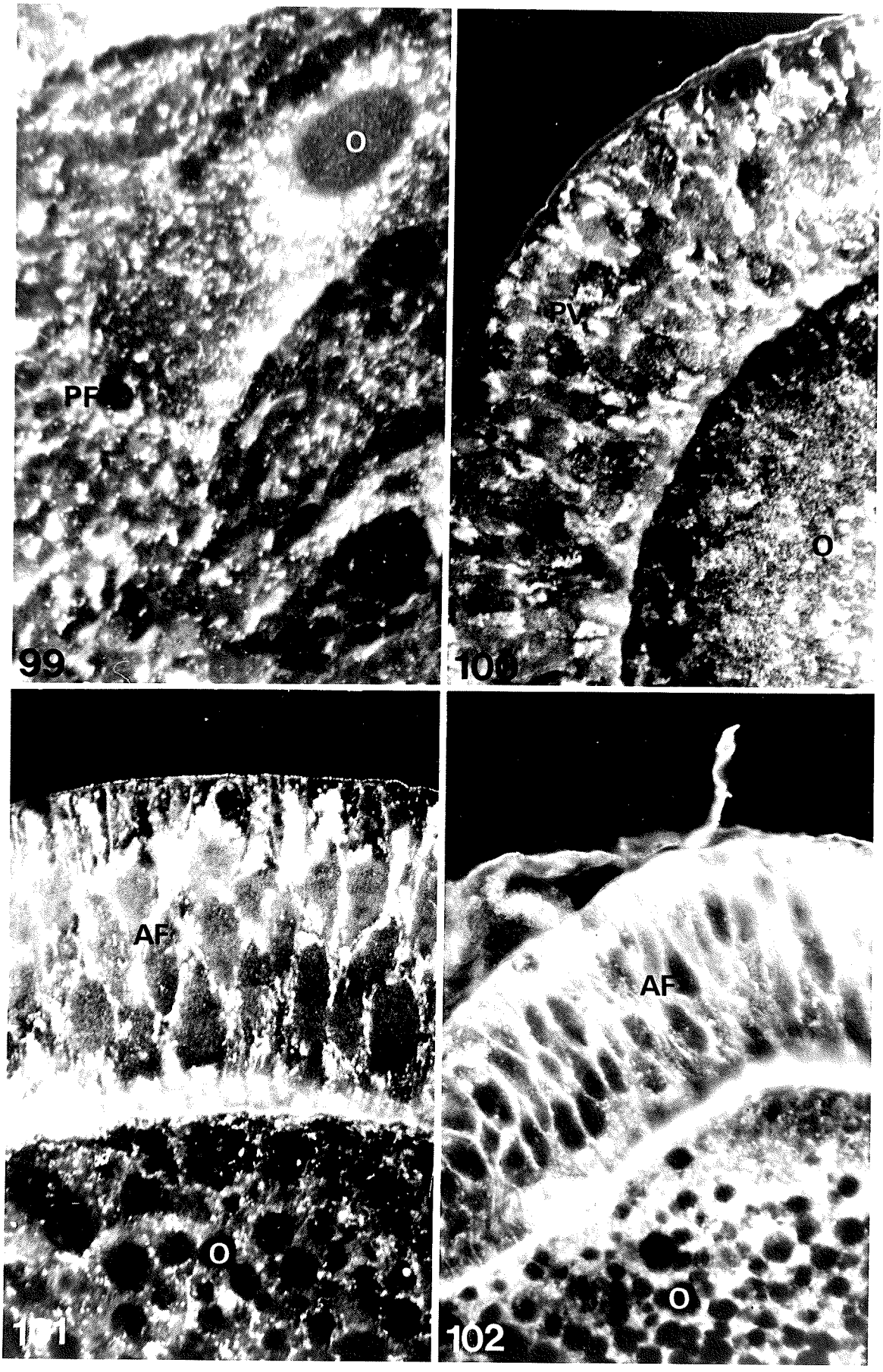
O
PF
99
PV
O
100
AF
O
101
AF
O
102

Plate 17

Prefollicular Cells

Figure 103. Anti-tubulin labelled fluorescence patterns of 3.0% paraformaldehyde - 0.5% glutaraldehyde fixed prefollicular tissue (5μ M paraffin sections). Note lateral bands of fluorescence as well as the fluorescence parallel to the basal lamina. X750.

Figure 104. Low magnification TEM of prefollicular cells. X16,900.

Figure 105. This TEM shows the lateral longitudinal distribution of microtubules (arrows) within the prefollicular cells. X33,000.

Figures 106 and 107. The presence of cross sectioned profiles of microtubules (arrows) with associated microfilamentous material concentrated at the basal ends of cells attached to the basal lamina, is illustrated in these TEM's. X25,000, X68,600.

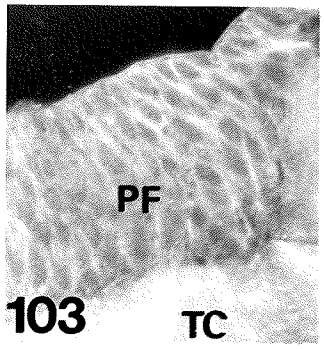

103

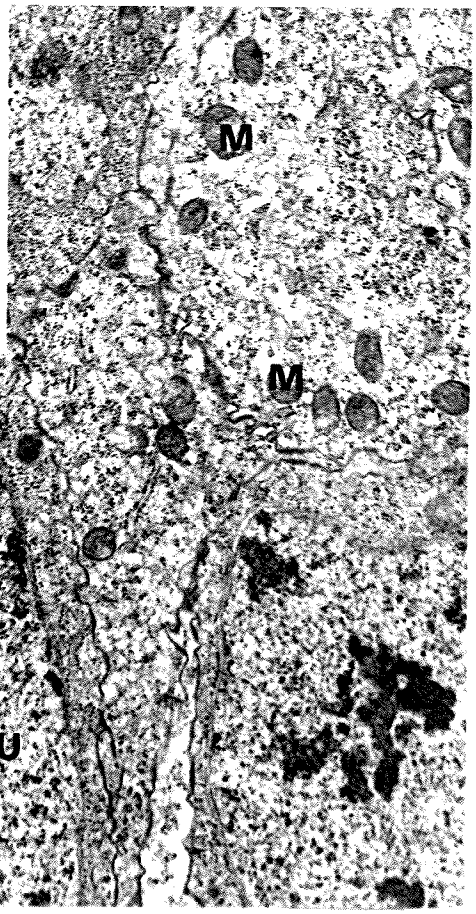

104



105

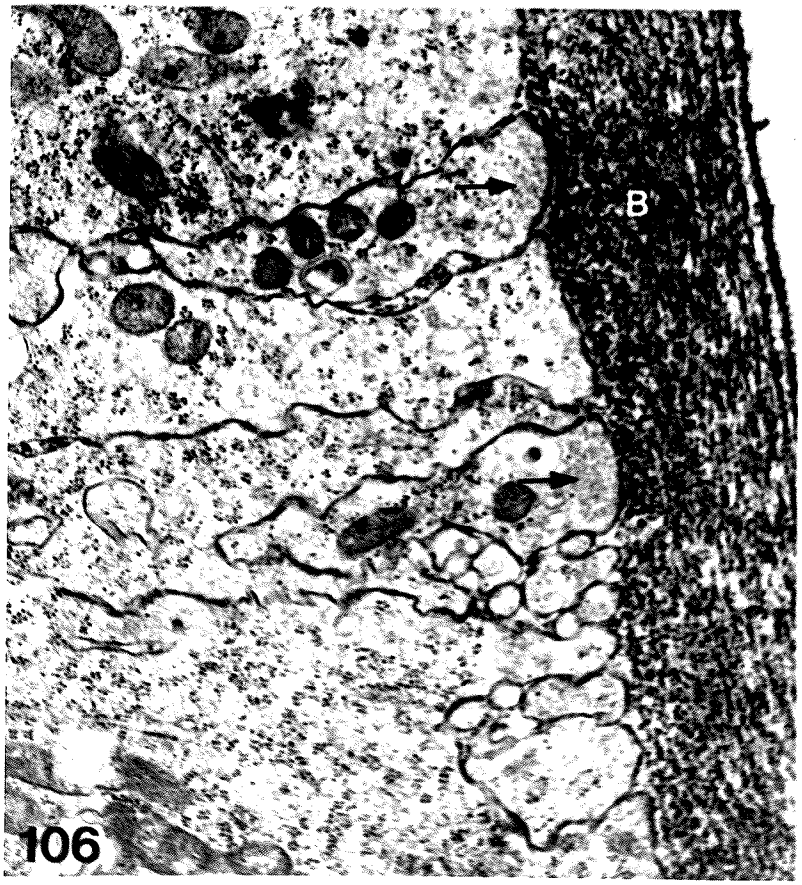

106



107

Plate 18

Previtellogenic Follicle Cells

Figure 108. This LM of a 1.0% paraformaldehyde, Epon-Araldite embedded 1 μM tissue section demonstrates the bright lateral bands of anti-tubulin fluorescence in previtellogenic follicle cells. X850.

Figure 109. This grazing TEM section reveals a dense array of longitudinally oriented microtubules (arrows) just under the plasmalemma. X31,000.

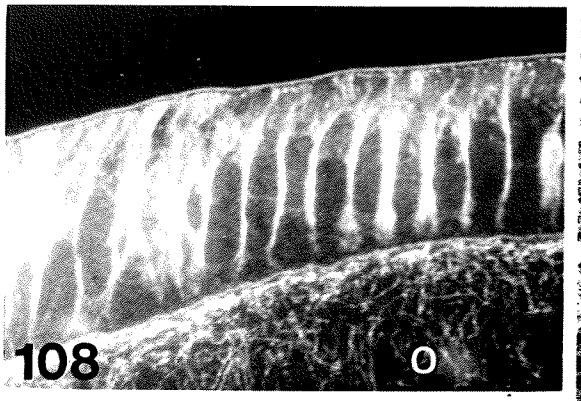
108
O

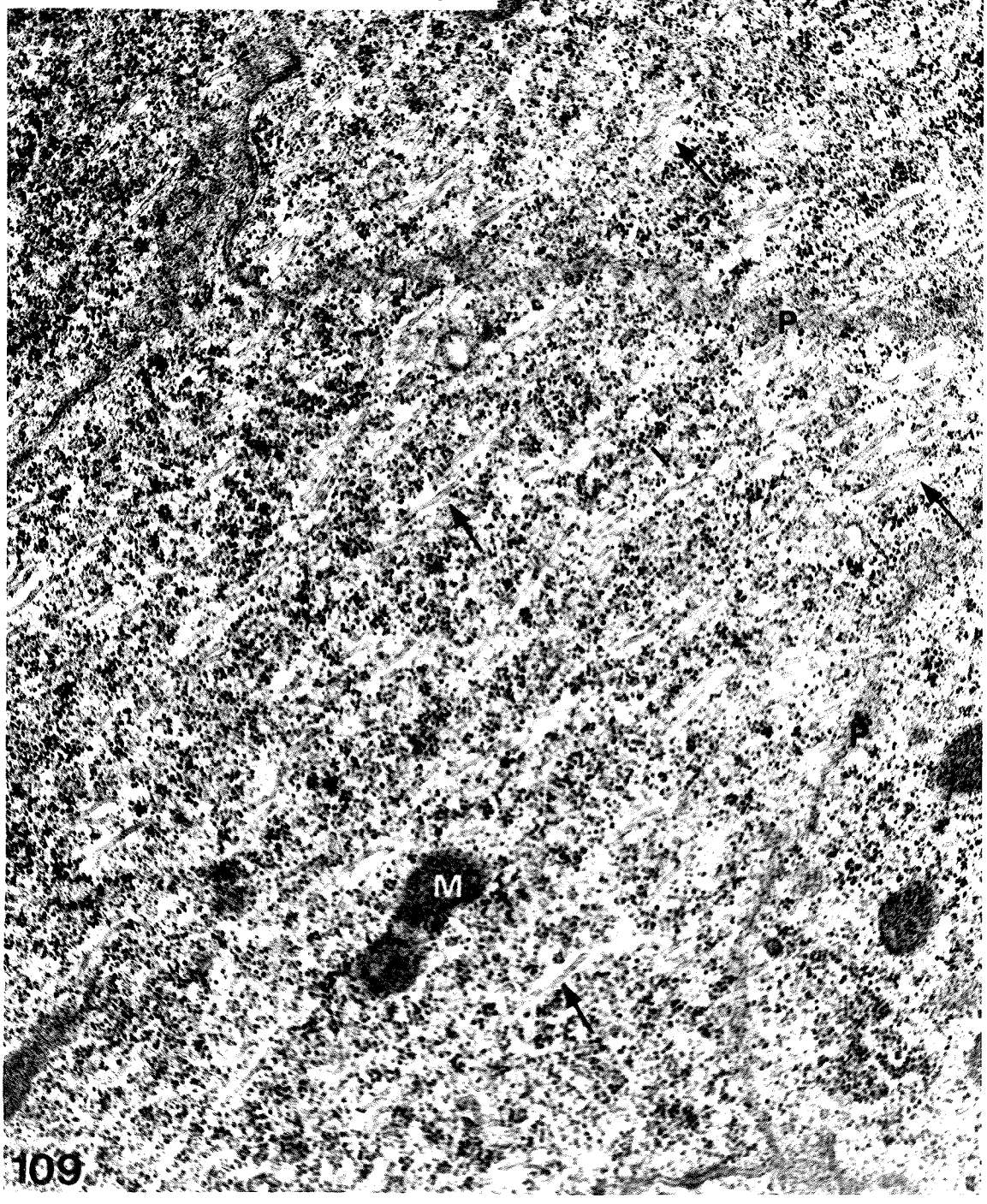
P
P
M
109

Plate 19

Previtellogenic Follicle Cells

Figures 110 and 111. Microtubules (arrows) are densely organized along the lateral edges of these cells as illustrated in these TEM's. X21,500, X32,700.

Figure 112. This Triton X-100 detergent extracted preparation also reveals numerous longitudinally oriented microtubules. (arrows) Note extracted areas (*). X44,000.

Figure 113. Oblique TEM section verifies the orientation of the microtubules (arrows) along the cell circumference. X23,000.

Figure 114. This TEM displays the subplasmalemmal microfilament band running parallel to the basal lamina. X47,000.

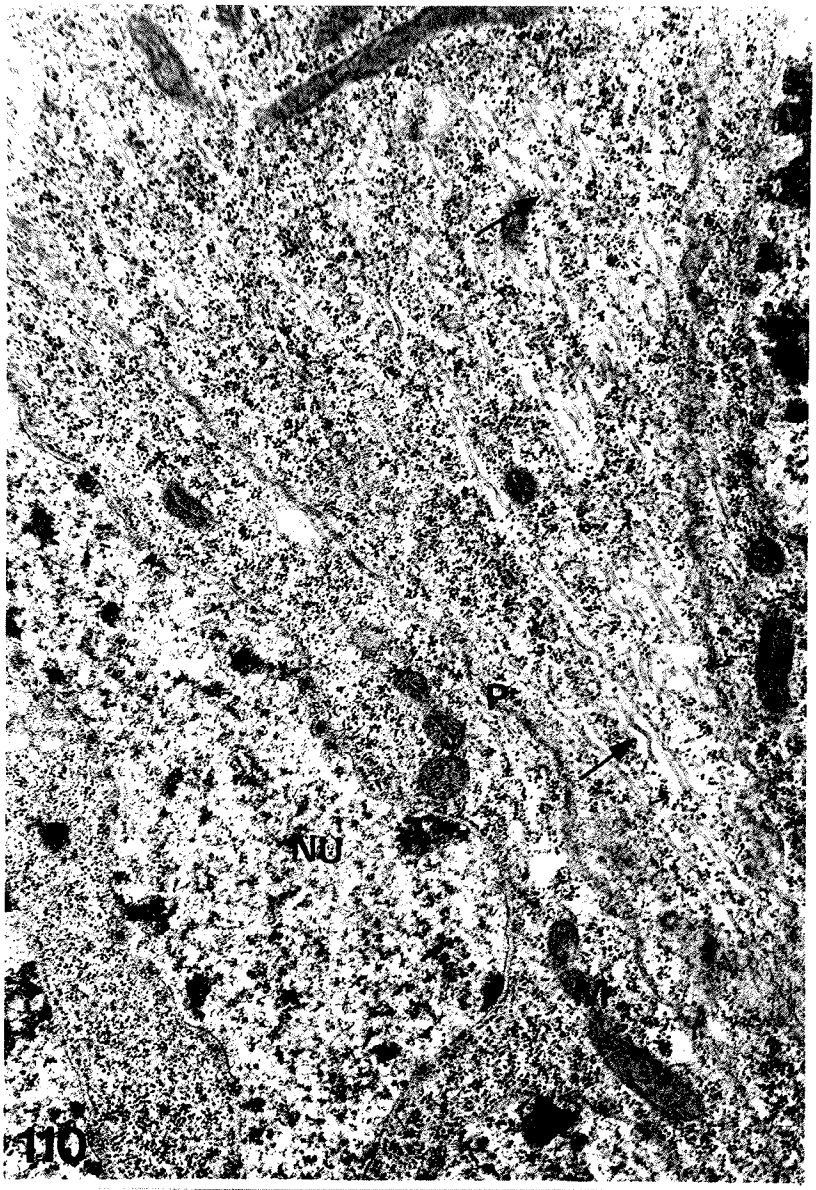

110



111



112

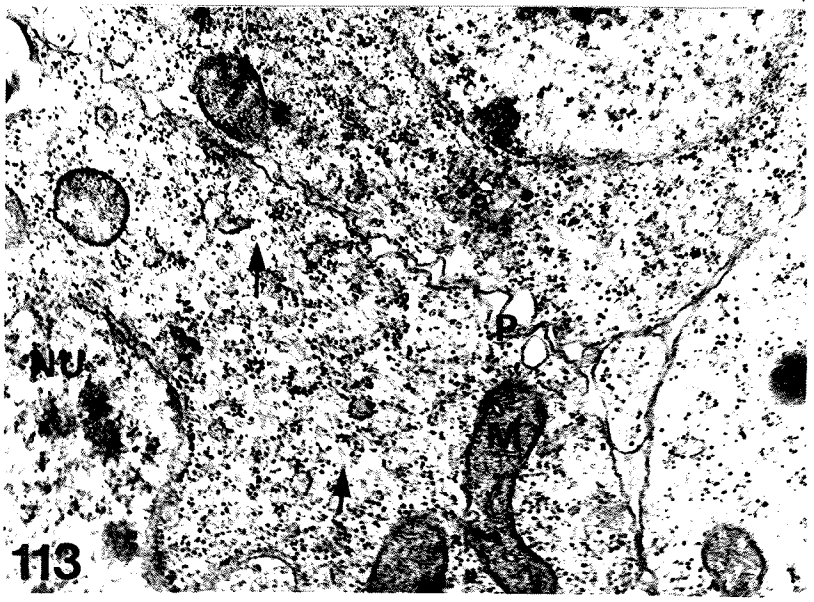

113

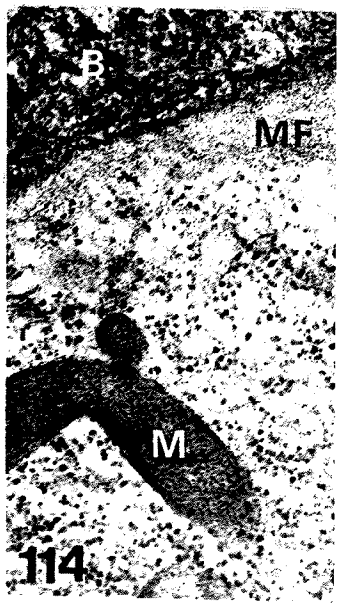

114

Plate 20

Previtellogenic Follicle Cells

Figures 115 and 116. Microtubules (arrows) are less numerous in the basal ends of these cells as revealed by these cross section TEM's. X29,000, X27,000.

Figure 117. Very early vitellogenic follicle cells retain a microtubule distribution (arrows) similar to previtellogenic cells. Cross section, TEM. X36,000.

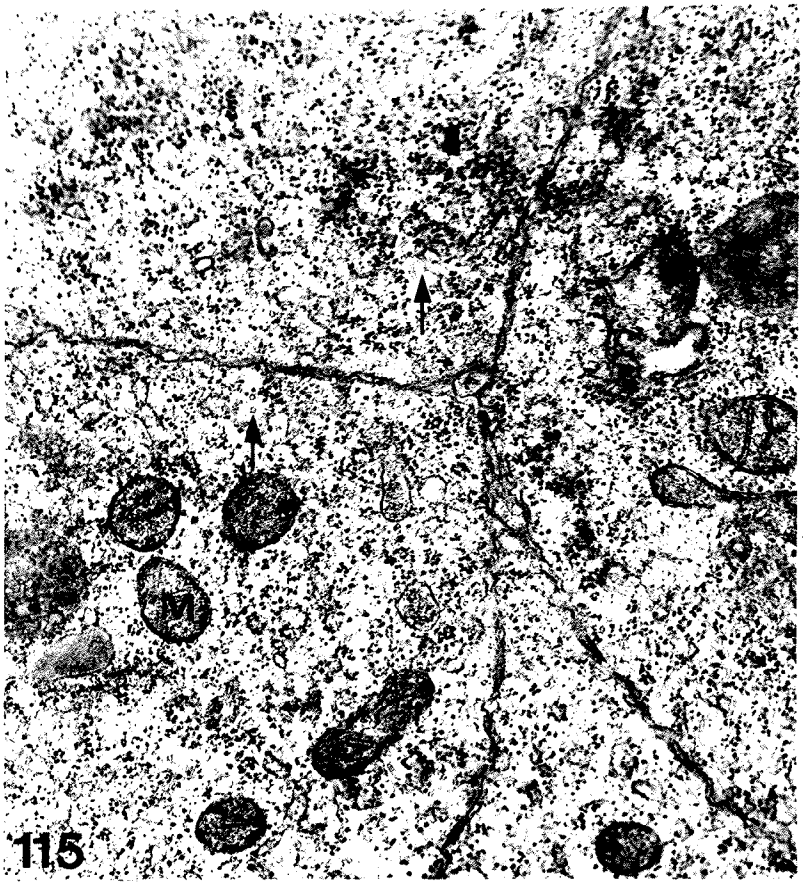
M
115


116

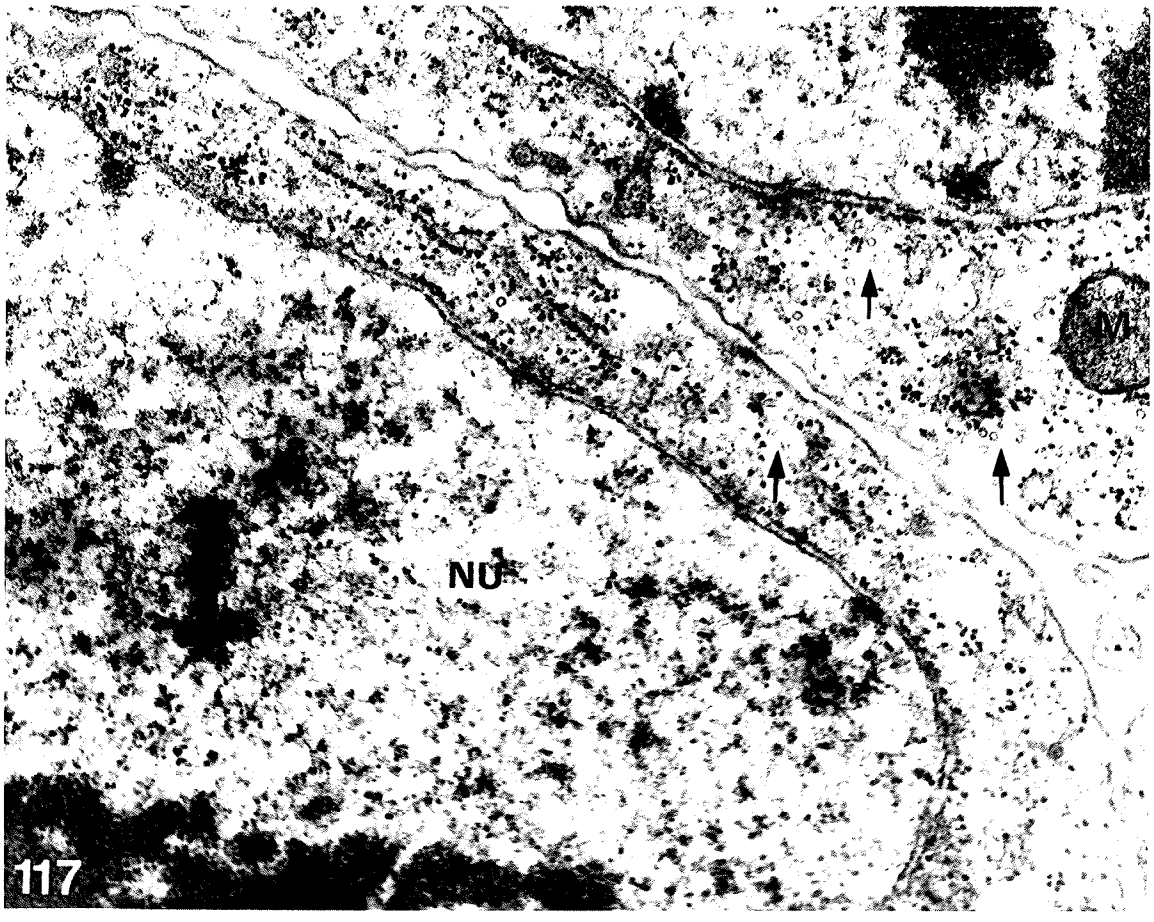
M
NU
117

Plate 21

Immunofluorescence: Vitellogenic Follicles

Figure 118. This 5 μM paraffin section displays the difference in the anti-tubulin fluorescence pattern between the lateral vitellogenic follicle cells and the apical follicle cells. X700.

Figures 119 and 120. Immunofluorescent anti-tubulin staining pattern of apical vitellogenic follicle cells is illustrated in these 5 μM paraffin section and 1 μM Epon-Araldite section, respectively. Note the finer detail at the cell's basal end (*) in the 1 μM epoxy section. X1,100, X900.


AF
O
118

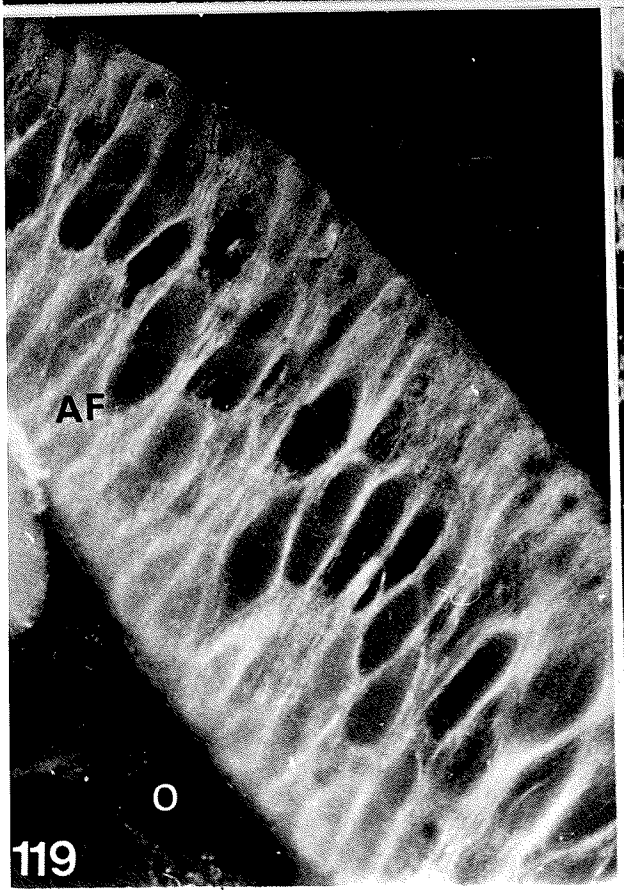
AF
O
119

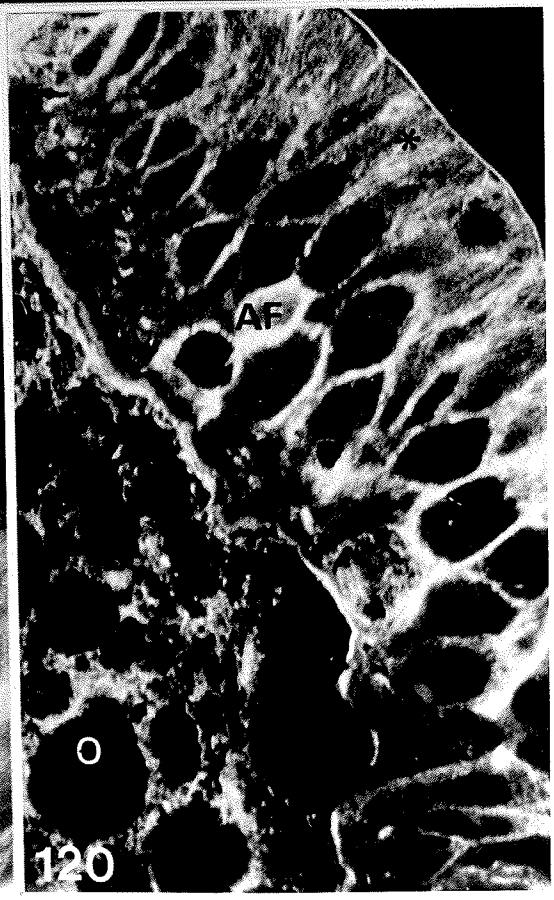
AF
O
120

Plate 22

Apical Vitellogenic Follicle Cells

Figures 121 and 122. TEM's showing a dense array of longitudinal microtubules (arrows) just beneath the cell membrane. X57,000, X29,000.

Figure 123. This thin section shows the lateral distribution of the longitudinal microtubules. Note the microtubules (arrows) proximity to the plasma membrane and that they are not structurally connected to each other. X43,000.

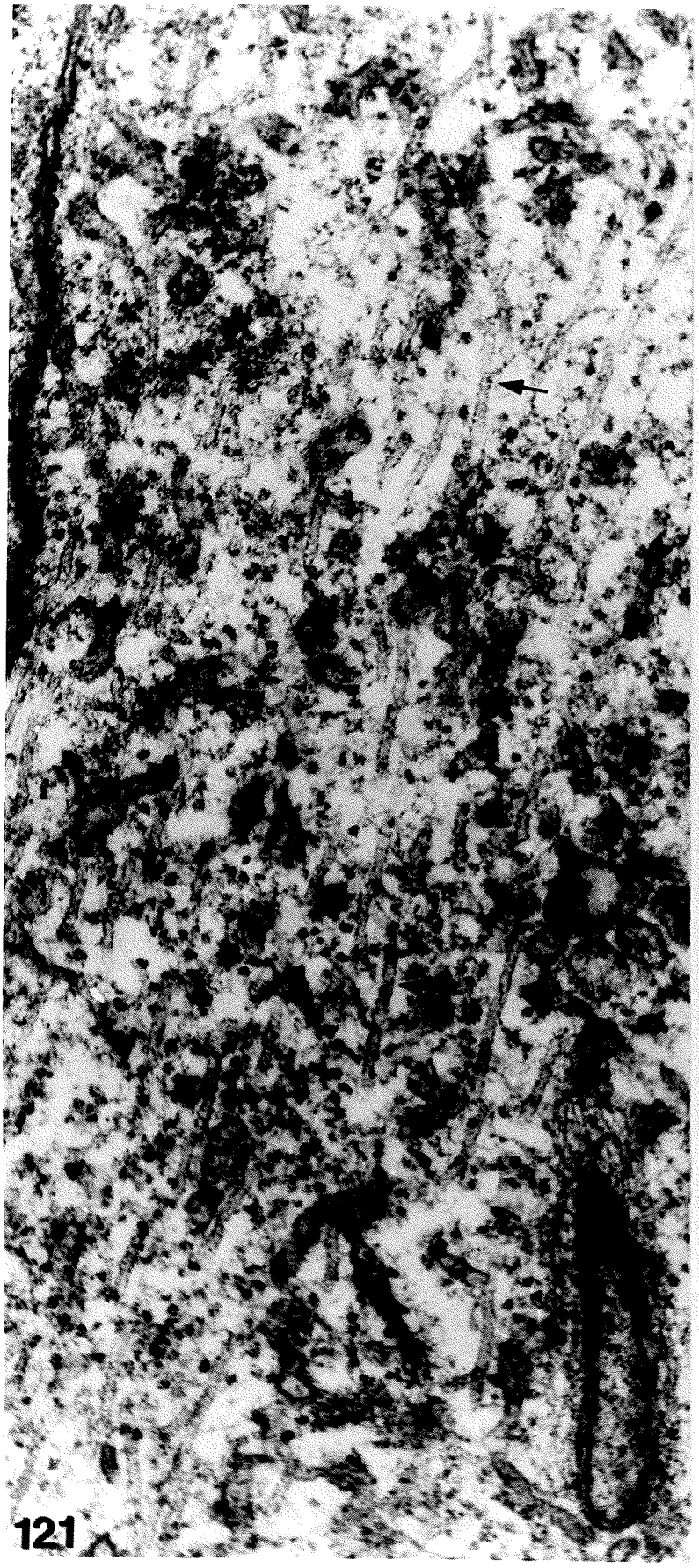

121



122



123

Plate 23

Apical Vitellogenic Follicle Cells

Figure 124. This TEM reveals the close apposition of the long microtubules. (arrows) X80,000.

Figure 125. This thin section demonstrates that the microtubules (arrows) are evently distributed along the lateral length of these cells. X31,000.

Figure 126 inset. The cross section TEM and LM inset show the tight apposition of apical cells during vitellogenesis. Extracellular spaces are absent. X8,500, X650.

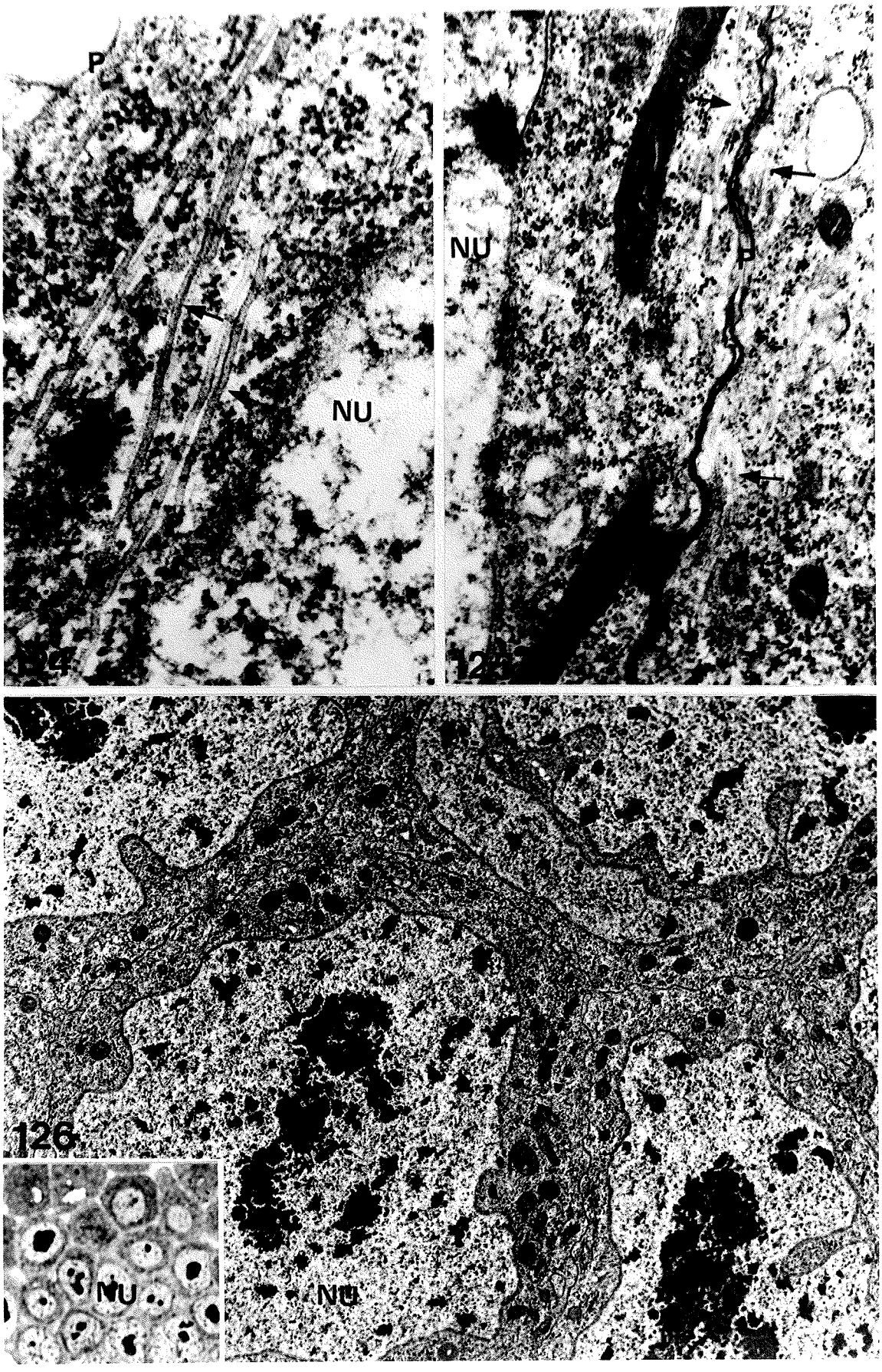
P
NU
NU
P
126
NU
NU

Plate 24

Apical Vitellogenic Follicle Cells

Figures 127 and 128. Microtubules (arrows) are not as densely distributed in the apical ends of these cells as revealed in cross section, TEM. X28,500, X25,700.

Figures 129 and 130. Cross section in the nuclear area of these cells demonstrate numerous cross section profiles of microtubules (arrows). X22,000, X25,000.

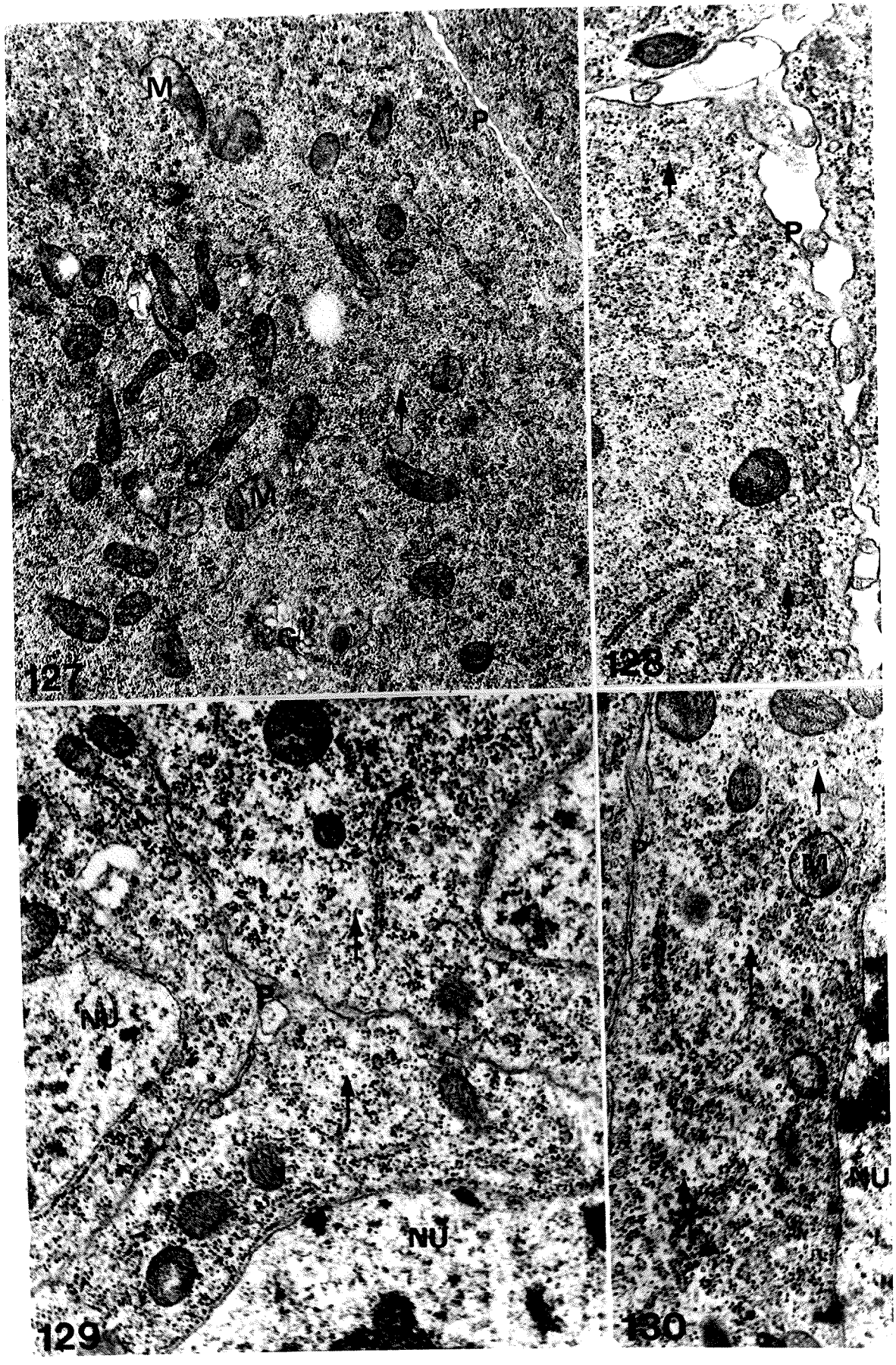
M
P
M
127
P
128
NU
P
NU
129
M
NU
130

Plate 25

Lateral Vitellogenic Follicle Cells

Figure 131 and inset. These fluorescence, LM's of anti-tubulin stained paraffin and Epon-Araldite sections show the diffuse pattern observed in the lateral vitellogenic cells. Note in the epoxy sections, thin discrete fluorescent lines can be resolved. X900, X750.

Figure 132 and inset. Numerous microtubules (arrows) in both longitudinal and transverse profiles are observed in longitudinal thin sections of these cells. Microfilaments also occur just beneath the cell membrane (inset). X16,300, X25,000.

Figure 133. The exclusion of ribosomes and other cell organelles by the subplasmalemmal band of microfilaments is revealed in this TEM. X31,600.

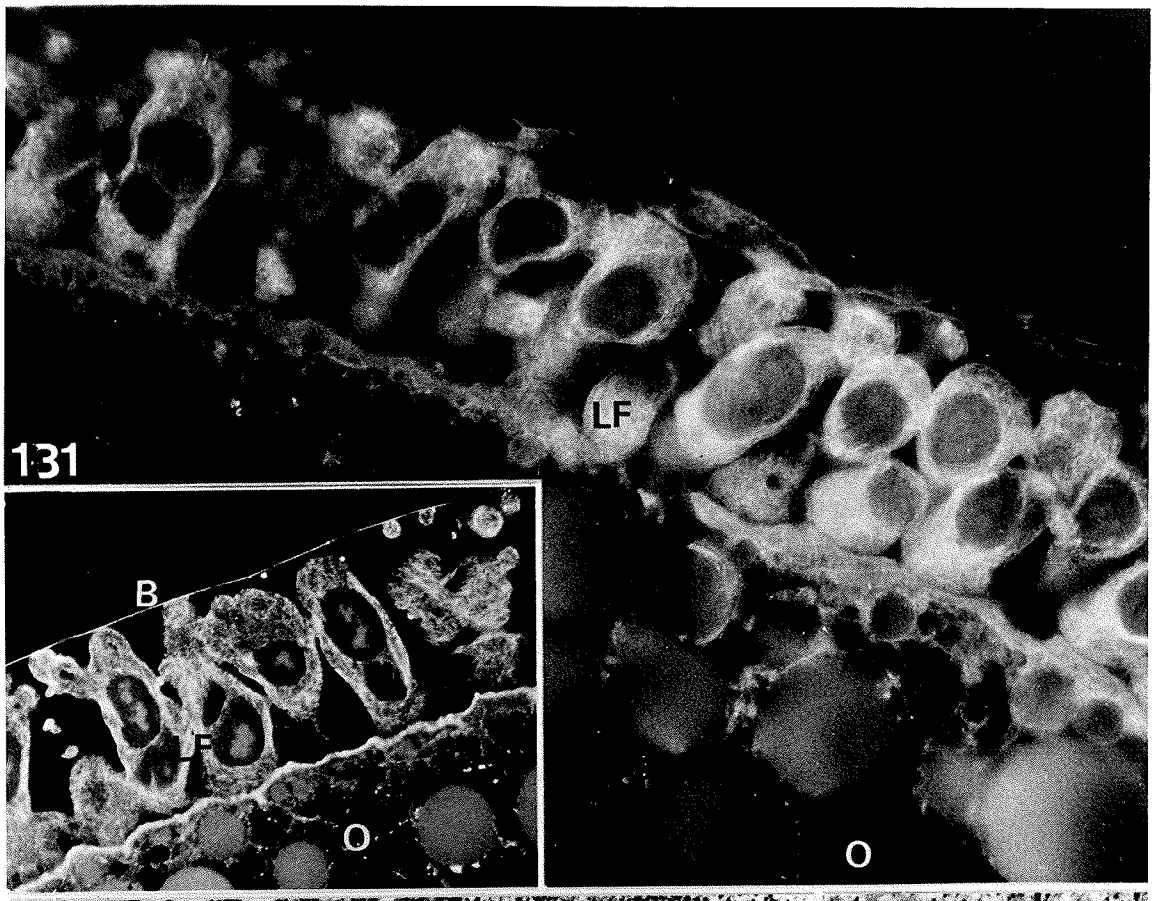
LF
131
B
F
O
O

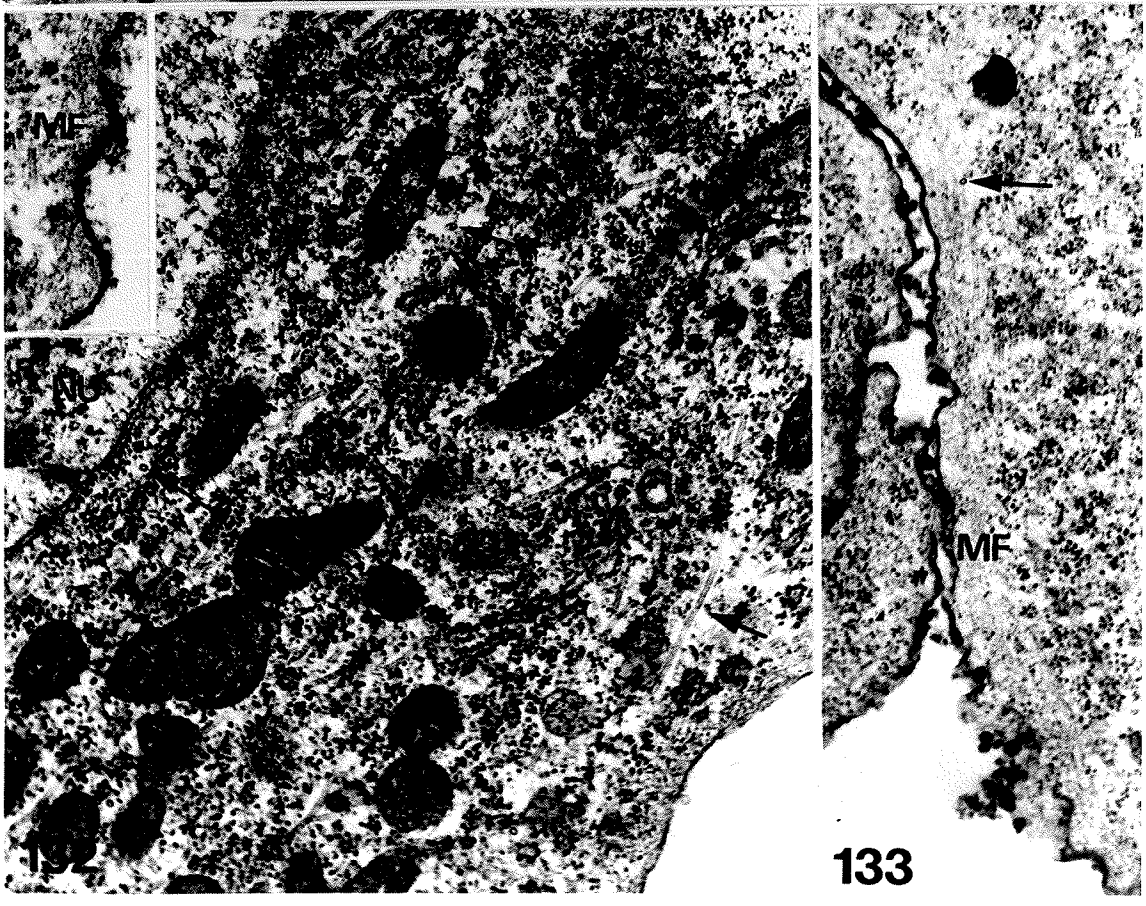
MF
Nu
MF
132
133

Plate 26

Vitellogenic Lateral Follicle Cells

Figure 134 and inset. These cross sections of lateral vitellogenic follicle cells (fig. 134) depicts the anti-tubulin fluorescence staining in 5 μM paraffin sections. Note the diffuse fluorescent staining pattern. The 1 μM epoxy section (inset) shows the cell nuclei and large extracellular spaces. (*) X900, X500.

Figures 135, 136 and inset. These cross section TEM's show the microtubule (arrows) and microfilament distribution within the lateral cells. Note there are both cross section and longitudinal profiles of microtubules. X34,300, X35,200, X73,000.

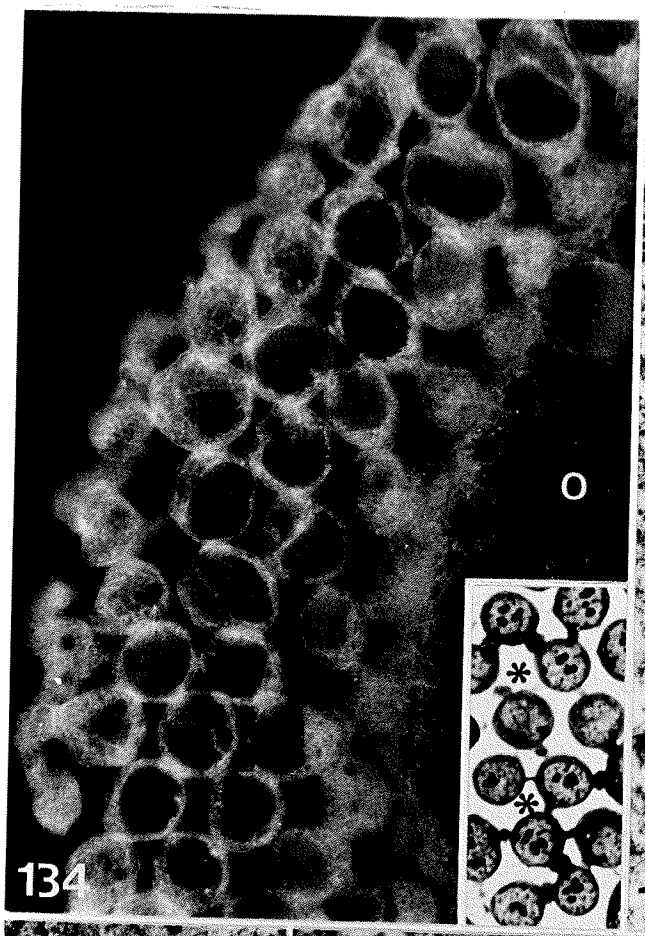
O
134

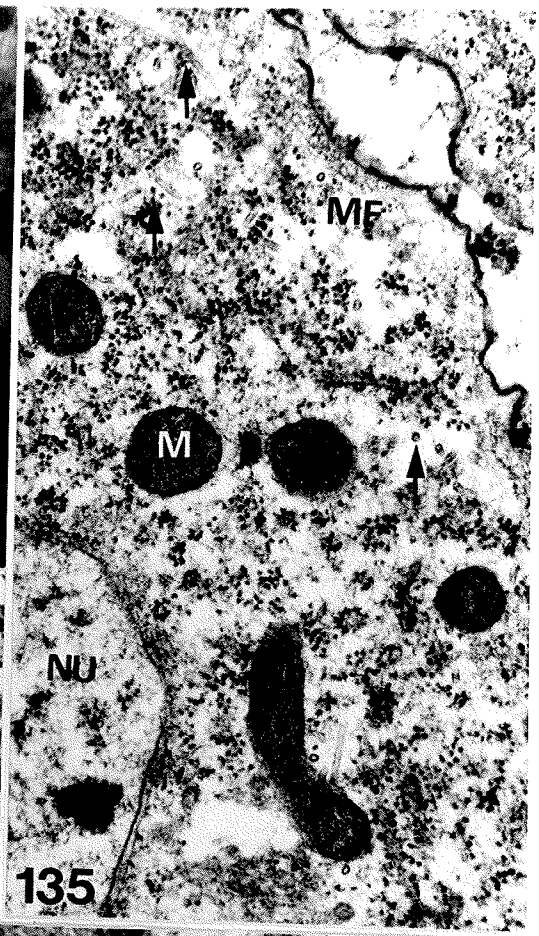
MF
M
NU
135

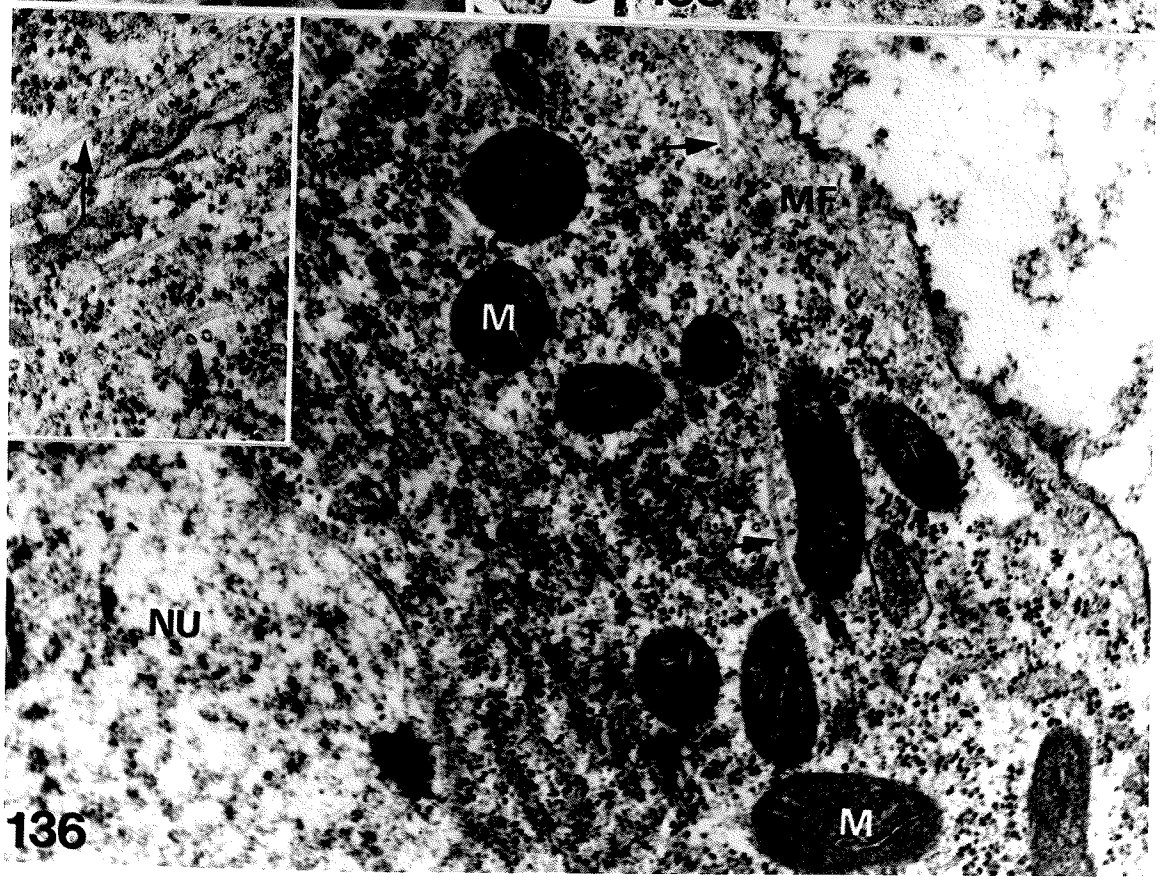
MF
M
NU
M
136

Plate 27

Vitellogenic Lateral Follicle Cells

Figure 137. The presence of microtubules (arrows) within the lateral arms is illustrated in this TEM. X34,000.

Figure 138. Microfilaments within the lateral arms are seen in this TEM. X35,200.

Figures 139 and 140. The microfilaments of the apical microvilli of the lateral vitellogenic follicle cells are noted in these TEM's. X65,000, X41,000.



137



138

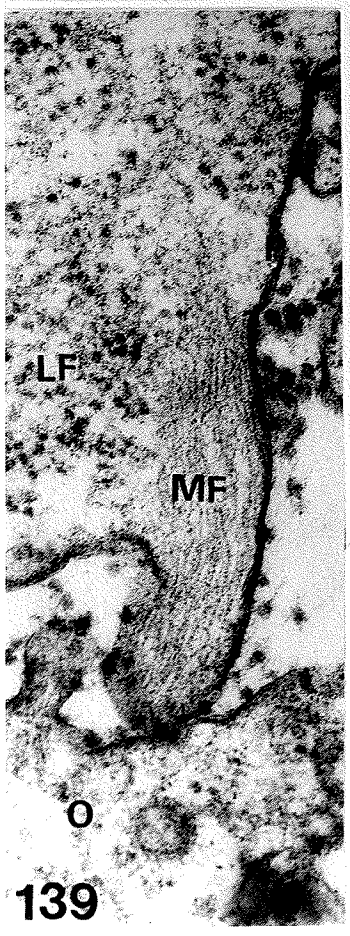

139

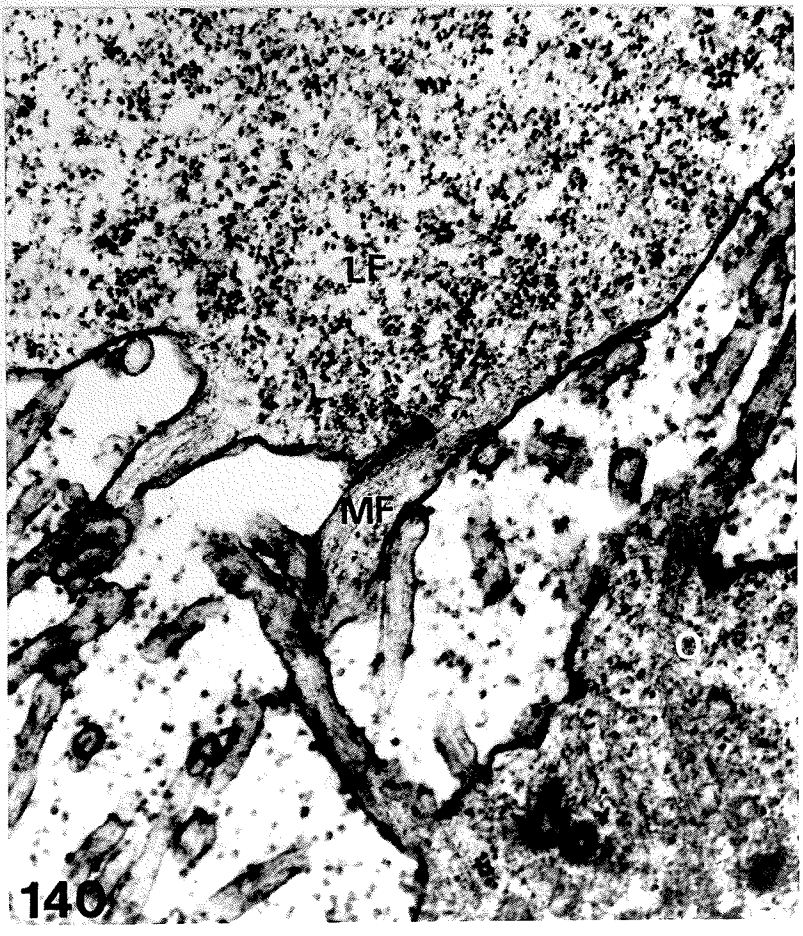

140

Plate 28

Post-Vitellogenic Follicle Cells

Figure 141. Microtubules (arrows) in the basal ends of these cells are illustrated in this TEM. X61,000.

Figure 142. This figure depicts the anti-tubulin staining fluorescence pattern in a 1μ M Epon-Araldite section. X550.

Figure 143. This TEM reveals the relative scarcity of microtubules in the apical part of the post-vitellogenic follicle cells. Note the beginning of chorion formation (arrows). X24,000.

Figure 144. A few microtubules (arrows) and disperse areas of microfilaments along the lateral cell edges are revealed in this TEM. X26,700.


B
141

O
142

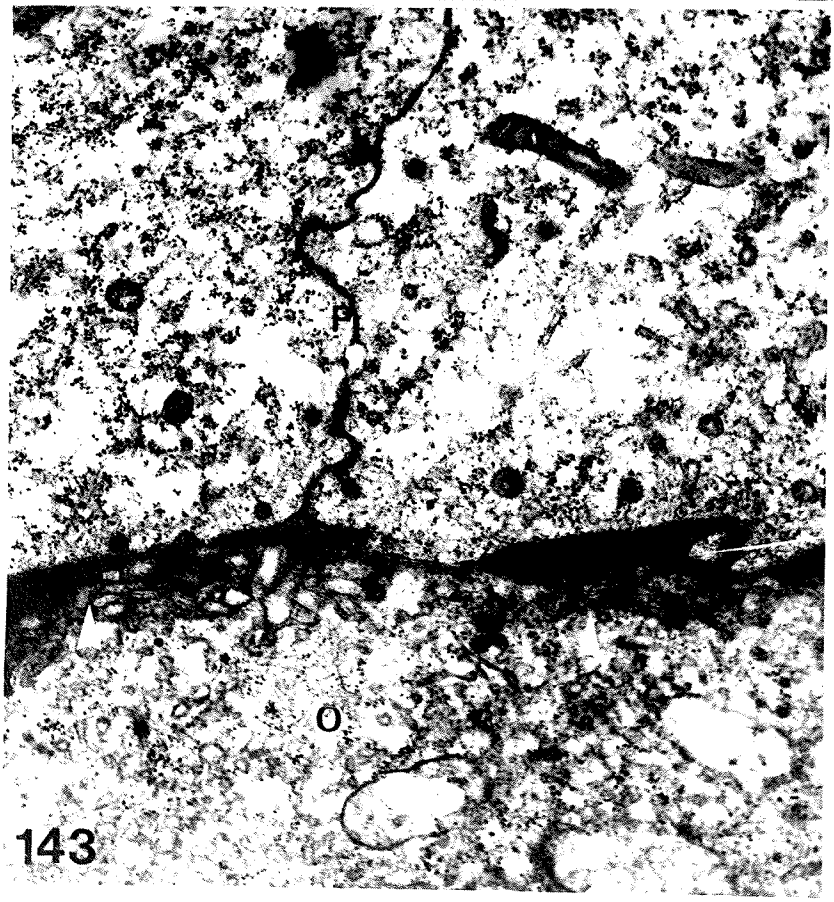
P
O
143

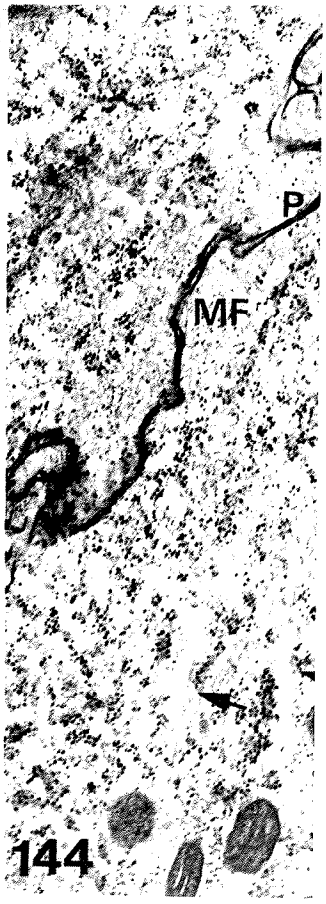
P
MF
144

Discussion

Methodology of Cytoskeletal Visualization and Isolation

Overview

Consideration and critical application of the methodology plays a very important role not only in the visualization of the cytoskeleton, but also in the validity and interpretation of the results relative to the *in vivo* situation. Several methods have been used to isolate cytoskeletal preparations in many diverse eukaryotic systems. These methods include: application of routine TEM and thin sectioning, of normal as well as detergent extracted cell and tissue preparations; high voltage electron microscopy (HVEM) (Glauert, 1974), on whole mounted critical point dried tissue culture cells (Buckley and Porter, 1975; Wolosewick and Porter, 1979 and Temmink and Spiele, 1980), or detergent extracted whole mounted critical point dried cells (Schliwa and Von Blerkom, 1981), as well as thick sections of tissue embedded in polyethylene glycol (PEG) (Wolosewick, 1980). A three dimensional model of the cytoskeletal organization can be generated by computer reconstruction of serial thin sections (Ghosh, 1981). The new quick freeze, freeze fracture-deep etch technique has provided dramatic views of cytoskeletal organization in some cell systems (Heuser and Kirshner, 1980 and Heuser, 1981). Batten *et al.* (1980) utilized physical lysis, freeze drying and rotary shadowing to achieve similar results. With the production of various antibodies specific for cytoskeletal proteins (Lazarides and Weber, 1974; Weber and Groeschel-Stewart, 1974; Weber *et al.*, 1975; Fujiwara and Pollard, 1976 and Franke *et al.*, 1978),

immunofluorescence methods are also extended to the localization of cytoskeletal proteins.

Application of some of these methods (HVEM, and freeze fracture-deep etch technique) requires access to very specialized equipment. Also, most of these methods were primarily developed for tissue culture cell systems. Application to whole tissues such as the follicle cell epithelium, necessitated the development of modified methods. In view of the facilities available, time constraints and feasibility, this study utilized TEM on normal and detergent extracted specimens as well as the indirect immunofluorescence methods.

Fixations and buffer composition

The most important factors influencing the preservation and visualization of the cytoskeletal elements includes the buffer composition, the addition of tannic acid (TA) to the prefixation and minimizing the exposure to OsO_4 during post fixation.

Modified Karnovsky's fixative provided excellent routine preservation of follicle cell cytoskeletal elements. Sodium cacodylate and sodium phosphate buffers are often used for routine aldehyde fixation (Sabatini et al., 1963), but they may not be the optimal buffers for the preservation of cytoskeletal elements, as microtubules isolated from chick brain can depolymerize upon exposure to these buffers (Luftig et al., 1977). The buffer composition becomes even more important with the application of detergent extraction techniques. The buffer under these conditions must maintain the organization of the cytoskeletal elements until fixation of the tissue has occurred.

The composition of cytoskeletal stabilization buffers is based upon biochemical studies of *in vitro* polymerization of microtubules (Synder and McIntosh, 1976 and Dustin, 1978). Weisenburg (1972) found that optimal polymerization of rat brain tubulin occurred under the following conditions: (1) tubulin concentration of at least 1 mg/ ml, (2) presence of guanosine nucleotides, (3) absence of Ca^{++} (removed by addition of EGTA) but not Mg^{++} and (4) a temperature of 37°C. The addition of 4M glycerol or 1M sucrose can substitute for the nucleotides, but microtubule assembly is greatly accelerated in the presence of guanosine nucleotides (Shelanski *et al.*, 1973). The addition of 4M glycerol to the detergent extraction medium and fixative is often required to achieve optimal retention of microtubules within the cells during cytoplasmic extraction (Bershadsky *et al.*, 1978 and Heuser and Kirschner, 1980). Upon lysis of the cell membrane (during detergent extraction) there is a large increase in the aqueous volume that cellular tubulin subunits are dissolved in (Bershadsky *et al.*, 1978). The concentration of tubulin may be lowered below 1mg/ml, upon which the microtubules begin to depolymerize (Bershadsky *et al.*, 1978). The glycerol maintains a higher concentration of tubulin subunits due to its viscosity and thus can inhibit the rate of microtubule depolymerization (Shelanski *et al.*, 1973). The exposure of ovarioles to concentrations of glycerol as low as 10% resulted in severe shrinkage of all the ovariole structural components including the follicle cells. This necessitated the discontinued use of glycerol, as any induced cell shrinkage in the follicle cells could affect the cytoskeletal organization, making the results obtained uninterpretable.

Schliwa and Von Blerkom (1981) tested over 25 different cytoskeletal stabilization buffers and concluded that the most critical factors for the maintainence of cytoskeletal elements, was the addition of high concentrations (10mM or higher) of EGTA to the buffer. They did not include GTP or glycerol in their buffer (Schliwa and Von Blerkom, 1981). Luftig et al., (1977) utilized a buffer composed of 100 mM Pipes pH 6.9 + 2mM EGTA, 1mM Mg SO_4 and 1mM GTP. They noted increased lengths of microtubules in interphase Hela cells over other fixations using sodium cacodylate or sodium phosphate buffers. This fixation however, did not prove optimal for Rhodnius ovarioles because of the induced tissue shrinkage due to the 5.0% glutaraldehyde and the 100mM Pipes buffer concentration. Similar shrinkage occurred using the cytoskeletal fixative of Batten et al.,. (1980). Since the ovarioles maintained excellent morphology in 60mM Pipes and 25mM Hepes buffer (Schliwa and Von Blerkom, 1981) a hybrid cytoskeletal stabilization buffer was used. The addition of 1mM GTP as recommended by Luftig et al., (1977) to the PHEM buffer (Schliwa and Von Blerkom, 1981), plus the addition of 3.0% glutaraldehyde resulted in the best cytoskeletal preservation of both normal and detergent extraction tissue preparations.

Since microfilaments are often difficult to detect in Epon embedded tissue sections the addition of TA during prefixation is a benefit as it increases the contrast of microfilaments. It also helps to prevent the disruption of microfilament structure in the subsequent OsO_4 postfixation (Maupin and Pollard, 1983). Use of the TA Saponin fixation did provide the easiest detection of microfilaments and microtubules within the follicle cells. The reduced OsO_4 postfixation did not reduce

the overall fixation quality, as membrane structures were still well preserved.

Detergent extractions

This is the first study to apply detergent extraction techniques to intact follicle cell epithelia, attempting to prepare isolated follicle cell cytoskeletons. Triton X-100 is commonly used in many tissue culture cell systems (Osborn and Weber, 1977; Trotter et al., 1978; Osborn et al., 1978; Bershadsky et al., 1978; Rubin et al., 1979; Pudney and Singer, 1980 and Heuser and Kirschner, 1980) with Saponin being less commonly used (Hirokawa and Heuser, 1980 and Parysek and Eckart, 1980).

Triton X-100 and other non-ionic detergents solubilize cell membranes by the formation of mixed micelles with the cell membrane lipid which creates the leakage of most cytoplasmic constituents (Helinius and Simons, 1975). Saponin, unlike Triton X-100 does not solubilize large areas of cell membrane (Hirokawa and Heuser, 1980) instead, tiny holes are produced in the cell membrane through which a rapid extraction of the cytoplasm occurs. Much lower concentrations of Saponin than Triton X-100 to achieve similar extraction of follicle cell constituents were found in this study. Similiar results were reported for human neutrophils where 0.4% Triton X-100 was as effective as 0.04% Saponin (Parysek and Eckart, 1980).

The detergent extractions revealed that unlike most tissue culture cells, the follicle epithelial cells do not contain a dense interacting network of cytoskeletal elements. Detergent extraction preparations of tissue culture cells show the presence of a dense fibrous network of microfilaments which radiate out from the nuclear region (Osborn and

Weber, 1977; Trotter et al., 1978 and Rubin et al., 1979). A dominant feature of their cytoskeleton is the presence of cytoplasmic fibrils consisting of bundles of microfilaments and accessory contractile proteins such as myosin and α-actinin, called stress fibers (Trotter et al., 1978; Pudney and Singer, 1980; Tomasek et al., 1982 and White et al., 1983). Stress fibers are involved in tissue culture cell spreading, attachment to substrate and cell migration or locomotion (Trotter et al., 1978; Tomasek et al., 1982 and Byers and Fujiwara, 1982). Until recently, they have been reported to exist only in tissue culture cells. Byers and Fujiwara (1982) and White et al., (1983) described their presence in fish scale scleroblasts and in vascular endothelial cells respectively. Stress fibers are not found in all endothelial cells or all scleroblasts but rather their presence was correlated with environmental factors such as increased hemodynamic pressure or position of the scleroblasts on the edge of the fibrillary plate, (conditions where large shear forces exist), (Byers and Fujiwara, 1982 and White et al., 1983). Apparently, stress fibres form when these cells require a greater adhesion and structural support to maintain their position in response to an environmental stress (White et al., 1983). These studies show that cells can regulate the organization of their cytoskeleton relative to environmental influences.

Trotter et al., (1978) indicated that there is a large exchangeable soluble pool of actin and myosin in 3T3 cells. This pool can be utilized during periods of environmental pressure to form a more complex cytoskeletal scaffolding to increase cell adhesiveness to its substrate or to initiate cell migration away from the source of stress.

The follicle cells of Rhodnius likely also contain large soluble pools of actin, myosin and other accessory contractile proteins. These cells however, are not exposed to drastic environmental conditions as are tissue culture cells or endothelial cells . One would thus expect to observe a less prominent network of microfilaments within the follicle cells as the detergent extraction experiments revealed. The stimulation of patency is the phase of oogenesis when the largest mechanical stress on the lateral follicle cells would occur. Interestingly this is also the stage when the largest areas of microfilamentous bands appear. As will be discussed further in a later section, one of the principle contributing factors to the observed lateral follicle cell shape change associated with patency, is likely the appearance of these microfilamentous bands.

A key area of concern with these detergent extraction experiments is the successful retention of microtubules and microfilaments, as well as their structural orientations as close to the in vivo condition as possible. Polymerized microtubules were retained in all the extraction experiments, but the maintainence of their position within the cell was not always achieved. The use of PHEM buffer, GTP and short extraction times accounts for the degree of retention of polymerized microtubules in my extraction preparations.

The additional problem of removing the basal lamina to achieve unrestricted cell extraction is obviously not encountered in the application of these methods to tissue culture cell systems. Although the basal lamina removal methods were successful, the retention of microtubules within extracted follicle cell preparations was decreased compared to normal non extracted fixations. This result indicated that

the microtubules are not held together in a fixed or integrated fashion within the follicle epithelial cells. Instead they seem to maintain their positions within the cells independently of one another.

Despite the displacement of some microtubules, detergent extractions show that the follicle cells do contain microtubules and except for vitellogenic lateral follicle cells, few areas of dense accumulations of microfilaments.

Basal lamina removal

Although basal lamina removal resulted in difficulties in obtaining optimal detergent extracted follicle cell cytoskeletons' several important observations were made pertaining to the effect of the basal lamina on the maintainence of ovariole morphology and ultrastructure. These experiments have clarified the potential function that the basal lamina plays in its contribution to the development and maintainence of the normal cell to cell interactions of Rhodnius oogenesis (see Huebner, 1984 a,b).

Basement membranes (basal lamina, tunica propria) can be defined as continuous sheets of extracellular matrix material, which in vertebrate systems are composed of type IV collagen, glycoproteins (fibronectin or laminin) and glycosaminoglycans or GAGS (hyaluronic acid, heparin sulfate or chondroitin sulfates) (Dutkowski, 1977; Laurie et al., 1980; Farquhar, 1981; Kleinman et al., 1981; Vaccaro and Brody, 1981; Hayman et al.,1982; Laurie et al., 1982; Sanders, 1983 and Scott, 1983). Basal laminae form substrates upon which all cell types, except connective tissue cells grow (Farquhar, 1981). All true epithelia are defined as resting upon a basal lamina (Bloom and Fawcett, 1975).

Many studies have investigated the role of the basal lamina by observing the effects of its removal via enzymatic digestion or exposure to salines containing high concentrations of EDTA or EGTA (Goel and Jurand, 1968; Jensen and Mottet, 1970; Dutkowski, 1977; Dybowska and Dutkowski, 1977; Banerjee et al., 1977; Vogel, 1978; Liotta et al., 1979 and Bradley, 1981). Bradley (1981) observed the complete removal of the malpighian tubule basal lamina of Rhodnius with elastase III (4 ug/ ml). Elastase type III did not remove the ovariole basal lamina using identical conditions. This suggests structural differences exist between the basal lamina of Rhodnius malpighian tubules and the basal lamina surrounding the ovariole. Collagenase was not effective in removing the malpighian tubule basal lamina (Bradley, 1981) as well as the ovarian basal lamina (this study). These results are not surprising in view of the results of Liotta et al., (1979) who were unable to digest type IV collagen with human skin collagenase although digestion of type I, II and III collagen did occur.

Calcium is known to influence, the effectiveness of enzymatic digestion of basal laminae (Banerjee et al., 1977). Hyaluronidase completely removed the basal lamina of embryonic salivary epithelial cells if calcium was deleted from the digestion medium (Banerjee et al., 1977). This parallels the results observed for trypsin digestion of the ovariole basal lamina. Chondroitin sulfates and other GAGS are known to bind calcium (Banerjee et al., 1977 and Dybowska and Dutkowski, 1977) and the presence of calcium is thought to stabilize the chondroitin sulfate component, which inhibits the rate of enzymatic digestion of the basal lamina (Banerjee et al., 1977). The presence of GAGS in insect basal laminae has not been verified as yet (Ashhurst, 1982).

Indirect evidence however, suggests GAGS may in fact be a component of insect basal laminae (Dutkowski, 1977 and Dybowska and Dutkowski, 1977). Digestion with neuraminidase, hyaluronidase and trypsin all greatly reduced the binding of ruthenium red (a cationic dye) to the fat body and neural lamella basal laminae of Gallaria mellonella (Dutkowski, 1977 and Dybowska and Dutkowski, 1977). This suggested that sialic acid and hyaluronic acid were responsible for the negative charge and thus the binding of the ruthenium red to the insect basal lamina. This could explain why trypsin did not remove the basal lamina in normal Rhodnius saline containing calcium.

The addition of 2mM EGTA to the calcium free saline accelerates the separation of the basal lamina from the ovariole surface. This EGTA effect was also observed in the basal lamina of chick limb buds (Goel and Jurand, 1968) and in the separation of chick embryonic epidermis from its attached mesenchyme (Jensen and Mottet, 1970). The chelation of calcium may weaken the GAG mediated attachment of the basal lamina to the ovariole.

The effectiveness of pronase in all salines is due to its non-specific proteolytic activity. Dutkowski (1977) reported that pronase digestion damaged the basal lamina and cell membranes of fat body cells, allowing ruthenium red to enter the cells. For this reason trypsin digestion of the basal lamina was used in favor of pronase digestion.

The ultrastructural changes associated with the 1 hour trypsin digestion have been observed in many other systems (Jensen and Mottet, 1970; Banerjee et al., 1977; Vogel, 1978 and Sugrue and Hay, 1981). These ultrastructural changes have demonstrated a function of the

ovarian basal lamina in the maintainance of normal ovariole shape and cell to cell interactions.

Basal laminae are involved in many processes such as tissue morphogenesis (Vaccaro and Brody, 1981), tissue repair (Fujikawa et al., 1974), regulation of the permeability of macromolecules (glomerular basement membrane) (Farquhar, 1981), modulation of epithelial cell polarity (Greenburg and Hay, 1982), maintainence of epithelial cell shape and cytoskeletal organization (Sugrue and Hay, 1981) and also mechanical roles such as the basal lamina of Aedes aegypti midgut (Reinhardt and Hecker, 1973).

The elegant study of Sugrue and Hay (1981) showed that loss of contact with basal lamina components directly induces morphological changes in corneal epithelial cells. These cells extend basal blebs after basal lamina removal. Associated with bleb formation there is a reorganization of the dense bands of microfilaments which underlie the cell membrane and normally run parallel to the basal lamina (Sugrue and Hay, 1981). Upon culturing, these microfilamentous bands reorganize to form a network underlying the cell membrane within each bleb (Sugrue and Hay, 1981). The prefollicular cells, previtellogenic follicle cells and nurse cells of Rhodnius produced similar surface projections and blebs upon basal lamina removal. Microfilamentous bands are also similarily observed in Rhodnius prefollicular, previtellogenic and in particular vitellogenic lateral follicle cells prior to basal lamina removal. Upon removal, these bands disappear and blebs form. No microfilamentous network was observed to form in the follicle cell blebs, during the short time prior to fixation. No attempts were made to culture these cells.

In vertebrate systems much is known about the interactions of the basal lamina components and associated glycoproteins such as fibronectin and laminin, in terms of modulating cell adhesion to basal laminae and the maintainence of cell shape and cytoskeletal organization (Kleinman et al., 1981; Sugrue and Hay, 1981; Greenburg and Hay, 1982 and Grinnel et al., 1982). Similiar work in insect systems is lacking with the presence of molecules like fibronectin and laminin unconfirmed (Ashhurst, 1982). The similarity of the response to basal lamina removal between the Rhodnius follicle cell epithelium and the vertebrate corneal epithelium is encouraging for the prospect that the maintainence of follicle cell polarity, shape and cytoskeletal organization is, at least in part, regulated by the basal lamina. I am unaware of any other study on insect epithelia concerning this aspect.

Immunofluorescence methods

Since Coomb's 1941 original methods, immunofluorescence has become a powerful technique, widely used to localize cytoskeletal proteins. Examples include the distribution of tubulin (Weber et al., 1975), actin (Lazarides and Weber, 1974), myosin (Weber and Groschel-Stewart, 1974) and intermediate filaments (Franke et al., 1978) in tissue culture cell systems. The use of tissue culture cells minimizes problems such as tissue handling, fixation, cell permeabilization and the use of embedding media. Immunofluorescence methods have only recently been extended to whole tissues in situ (Bretscher and Weber, 1978; Berthold, 1980; Harris et al., 1980; Byers and Fujiwara, 1982 and White et al., 1983). Immunofluorescence has also been applied to frozen cryostat sections (Franke et al., 1978), paraffin embedded tissue sections

(Bussolati et al., 1980; Kramer, 1981 and Valnes and Brandtzaeg, 1981), polyethylene glycol (PEG) embedded tissue sections (Repetto-Antoine et al., 1982 and Wolosewick and DeMay, 1982) and most recently to plastic embedded tissue sections (Rodning et al., 1980; Hogan and Smith, 1982 and this study).

The adaptation of these methods to whole cells, such as isolated intestinal epithelial cells (Bretscher and Weber, 1978), sea urchin oocytes (Harris et al., 1980) or intact follicle epithelial cells, as in this study, results in a decreased fluorescence resolution due to the cell thickness. Tissue culture cell systems offer high resolution due to their thinness, resultant from spreading in culture (Lazarides and Weber, 1974; Weber and Groschel-Stewart, 1974; Weber et al., 1975; Cande et al., 1977; Franke et al., 1978 and Osborn et al., 1978). Application of these methods to whole cells would provide the most ideal and direct way of visualizing the cytoskeleton (Berthold, 1980; Byers and Fujiwara, 1982 and White et al., 1983). However the poor fluorescence resolution necessitates using sectioned material.

Commonly, formaldehyde fixation is combined with either postfixation in acetone and methanol at -20°C (Lazarides and Weber, 1974; Weber et al., 1975; Schliwa et al., 1978 and White et al., 1983) or with detergent extraction with Triton X-100 prior to fixation (Cande et al., 1977; Osborn et al., 1978; Webster et al., 1978; Drenckhahn and Groschel-Stewart, 1980 and Byers and Fujiwara, 1982) to permeablize the tissue allowing the antibodies access to the cytoskeletal proteins. Fixation of sea urchin oocytes with 90% methanol + 50mM EGTA was suitable for microtubule localization, while fixation with 100% methanol was not (Harris et al., 1980).Possibly microtubules depolymerized due to the

release of intracellular calcium in the 100% methanol fixation (Harris et al., 1980). Classical fixations with Bouins or buffered formalin are also used with success (Lazarides and Weber, 1974; Weber et al., 1975; Bussolati et al., 1980 and Kramer, 1981).

Fixation with paraformaldehyde and glutaraldehyde should be used with some caution. Glutaraldehyde fixation results in the best preservation of intracellular constituents, but also creates a bright nonspecific background fluorescence. This is due to the crosslinking action of glutaraldehyde fixation and the number of bound aldehyde groups in the tissue (Cande et al., 1977; Harris et al., 1980 and Osborn and Weber, 1982).

Specialized methods, such as exposure of tissues to a sodium borohydride ($NaBH_4$) (an aldehyde reducing agent) solution following glutaraldehyde fixation are suggested to suppress the nonspecific background fluorescence (Osborn and Weber, 1982 and Wolosewick and DeMay, 1982). In this study, however, I chose to minimize the nonspecific fluorescence by selection of the fixation components. The use of paraformaldehyde fixation alone was criticized by Harris et al., (1980) due to the poor ultrastructural preservation and shrinkage it can cause in tissues. It does however, preserve microtubule arrays and yields very little nonspecific background fluorescence (Harris et al., 1980 and Osborn and Weber, 1982). In combination with plastic embedding and its removal after sectioning, only the paraformaldehyde fixations resulted in acceptable levels of nonspecific background fluorescence.

For paraffin embedded tissues the problems of nonspecific fluorescence were less severe and thus the paraformaldehyde-

glutaraldehyde fixation method of Repetto-Antoine et al., (1982) was used. Incubation of the tissue sections in BSA solution prior to exposure to the antibodies also reduced the incidence of non-specific fluorescence (Bussolati et al., 1980; Kramer, 1981; Repetto-Antoine et al., 1982 and Wolosewick and DeMay 1982). Embedding tissue in paraffin may reduce antigenicity and thus the intensity and specificity of labelling (Feteanu, 1978). This did not appear to be a problem in the application of these methods to Rhodnius follicles. The fluorescent pattern observed within the follicle cell epithelium was very bright and consistent, suggesting that if the antigenicity was impaired, it was not by a significant amount.

The application of immunofluorescence methods to plastic embedded tissues has only recently been successfully accomplished (Rodning et al., 1980). The general application of these methods to plastic embedded tissue is largely unsuccessful. Steinberger (1967) in Rodning et al., (1980) suggested that the antigenic determinants become so enmeshed by the embedding matrix that antigen-antibody reactions are inhibited. The key to successfully adapting these methods to plastic embedded tissue sections lies in the complete removal of the embedding media. Of the 2 plastic removal methods (Lane and Europa, 1965; Maxwell, 1978; Rodning et al., 1980 and Hogan and Smith, 1982) the NaOH method consistently removed the plastic embedding media from the tissue sections for all the plastics used in this study. The Epon-Araldite embedding medium (Anderson and Ellis, 1965) gave the best combination of lowest background, with ease of sectioning and subsequent removal from the sections. Rodning et al., (1980) embedded tissue in various media including, Spurr's (Spurr, 1969), Epon 812 (Luft, 1961) and

Epon-Araldite (Mollenhauer, 1963). They reported no variation in these 3 media for ease of removal from the sections, relative degree of background fluorescence and most important, the patterns of antigen localization. My results show that immunofluorescent localization of tubulin can be applied to plastic embedded follicle cell sections. The increased resolution observed allowed for a more precise assessment of tubulin distribution within the follicle cells.

Fujiwara and Pollard (1976) and Byers and Fujiwara (1982) used the following controls in their studies: (A) absorbed antibody (to isolated protein) followed by fluorescein conjugated goat anti-rabbit IgG (Fl-GAR); (B) preimmune serum + FL-GAR; (C) FL-GAR alone; and (D) a different 1° antibody and then FL-GAR. The application of controls A and B were not possible in this study as the antibodies used were either purchased (Miles Laboratories) or the gift of Dr. Fujiwara. No preimmune serum was available, nor was a source of tubulin to absorb the antibody. Dr. Fujiwara's anti-tubulin is one of the best available and has been successfully used in a large number of diverse studies. Results of my work with his antibody were sent to him for evaluation and received very favourable comments. The quality of his antibody, his evaluation of my results, combined with the other controls I ran indicated a high degree of confidence can be placed on the results obtained. These immunofluorescence results also agree closely with the TEM findings on microtubule distribution.

Characterization and Organizational Dynamics of the Follicle Cell Cytoskeleton During Oogenesis

The formation of intercellular spaces between the oocyte and follicle cells occurs in groups as diverse as teleosts (Selman and Wallace, 1982 and Abraham et al., 1984), amphibian (Dumont, 1972, 1979), lizards (Neaves, 1972), birds (Perry and Gilbert, 1979) and many insects (Anderson, 1969; Anderson and Spielman, 1971; Kelly and Telfer, 1979; Huebner and Injeyan, 1980 and Telfer et al., 1982).

It is a widespread phenomenon which provides a pathway for yolk proteins (synthesized at extraovarian sites, like the liver or fat body) to reach the oolemma for pinocytotic incorporation. Insects such as Glossina austeni, which do not form a patent follicle cell epithelium, produce their yolk proteins from intraovarian sources in either the follicle epithelium or the oocyte directly (Huebner et al., 1975 a,b). In Drosophila, yolk proteins may arise from both the extra or intraovarian sources (Cummings and King, 1963; Mahowald, 1972 and Postlethwait and Shirk, 1981).

The insects Rhodnius prolixus and Hyalophora cecropia are the best systems studied in terms of the details and mechanisms involved with patency formation. They also illustrate two different mechanisms by which the spaces are formed. In Hyalophora the spaces arise due to the secretion of a proteoglycan matrix inbetween adjacent follicle cells, beginning at the onset of vitellogenesis (Telfer, 1979 and Telfer et al., 1982). For details on the biochemistry and cellular events inherent in the cecropia system see Rubinstein (1979), Telfer (1979) and Telfer et al. (1982).

The mechanism of patency formation in Rhodnius is quite different. As suggested in the introduction, Davey (1981) has concluded that in Rhodnius patency occurs due to a JH stimulated activity of Na^+K^+

ATPase's in the follicle cell membranes and the subsequent pumping out of fluid from the cytoplasm.

The role of JH in stimulating patency in Rhodnius is established (Pratt and Davey, 1972 a,b,c; Davey and Huebner, 1974 and Huebner and Injeyan, 1980). An action during both previtellogenesis and vitellogenesis has also been suggested (Abu-Hakima and Davey, 1975). During previtellogenesis, JH is required to "prime" the follicle cells to become responsive to the second action of JH, which is the initiation of patency at the onset and during vitellogenesis (Abu-Hakima and Davey, 1975). Abu-Hakima and Davey (1977a) showed that the appearance of spaces is correlated with a 50% reduction in lateral follicle cell volume. This value was determined in using interference microscopy to measure the change in cell volume of isolated follicle cells upon JH treatment (Abu-Hakima and Davey 1977a). Volume change appears to be dependent on the effect of JH on Na^+K^+ ATPase, as significant increases in enzyme activity occur with JH exposure and this response in inhibited by ouabain (Abu-Hakima and Davey, 1979 and Ilenchuk, 1980). Ilenchuk and Davey (1983) have proposed that a specific Na^+ K^+ ATPase develops as the lateral follicle cells enter vitellogenesis. These results convincingly support Davey's (1981) explanation of patency formation.

Further evidence, illustrating that cytoskeletal disruptors, such as cytochalasin B and colchicine, inhibit the JH induced patency response (Huebner, 1976 and Abu-Hakima and Davey, 1977b) suggest an involvement of the follicle cell cytoskeleton to the overall mechanism of patency formation. Although Huebner and Anderson (1970, 1972a) and Abu-Hakima and Davey (1977c) described the presence of microtubules and microfilaments in Rhodnius follicle cells, no study until now has

compared the changes in the arrangement and abundance of these cytoskeletal elements in the follicle cells during oogenesis.

The immunofluorescence and TEM results both substantiate that initiation of patency is correlated with a microtubular reorganization in the lateral follicle cells. This is reflected in a change from the highly organized cylindrically arranged microtubules of the previtellogenic cells to the random pattern observed within the mid-vitellogenic lateral follicle cells. The apical and basal follicle cells maintain this regular cylindrical microtubular arrangement throughout oogenesis. Huebner and Anderson (1972) first reported that the apical follicle cells remain tall and tightly apposed during patency. It is tempting to explain this observation by suggesting the maintainence of a well organized microtubular cytoskeleton precludes any possible cell shape change.

These results confirm the presence of sub-populations of follicle cells. This is the first study to ultrastructurally define a subpopulation of follicle cells in Rhodnius prior to chorion formation. The apical follicle cells are responsible for chorion cap formation (Beament, 1946). The production of this specialized region seems to require the maintenance of tall columnar follicle cells as a template for cap formation (Beament, 1946). Margarites et al., (1980) has defined up to 10 different populations of follicular epithelial cells in Drosophila. The identification of these sub-populations was also based upon follicle cell synthetic differences during chorion formation.

The involvement of microtubules and microfilaments in the dynamics of lateral follicle cell shape in Rhodnius is not surprising since an abundant literature has implicated their role in cell shape in other

systems. Examples include Dictyostelium amebae (Roos et al., 1984 and Rubino et al., 1984), flagellates Naegleria gruberi and Ochromonas (Bouck and Brown, 1973; Brown and Bouck, 1973 and Walsh, 1984), volvox inversion (Vicmontes and Kirk, 1977), rat mast cells (Lagunoff and Chi, 1976), cultured mammalian granulosa cells (Herman et al., 1983 and Albertini et al., 1984) and nonmammalian nucleated erythrocytes (Barrett and Dawsen, 1974; Bertolini and Monaco, 1976 and Cohen, 1978). Microtubules are associated with the maintainence of cell shape and pigment granule migration in crayfish retinula cells (Frixione, 1983) and erythrophores and melanophores (Schliwa et al., 1978 and Beckerle and Porter, 1983).

The orientation of microtubules within the follicle cells of the gall midge Heteropeza and the cockroach Periplaneta not only modulate follicle cell shape but also contribute to the formation of the long ovoid shape of oocytes (Tucker and Meats, 1978). Microtubules in the follicle cells are arranged so that tension is applied around the circumference of the growing oocyte. Oocytes which are cultured without the follicle epithelium become spherical, similiar to mammalian oocytes as opposed to the long ovoid shape of the most insect oocytes (Went, 1978).

Microfilaments are thought to influence cell shape by the creation of contractile forces which physically compresses the shape of the cell. Microfilaments are often transistory structures such as in the case of the formation of the contractile ring or cleavage furrow of dividing cells (Schroeder, 1972, 1973, 1981 and Fujiwara et al., 1978). Microfilaments can also form the main cytoskeletal constituent of very stable cell structures such as the intestinal brush border (Mooseker,

1976; Hirokawa and Heuser, 1981 and Hirokawa et al., 1982) or the stereocilia structures of the cochlear hair cells (Flock and Cheung, 1977; Tilney et al., 1980; Hirokawa and Tilney, 1982; Tilney and Saunders, 1983 and Tilney et al., 1983).

Additionally the processes of amphibian neurulation (Handel and Roth, 1970 Karfunkel, 1971 and Burnside 1973) and the mechanism of light and dark adaptation of fish photoreceptor cells (Burnside, 1978 and Warren and Burnside, 1978) both illustrate clearly how cell shape control can be mediated by the interaction of microfilaments and microtubules.

The vitellogenic lateral follicle cells decrease in height at the onset of patency (Abu-Hakima and Davey, 1977a). This decrease in height is correlated with the reorganization of microtubules in the lateral follicle cells. The formation of a random distribution of microtubules would greatly decrease the resistance an organized cylindrical arrangement of microtubules would produce against a change in cell height or volume.

The microtubules arranged randomly would still support the new cell shape, but at the same time would not inhibit any inward movement of the cell boundaries that would be associated with the cell shrinkage. The overall process of cell shrinkage by $Na^{+}K^{+}$ATPase mediated pumping of fluid out of the cell, would thus be restrained until the microtubular cytoskeleton becomes rearranged.

The maintainence of the columnar, closely apposed shape of the apical and basal follicle cells during vitellogenesis is certainly related to the maintanence of the regular cylindrical arrangement of microtubules found in these cells. This further strengthens the

hypothesis that a rearrangement of the microtubular cytoskeleton is a requirement for the observed cell shape and volume changes to appear in the lateral follicle cells.

The complete involvement of microfilaments to the overall process cannot be conclusively assessed by this study. Microfilaments are most prominant within the patent lateral follicle cells. The appearance of microfilaments at this stage could take on a similiar function as observed with the contractile ring in providing an inward contractile force. This would definitely assist with the modulation of cell shape and is likely involved with the formation of the lateral connections between patent lateral follicle cells.

In addition to cytoskeletal reorganization and $Na^{+}K^{+}$ATPase mediated cell shrinkage, patency, also involves the disassembly and reformation of junctional complexes between the lateral follicle cells (Huebner and Injeyan, 1981 and Huebner, 1984b). By late previtellogenesis well developed areas of septate and E type gap junctions are formed within the cell membranes of adjacent previtellogenic follicle cells (Huebner and Injeyan, 1981). These cell junctions, along with the cylindrically arranged microtubular cytoskeleton contribute to the maintainence of the tightly apposed columnar epithelium observed during previtellogenesis. By mid-vitellogenesis the regions of junctional contact are limited to the lateral connections which form between patent lateral follicle cells (Huebner and Injeyan, 1981). The actual stimulatory factor for this disassembly and reorientation is unknown.

Since in some systems the cytoskeleton is also involved in the translocation of membrane components (Albertini and Clark, 1975), it is possible that the follicle cell junctional reorganization may also

depend on the alteration of the cytoskeletal components. JH could also directly affect the cell junction dynamics, as the action of gonadotropin on the mammalian granulosa cell oocyte gap junctions is well characterized (Burghardt and Anderson, 1981 and Dekel et al., 1981). Further research is required to clarify these points.

In conclusion, the mechanism of lateral follicle cell patency in Rhodnius is a more complex process than generally viewed. JH exposure either directly or indirectly appears to stimulate the observed change in lateral follicle cell shape by intergrating at least 3 separate cellular processes. Namely, the rearrangement of the microtubular and microfilamentous elements of the lateral follicle cell cytoskeleton, the disassembly and rearrangement of cell junctions and the stimulation of Na^+ K^+ ATPase.

The details of the dynamics of the follicle cell cytoskeleton during oogenesis ellucidated in this thesis add important elements to our understanding of the overall process of patency. The results also verify that Rhodnius follicle cells provide a good model system to study the role of cytoskeletal organization in the modulation of cell shape in a tissue. The application of the detergent extraction techniques and in particular the immunofluorescence techniques to paraffin and plastic embedded tissues sections, will hopefully encourage the further application and extension of these techniques to intact tissues of other research systems.

References

Abraham, M., Hilge, V., Lison, S. and Tibika, H., 1984. The cellular envelope of oocytes in teleosts. Cell Tiss. Res. 235: 403-410.

Abu-Hakima, R. and Davey, K.G., 1975. Two actions of juvenile hormone on the follicle cells of Rhodnius prolixus. (Stal). Can. J. Zool. 53: 1187-1188.

Abu-Hakima, R. and Davey, K.G., 1977a. The action of juvenile hormone on the follicle cells of Rhodnius prolixus: The importance of volume changes. J. Exp. Biol. 69: 33-44.

Abu-Hakima, R. and Davey, K.G., 1977b. Effects of hormones and inhibitors of macromolecular synthesis on the follicle cells of Rhodnius. J. Insect Physiol. 23: 913-917.

Abu-Hakima, R. and Davey, K.G., 1977c. The action of juvenile hormone on follicle cells of Rhodnius prolixus in vitro: The effect of colchicine and cytochalasin B. Gen. and Comp. Endocrin. 32: 360-370.

Abu-Hakima, R. and Davey, K.G., 1979. A positive relationship between ouabain-sensitive Na^+ - K^+ dependent ATPase and the effect of juvenile hormone on the follicle cells of Rhodnius prolixus. Insect Biochem. 9: 195-198.

Albertini, D.F., and Clark, J.I., 1975. Membrane-microtubule interactions: concanavalin A capping induced redistribution of cytoplasmic microtubules and colchicine binding proteins. Proc. Natl. Acad. Sci. USA. 72: 4976-4980.

Albertini, D.F., Herman, B. and Sherline, P., 1984. In vivo and in vitro studies on the role of HMW-MAP's in taxol induced microtubule bundling. Eur. J. Cell Biol. 33: 134-143.

Anderson, E., 1969. Oogenesis in the cockroach, Periplaneta americana, with special reference to the specialization of the oolemma and the fate of coated vesicles. J. Microscopie 8 : 721-738.

Anderson, W.A. and Ellis, R.A., 1965. Ultrastructure of Trypanosoma lewisi flagellum, microtubules and the kinetoplast. J. Protozool. 12: 483-499.

Anderson, W.A. and Spielman, A., 1971. Permeability of the ovarian follicle of Aedes aegypti, mosquitoes. J. Cell Biol. 50: 201-221.

Ashurst, D.E., 1982. The structure and development of insect connective tissues. In. Insect Ultrastructure, Vol. 1, R.C. King and H. Akai (Eds.) Plenum Press, New York, pgs. 313-351.

Banerjee, S.D., Cohn, R.H. and Bernfield, M.R., 1977. Basal lamina of embryonic salivary epithelia. Production by the epithelium and role in maintaining lobular morphology. J. Cell Biol. 73 : 445-465.

Barrett, L.A. and Dawson, R.B., 1974. Avian erythrocyte development: Microtubules and the formation of the disk shape. Dev. Biol. 36: 72-81.

Batten, B.E., Aalberg, J.J. and Anderson, E., 1980. The cytoplasmic filamentous network in cultured ovarian granulosa cells. Cell 21: 885-895.

Beament, J.W.L., 1946. The formation and structure of the chorion of the egg in an hemipteran: Rhodnius prolixus. Quart. J. Microsop. Sci. 87: 393-439.

Beckerle, M.C., and Porter, K.R., 1983. Analysis of the role of microtubules and actin in erythrophore intracellular motility. J. Cell Biol. 96 : 354-362.

Bershadsky, A.D., Gelfand, V.I., Svitkina, T.M. and Tint, I.S., 1978. Microtubules in mouse embryo fibroblasts extracted with Triton X-100. Cell Biol. Inter. Rep. 2 : 425-432.

Berthold, G., 1980. Microtubules in the epidermal cells of Carausius morosus (BR). Their pattern and relation to pigment migration. J. Insect Physiol. 26: 421-425.

Bertolini, B. and Monaco, G., 1976. The microtubule marginal band of the newt erythrocyte. J. Ultrastruct. Res. 54: 59-67.

Bloom, W. and Fawcett, D., 1975. A Textbook of Histology, 10th ed.,W.B. Saunders Company, Toronto. 1033 pgs.

Bouck, G.B. and Brown, D.L., 1973. Microtubule biogenesis and cell shape in Ochromonas. I. The distribution of cytoplasmic and mitotic microtubules. J. Cell Biol. 56: 340-359.

Bradley, T.J., 1981. Elastase fully removes the basal lamella of insect malpigian tubules. J. Cell Biol. 91 : pt. 2. 153a.

Bretscher, A. and Weber, K., 1978. Localization of actin and microfilament associated proteins in the microvilli and terminal web of the intestinal brush border by immunofluorescence microscopy. J. Cell Biol. 79 : 839-845.

Brown, D.L. and Bouck, G.B., 1973. Microtubule biogenesis and cell shape in Ochromonas II. The role of nucleating sites in shape development. J. Cell Biol. 56: 360-378.

Buckley, I.K. and Porter, K.R., 1978. Electron microscopy of critical point dried whole culture cells. J. Microscopie 104: 107-120.

Burghardt, R.C. and Anderson, E., 1981. Hormonal modulation of gap junctions in rat ovarian follicles. Cell Tiss. Res. 214: 181-193.

Burnside, B., 1973. Microtubules and microfilaments in amphibian neurulation. Amer. Zool. 13: 989-1006.

Burnside, B., 1978. Thin (actin) and thick (myosin-like) filaments in cone contraction in the teleost retina. J. Cell Biol. 78 : 227-246.

Bussolati, G., Alfani, V., Weber, K. and Osborn, M., 1980. Immunocytochemical detection of actin on fixed and embedded tissues: Its potential use in routine pathology. J. Histochem. Cytochem. 28 : 169-173.

Byers, H.R. and Fujiwara, K., 1982. Stress fibers in cells in situ: Immunofluorescence visualization with anti-actin, anti-myosin and anti-alpha-actinin. J. Cell Biol. 93 : 804-811.

Cande, W.Z., Lazarides, E. and McIntosh, J.R., 1977. A comparison of the distributions of actin and tubulin in the mammalian mitotic spindle as seen by indirect immunofluorescence. J. Cell Biol. 72: 552-567.

Cohen, W.H., 1978. Observations on the marginal band system of nucleated erythrocytes. J. Cell Biol. 78 : 260-273.

Coulter, H.D., 1967. Rapid and improved methods for embedding biological tissues in Epon 812 and Araldite 502. J. Ultrastruct. Res. 20: 346.

Cummings, M.R. and King. R.C., 1969. The cytology of the vitellogenic stages of oogenesis in Drosophila melanogaster. General staging characteristics. J. Morph. 128: 427-442.

Davey, K.G., 1981. Hormonal control of vitellogenin uptake in Rhodnius prolixus (Stal). Amer. Zool. 21: 701-705.

Davey, K.G. and Huebner, E., 1974. The response of the follicle cells of Rhodnius prolixus to juvenile hormone and antigonadotropin in vitro. Can. J. Zool. 52 : 1407-1412.

Dekel, W., Lawrence, T.S., Gilula, N.B. and Beers, W.H., 1981. Modulation of cell to cell communication in the cumulus-oocyte complex and the regulation of oocyte maturation by LH. Dev. Biol. 86: 356-362.

Drenckhahn, D. and Groschel-Stewart, U., 1980. Localization of myosin, actin, and tropomyosin in rat intestinal epithelium: Immunohistochemical studies at the light and electron microscope levels. J. Cell Biol. 86 : 475-482.

Dumont, J.N., 1972. Oogenesis in Xenopus laevis (Daudin). I. Stages of oocyte development in laboratory maintained animals. J. Morph. 136: 153-180.

Dumont, J.W., 1978. Oogenesis in Xenopus laevis (Daudin). VI. The route of injected tracer transport in the follicle and developing oocyte. J. Exp. Zool. 204: 193-208.

Dustin, P., 1978. Microtubules. Springer- Verlag. New York. 425p.

Dutkowski, A.B., 1977. The ultrastructure and ultracytochemistry of the basement membrane of the Galleria mellonella fat body. Cell Tiss. Res. 176: 417-429.

Dybowska, H.E. and Dutkowski, A.B., 1977. Ruthenium red staining of the neural lamella of the brain of Galleria mellonella. Cell Tiss. Res. 176: 275 - 284.

Farquhar, M.G., 1981. The glomerular basement membrane, a selective macromolecular filter. In Cell Biology of Extracellular Matrix, Chapter II, E. Hay. (Ed.) Plenum Press. New York pgs. 335-378.

Feteanu, A., 1978. Labelled Antibodies in Biology and Medicine, McGraw Hill Publ., Toronto. 411pgs.

Flock, A. and Cheung, H.C., 1977. Actin filaments in sensory hairs of inner ear receptor cells. J. Cell Biol. 75 : 339-343.

Franke, W.W., Schmid, E., Osborn, M. and Weber, K., 1978. Different intermediate-sized filaments distinguished by immunofluorescence microscopy. Proc. Natl. Acad. Sci. USA. 75 : 5034-5038.

Frixione, E., 1983. Firm structural associations between migratory pigment granules and microtubules in crayfish retinula cells. J. Cell Biol. 96 : 1258-1265.

Fijikawa, L.S., Foster, C.S., Gipson, I.K. and Colvin, R.B., 1984. Basement membrane components in healing rabbit corneal epithelial wounds: Immunofluorescence and ultrastructural studies. J. Cell Biol. 98 : 128-138.

Fujiwara, K., Porter, M.E. and Pollard, T.D., 1978. Alpha-actinin localization in the cleavage furrow during cytokinesis. J. Cell Biol. 79: 268-275.

Fujiwara, K. and Pollard, T.D., 1976. Fluorescent antibody localization of myosin in the cytoplasm, cleavage furrow, and mitotic spindle of human cells. J. Cell Biol. 71 : 848-875.

Ghosh, S.K., 1981. Quantitative methods applied to stereo imaging hardware and software. In. Methods in Cell Biology, Vol. 22., Three Dimensional Ultrastructure in Biology. J.W. Turner (Ed.). Academic Press Toronto. pgs. 155-176.

Glauert, A., 1974. The high voltage electron microscope in biology. J. Cell Biol. 63: 717-748.

Goel, S.C. and Jurand. A., 1968. Electron microscopic observations on the basal lamina of chick limb buds after trypsin treatment and

EDTA treatment. J. Cell Sci. 3: 373-380.

Greenburg, G. and Hay, E.D., 1982. Epithelia suspended in collagen gells can loose polarity and express characteristics of migrating mesenchymal cells. J. Cell Biol. 95 : 333-339.

Grinnell, F., Head, J.R. and Hoffpauir, J., 1982. Fibronectin and cell shape in vivo: Studies on the endometrium during pregnancy. J. Cell Biol. 94 : 596-606.

Harris, P., Osborn, M. and Weber, K., 1980. Distribution of tubulin containing structures in the egg of the sea urchin, Strongylocentrotus purpuratus from fertilization through first cleavage. J. Cell Biol. 84: 668-679.

Handel, M.A. and Roth, L.E., 1971. Cell shape and morphology of the neural tube: Implications for microtubule function. Dev. Biol. 25: 78-95.

Hayman, E.G., Oldberg, A., Martin, G.R. and Russlahti, E., 1982. Co-distribution of heparan sulfate proteoglycan, laminin, and fibronectin in the extracellular matrix of normal rat kidney cells and their coordinate absence in transformed cells. J. Cell Biol. 94 : 28-35.

Helenius, A. and Simions, K., 1975. Solubilization of membranes by detergents. Biochem. et Biophys. Acta. 415: 29-79.

Herman, B., Langevin, M.A. and Albertini, D.F., 1983. The effects of taxol on the organization of the cytoskeleton in cultured ovarian granulosa cells. Eur. J. Cell Biol. 31: 34-45.

Heuser, J., 1981. Preparing biological samples for stereomicroscopy by the quick-freeze, deep etch, rotary replication technique. In Methods in Cell Biology, Vol. 22., J.W. Turner (Ed.). Academic Press, Toronto, pgs. 97-122.

Heuser, J.E. and Kirschner, M.W., 1980. Filament organization revealed in platinum replicas of freeze-dried cytoskeletons. J. Cell Biol. 86 : 212-234.

Hirokawa, N. and Heuser, J., 1980. Methods for visualizing the relationships between cell membranes and cytoskeletal elements. J. Cell Biol. 87: 219a.

Hirokawa, N. and Heuser, J.E., 1981. Quick-freeze, deep etch, visualization of the cytoskeleton beneath surface differentiations of intestinal epithelial cells. J. Cell Biol. 91 : 399-409.

Hirokawa, D., Keller, T.C.S., Chason, R. and Mooseker, M.S., 1983. Mechanism of brush border contractility studied by quick freeze deep etch method. J. Cell Biol. 96 : 1325-1336.

Hirokawa, N. and Tilney, L.G., 1982. Interactions between actin filaments and between actin filaments and membranes in quick frozen and deeply etched hair cells of the chick ear. J. Cell Biol. 95: 249-261.

Hirokawa, N., Tilney, L.G., Fujiwara, K. and Heuser, J.E., 1982. Organization of actin, myosin, and intermediate filaments in the brush border of intestinal epithelial cells. J. Cell Biol. 94 : 425-443.

Hogan, D.L. and Smith, G.H., 1982. Unconventional application of standard light and electron immunocytochemical analysis to aldehyde-fixed, Araldite embedded tissues. J. Histochem. Cytochem. 30 : 1301-1306.

Huebner, E., 1976. Experimental modulation of the follicular epithelium of Rhodnius oocytes by juvenile hormone and other agents. J. Cell Biol. 70: 251a.

Huebner, E., 1982. Ultrastructure and development of the telotrophic ovary. In. The Ultrastructure and Functioning of Insect Cells., H. Akai, R.C. King and S. Morohoshi (Eds.), Soc. for Insect Cells, Japan, pgs. 9-12.

Huebner, E., 1984a. Developmental cell interactions in female insect reproductive organs. In. Advances in Invertebrate Reproduction, W. Engels, (Ed.), Elsevier Science Publishers, Amsterdam, pgs. 97-105.

Huebner, E., 1984b. The Ultrastructure and development of the telotrophic ovary. In. Insect. Ultrastructure, Vol. 2, R.C. King and H. Akai (Eds.), Plenum Press, New York, In Press.

Huebner, E. and Anderson, E., 1970. The effects of vinblastine sulfate on the microtubular organization of the ovary of Rhodnius prolixus. J. Cell Biol. 46: 191-198.

Huebner, E. and Anderson, E., 1972a. A cytological study of the ovary of Rhodnius prolixus. I. The ontogeny of the follicular epithelium. J. Morph. 136: 459-494.

Huebner, E. and Injeyan, H.S., 1980. Patency of the follicular epithelium in Rhodnius prolixus: A re-examination of the hormone response and technique refinement. Can. J. Zool. 58 : 1617-1625.

Huebner, E. and Injeyan, H., 1981. Follicular modulation during oocyte development in an insect: Formation and modification of septate and gap junctions. Dev. Biol. 83: 101-113.

Huebner, E., Tobe, S.S. and Davey, K.G., 1975a. Structural and functional dynamics of oogenesis in Glossina austeni: General

features, previtellogenesis and nurse cells. Tissue & Cell 7 : 297-317.

Huebner, E., Tobe., S.S. and Davey, K.G., 1975b. Structural and functional dynamics of oogenesis in Glossina austeni: Vitellogenesis with special reference to the follicular epithelium. Tissue & Cell 7 : 535-558.

Humason, G.L., 1979. Animal Tissue Techniques, 4th ed., W.H. Freeman and Company, San. Francisco, 661pgs.

Ilenchuk, T.T., 1980. Juvenile hormone stimulates $Na^{+}K^{+}$ ATPase in vitellogenic follicle cells of Rhodnius prolixus. Amer. Zool. 20: 900.

Ilenchuk, T.T. and Davey, K.G., 1983. Juvenile hormone increases ouabain-binding capacity of microsomal preparations from vitellogenic follicle cells. Can. J. Biochem. Cell. Biol. 61: 826-831.

Jensen, H.M. and Mottet, W.K., 1970. Ultrastructural changes in keratinizing epithelium following trypsinization, epidermal detachment and apposition to mesenchymes. J. Cell Sci. 6: 511-535.

Juurlink, B.H.J. and Dell, R., 1980. A simple method for producing fine stainless steel dissecting needles and microscalpels. Experientia 36: 1335.

Karfunkel, P., 1971. The role of microtubules and microfilaments in neurulation in Xenopus. Dev. Biol. 25: 30-56.

Karnovsky, M.J., 1965. A formaldehyde-glutaraldehyde fixative of high osmolality for use in electron microscopy. J. Cell Biol. 27: 137A.

Kelly, T.J. and Telfer, W.H., 1979. The function of the follicular epithelium in vitellogenic Oncopeltus follicles. Tissue & Cell 11: 663-672.

King, R.C. and Koch, E.A., 1963. Studies on the ovarian follicle cells of Drosophila. Quart. J. Microscop. Sci. 104 : 297-320.

Kleinman, H.K., Klebe, R.J. and Martin, G.R., 1981. Role of collagenous matrices in the adhesion and growth of cells. J. Cell Biol. 88 : 473-485.

Kramer, J.M. 1981. Immunofluorescent localization of PGK-1 and PGK-2 isozymes with specific cells of the mouse testis. Dev. Biol. 87: 30-36.

Lagunoff, D. and Chi, E.Y., 1976. Effect of colchicine on rat mast cells. J. Cell Biol. 71 : 182-195.

Lane, B.P. and Europa, D.L., 1965. Differential staining of ultrathin sections of Epon embedded tissues for light microscopy. J. Histochem. Cytochem. 13: 579.

Lazarides, E. and Weber, K., 1974. Actin antibody. The specific visualization of actin filaments in non-muscle cells. Proc. Natl. Acad. Sci. USA. 71 : 2268-2272.

Laurie, G.W., Leblond, C.P., Cournil, I. and Martin, G.R., 1980. Immunohistochemical evidence for the intracellular formation of basement membrane collagen (Type IV) in developing tissues. J. Histochem. Cytochem. 28 : 1267-1274.

Laurie, G.W., Leblond, C.P. and Martin, G.R., 1982. Localization of Type IV collagen, laminin, heparin sulfate proteoglycan and fibronectin to the basal lamina of basement membranes. J. Cell Biol. 95 340-344.

Liotta, L.A., Abe, S., Robey, P.G. and Martin, G.R., 1979. Preferential digestion of basement membrane collagen by an enzyme

derived from a metastatic murine tumor. Proc. Natl. Acad. Sci. USA. 76 : 2268-2272.

Luft, J.H., 1961. Improvements in epoxy resin embedding methods. J. Biophys. Biochem. Cytol. 9: 409.

Luftig, R.B., McMillan, P.W., Weatherbee, J.A. and Weihing R.R., 1977. Increased visualization of microtubules by an improved fixation procedure. J. Histochem. Cytochem. 25 : 175-187.

Lutz, D.A. and Huebner, E., 1980. Development and cellular differentiation of an insect telotrophic ovary, Rhodnius prolixus. Tissue and Cell 12 : 773-794.

Maddrell, S.H.P., 1969. Secretion by the malphigian tubules of Rhodnius. The movements of ions and water. J. Exp. Biol. 51: 71-97.

Mahowald, A.P., 1972. Ultrastructural observations on oogenesis in Drosophila. J. Morph. 137: 29-48.

Margaritis, L.H., Kafatos, F.C. and Petri. W.H., 1980. The eggshell of Drosophila melanogaster. 1. Fine structure of the layers and regions of the wild-type eggshell. J. Cell Sci. 43: 1-35.

Masner, P., 1968. The inductors of differentiation of prefollicular tissue and the follicular epithelium in ovarioles of Pyrrhocoris apterus (Heteroptera). J. Embryol. exp. Morph. 20 : 1-13.

Maupin-Szamier, P. and Pollard, T.D., 1978. Actin filament destruction by osmium tetroxide. J. Cell Biol. 77 : 837-852.

Maupin, P. and Pollard, T.D., 1983. Improved preservation and staining of Hela cell actin filaments, clathrin coated membranes and other cytoplasmic structures by tannic acid-glutaraldehyde-saponin fixation. J. Cell Biol. 96 : 51-62.

Maxwell, M.H., 1978. Two rapid and simple methods used for the removal of resins from 1.0 M thick epoxy sections. J. Microscopie 112: 253-255.

Mooseker, M.S., 1976. Brush border motility, microvillar contraction in Triton-treated brush borders isolated from intestinal epithelium. J. Cell Biol. 71 : 417-432.

Mollenhauer, H., 1964. Plastic embedding mixtures for use in electron microscopy. Stain Technol. 39: 111.

Neaves, W.B., 1972. The passage of extracellular tracers through the follicular epithelium of lizard ovaries. J. Exp. Zool. 179 : 339-364.

Osborn, M. and Weber, K., 1977. The detergent resistant cytoskeleton of tissue culture cells includes the nucleus and the microfilament bundles. Exp. Cell Res. 106: 339-350.

Osborn, M. and Weber, K., 1982. Immunofluorescence and immunocytochemical procedures with affinity purified antibodies: Tubulin containing structures In. Methods in Cell Biology, Vol. 24. Part A. The Cytoskeleton., L. Wilson (Ed.), Academic Press, Toronto. pgs. 97-132.

Osborn, M., Webster, R.E. and Weber, K., 1978. Individual microtubules viewed by immunofluorescence and electron microscopy in the same Ptk2 cell. J. Cell Biol. 77 : R27.

Parysek, L.M. and Eckert, B.S., 1980. Cytoskeletal elements of detergent extracted human neutrophils. J. Cell Biol. 87: 222a.

Perry, M.M. and Gilbert, A.B., 1979. Yolk transport in the ovarian follicle of the hen (Gallus domesticus): Lipoprotein-like particles at the periphery of the oocyte in the rapid growth phase. J. Cell Sci. 39: 257-272.

Postlethwait, J.H. and Shirke, P.D., 1981. Genetic and endocrine regulation of vitellogenesis in Drosophila. Amer. Zool. 21: 687-700.

Pratt, G.E. and Davey, K.G., 1972a. The corpus allatum and oogenesis in Rhodnius prolixus (Stal) I. The effects of allatectomy. J. Exp. Biol. 56: 201-214.

Pratt, G.E. and Davey, K.G., 1972b. The corpus allatum and oogenesis in Rhodnius prolixus (Stal) II. The effects of starvation. J. Exp. Biol. 56: 215-221.

Pratt, G.E. and Davey, K.G., 1972c. The corpus allatum and oogenesis in Rhodnius prolixus (Stal) III. The effects of mating. J. Exp. Biol. 56: 223-237.

Pudney, J. and Singer, R.H., 1980. Intracellular filament bundles in whole mounts of chick and human myoblasts extracted with Triton X-100. Tissue & Cell 12 : 595-612.

Reinhardt, C. and Hecker, H., 1973. Structure and function of the basal lamina and of the cell junctions in the midgut epithelium (stomach) of female Aedes aegypti L. (Insecta, Diptera). Acta. Trop. Parasit. 30 : 213-233.

Repetto-Antoine, M., DeMey, J. and Meininger, V., 1982. In situ distribution of microtubules in the rat tectal plate at the earliest stages of cell differentiation using indirect immunofluorescence. Biol. Cell 44: 325-328.

Rodning, C.B., Erlandsen, S.L., Coulter, D.H. and Wilson, I.D., 1980. Immunohistochemical localization of IgA antigens in sections embedded in epoxy resin. J. Histochem. Cytochem. 28 : 199-205.

Roos, V.P., Brabander, M. and DeMey, J., 1984. Indirect immunofluorescence of microtubules in Dictyostelium discoideum. A study with polyclonal and monoclonal antibodies to tubulins. Exp. Cell Res. 151: 183-193.

Rubenstein, E., 1979. The role of anepithelial occlusion zone in the termination of vitellogenesis in Hyalophora cecropia ovarian follicles. Dev. Biol. 71: 115-127.

Rubin, R.W., Howard, J. and Leonardi, C., 1979. A biochemical and ultrastructural comparison of Triton X-100 models of normal and transformed cells. Tissue & Cell 11 : 413-423.

Rubino, S., Fighetti, M., Unger, E. and Cappucinelli, P., 1984. Location of actin, myosin and microtubular structures during directed locomotion of Dictyostelium amebae. J. Cell Biol. 98 : 382-390.

Sabatini, D.D., Bensch, K. and Barrnett, R.J., 1963. Cytochemistry and electron microscopy. The preservation of cellular ultrastructure and enzymatic activity by aldehyde fixation. J. Cell Biol. 17: 19-58.

Sanders, E.J., 1983. Recent progress towards understanding the roles of the basement membrane in development. Can. J. Biochem. Cell Biol. 61: 949-956.

Schliwa, M. Osborn, M. and Weber, K., 1978. Microtubule system of isolated fish melanophores as revealed by immunofluorescence microscopy. J. Cell Biol. 76 : 229-236.

Schliwa, M. and Von Blerkom, J., 1981. Structural interaction of cytoskeletal components J. Cell Biol. 90 : 222-235.

Schroeder, T.E., 1972. The contractile ring: II. Determining its brief existence, volumetric changes and vital role in cleaving Arbacia eggs. J. Cell Biol. 53: 419-434.

Schroeder, T.E., 1973. Actin in dividing cells: Contractile ring filaments bind heavy meromyosin. Proc. Natl. Acad. Sci. USA. 70 : 1688-1692.

Schroeder, T.E., 1981. The origin of cleavage forces in dividing eggs. A mechanism in two steps. Exp. Cell Res. 134: 231-240.

Scott, P.G., 1983. Macromolecular constituents of basement membranes: A review of current knowledge on their structure and function. Can. J. Biochem. Cell Biol. 61: 942-948.

Selmon, K. and Wallace, R.A., 1982. Oocyte growth in the sheepshead minnow: Uptake of exogenous proteins by vitellogenic oocytes. Tissue & Cell 14 : 555-571.

Shelanski, M.L., Gaskin, F. and Cantor, C.R., 1973. Microtubule assembly in the absence of added nucleotides. Proc. Natl. Acad. Sci. USA. 70 : 765-768.

Snyder, J.A. and McIntosh, J.R., 1976. Biochemistry and physiology of microtubules. Ann. Rev. Bioochem. 45: 699-720.

Spurr, A.R., 1969. A low viscosity epoxy resin embedding medium for electron microscopy. J. Ultrastruct. Res. 26: 31.

Sugrue, S.P. and Hay, E.D., 1981. Response of basal epithelial cell surface and cytoskeleton to solubilized extracellular matrix molecules. J. Cell Biol. 91 : 45-54.

Temmink, J.H.M. and Spiele, H., 1978. Preservation of cytoskeletal elements for electron microscopy. Cell Biol. Int. Rep. 2 : 51-59.

Telfer, W.H., 1979. Sulfate and glucosamine labelling of the intercellular matrix in vitellogenic follicles of a moth. W. Roux's Arch. 185: 347-362.

Telfer, W.H., Huebner, E. and Smith, D.S., 1982. The cell biology of vitellogenic follicles in Hyalophora and Rhodnius. In. Insect Ultrastructure, Vol. 1, R.C. King and H. Akai, (Eds.), Plenum Press, New York, pgs. 118-149.

Tilney, L.G., Derosier, D.J. and Mulroy. M.J., 1980. The organization of actin filaments in the stereocilia of cochlear hair cells. J. Cell Biol. 86 : 244-259.

Tilney, L.G. and Saunders, J.C., 1983. Actin filaments, stereocilia, and hair cells of the bird cochlea. I. Length, number, width and distribution of stereocilia of each hair cell are related to the position of the hair cell on the cochlea. J. Cell Biol. 96 : 807-821.

Tilney, L.G., Egelman, E.H., Derosier, D.J. and Saunders, J.C., 1983. Actin filaments, sterocilia and hair cells of the bird cochlea. II. Packing of actin filaments in the stereocilia and in the cuticular plate and what happens to the organization when the stereocilia are bent. J. Cell Biol. 96 : 822-834.

Tomasek, J.J., Hay, E.D. and Fujiwara, K., 1982. Collagen modulates cell shape and cytoskeleton of embryonic corneal and fibroma fibroblasts: Distribution of actin, - actinin and myosin. Dev. Biol. 92: 107-122.

Trotter, J.A., Foerder, B.A. and Keller, J.M. 1978. Intracellular fibers in cultured cells: Analysis by scanning and transmission electron microscopy and by SDS-polyacrylamide gel electrophoresis. J. Cell Sci. 31: 359-392.

Tucker, J.B. and Meats, M., 1976. Microtubules and control of insect egg shape. J. Cell Biol. 71: 207-217.

Vaccaro, G.A. and Brody, J.S., 1981. Structural features of alveolar wall basement membrane in the adult rat lung. J. Cell Biol. 91: 427-437.

Valnes, K. and Brandtzaeg, P., 1981. Unlabelled antibody peroxidase-antiperoxidase method combined with direct immunofluorescence. J. Histochem. Cytochem. 29 : 703-711.

Venable, J.M. and Coggershall, R., 1965. A simplified lead citrate stain for use in electron microscopy. J. Cell Biol. 25: 407.

Viamontes, G.I. and Kirk., D.L., 1977. Cell shape changes and the mechanism of inversion in Volvox. J. Cell Biol. 75 : 719-730.

Vogel, K., 1978. Effects of hyaluronidase, trypsin and EDTA on surface composition and topography during detachment of cells in culture. Exp. Cell Res. 113: 345-357.

Walsh, C., 1984. Synthesis and assembly of the cytoskeleton of Naegleria gruberi flagellates. J. Cell Biol. 98 : 449-456.

Warren, R.H. and Burnside, B., 1978. Microtubules in cone myoid elongation in the teleost retina. J. Cell Biol. 78 : 247-259.

Weber, K. and Groschel-Stewart, U., 1974. Antibody to myosin. The specific visualization of myosin-containing filaments in non-muscle cells. Proc. Natl. Acad. Sci. USA. 71 : 4561-4564.

Weber, K., Pollack, R. and Bibring, T., 1975. Antibody against tubulin: The specific visualization of cytoplasmic microtubules in tissue culture cells. Proc. Natl. Acad. Sci. USA. 72 : 459-463.

Webster, R.E., Henderson, D., Osborn, M. and Weber, K., 1978. Three dimensional electron microscopical visualization of the cytoskeleton of animal cells: immunoferritin identification of actin and tubulin containing structures. Proc. Natl. Acad. Sci. USA. 75 5511-5515.

Weisenberg, R.C., 1972. Microtubule formation *in vitro* in solutions containing low calcium concentrations. Science 177: 1104-1105.

Went, D.F., 1978. Oocyte maturation without follicular epithelium alters egg shape in a dipteran insect. J. Exp. Zool. 205 : 149-155.

White, G.E., Gimbrone, M.A. and Fujiwara, K., 1983. Factors influencing the expression of stress fibers in vascular endothelial cells *in situ*. J. Cell Biol. 97 : 416-424.

Wolosewick, J.J., 1980. The application of polyethylene glycol (PEG) to electron microscopy. J. Cell Biol. 86 : 675-681.

Wolosewick, J.J. and Porter, K.R., 1979. Microtrabecular lattice of the cytoplasmic ground substance. Artifact or reality. J. Cell Biol. 82 : 114-139.

Wolosewick, J. and De Mey, J., 1982. Localization of tubulin and actin in polyethylene glycol embedded rat seminiferous epithelium. Biol. Cell 44: 85-88.